EXPERIMENTAL COMPARISON OF DIFFERENT MINICHANNEL GEOMETRIES FOR USE IN EVAPORATORS

YİĞİT ATA AĞARTAN

FEBRUARY 2012

EXPERIMENTAL COMPARISON OF DIFFERENT MINICHANNEL GEOMETRIES FOR USE IN EVAPORATORS

A THESIS SUBMITTED TO
THE GRADUATE SCHOOL OF NATURAL AND APPLIED SCIENCES
OF
MIDDLE EAST TECHNICAL UNIVERSITY

BY

YİĞİT ATA AĞARTAN

IN PARTIAL FULFILLMENT OF THE REQUIREMENTS
FOR
THE DEGREE OF MASTER OF SCIENCE
IN
MECHANICAL ENGINEERING

FEBRUARY 2012

Approval of the thesis:

EXPERIMENTAL COMPARISON OF DIFFERENT MINICHANNEL GEOMETRIES FOR USE IN EVAPORATORS

Submitted by **YİĞİT ATA AĞARTAN** in partial fulfillment of the requirements for the degree of **Master of Science in Mechanical Engineering Department, Middle East Technical University** by,

Prof. Dr. Canan Özgen
Dean, Graduate School of **Natural and Applied Sciences** _____

Prof. Dr. Suha Oral
Head of Department, **Mechanical Engineering** _____

Assoc. Prof. Dr. Almıla Güvenç Yazıcıoğlu
Supervisor, **Mechanical Engineering Dept., METU** _____

Examining Committee Members:

Assoc. Prof. Dr. Cemil Yamalı
Mechanical Engineering Dept., METU _____

Assoc. Prof. Dr. Almıla Güvenç Yazıcıoğlu
Mechanical Engineering Dept., METU _____

Assoc. Prof. Dr. Derek Baker
Mechanical Engineering Dept., METU _____

Assist. Prof. Dr. Tuba Okutucu Özyurt
Mechanical Engineering Dept., METU _____

Assist. Prof. Dr. Nilay Sezer Uzol
Mechanical Engineering Dept., TOBB ETU _____

Date: **09.02.2012**

I hereby declare that all information in this document has been obtained and presented in accordance with academic rules and ethical conduct. I also declare that, as required by these rules and conduct, I have fully cited and referenced all material and results that are not original to this work.

Name, Last name : Yiğit Ata Ağartan

Signature :

ABSTRACT

EXPERIMENTAL COMPARISON OF DIFFERENT MINICHANNEL GEOMETRIES FOR USE IN EVAPORATORS

Ağartan, Yiğit Ata

M.Sc., Department of Mechanical Engineering

Supervisor : Assoc. Prof. Dr. Almıla G. Yazıcıoğlu

February 2012, 148 pages

This thesis investigates the refrigerant (R-134a) flow in three minichannels having different geometries experimentally. During the last 40 years heat transfer in small scales has been a very attractive research area. Improvements in heat transfer in the refrigeration applications by means of usage of micro/minichannels provide significant developments in this area. Also it is known that experimental studies are very important to constitute a database which is beneficial for new developments and research. During the two-phase flow experiments conducted in the minichannels, low mass flow rates and constant wall temperature approach, which are the conditions in the evaporators of the refrigerator applications were applied because one of the purposes of this study is to determine the most ideal minichannel among the tested minichannels for usage in the evaporator section of the refrigerators. Two-phase flow experiments were made with refrigerant R134a in the three minichannels having hydraulic diameters of 1.69, 3.85 and 1.69 mm respectively. As distinct from the others, the third minichannel has a rough inner surface. Comparison of the experimental results of the three minichannels was made in terms of forced convection heat transfer coefficients and pressure drop at constant quality and mass flux values. As a result of the experiments, the most ideal minichannel among the tested minichannels was determined for the evaporator applications in the refrigerators.

Keywords: Minichannels, forced convection heat transfer, pressure drop, refrigerant, R134a, two-phase flow, experimental study.

ÖZ

EVAPORATÖRLERDE KULLANILMAK ÜZERE FARKLI MİNİKANAL GEOMETRİLERİNİN DENEYSEL KARŞILAŞTIRILMASI

Ağartan, Yiğit Ata
Yüksek Lisans, Makina Mühendisliği Bölümü
Tez Yöneticisi : Doç. Dr. Almıla G. Yazıcıoğlu

Şubat 2012, 148 Sayfa

Bu tez farklı geometrilere sahip üç minikanaldaki R134a soğutkan akışını deneysel olarak incelemektedir. Son 40 yıldır küçük boyutlardaki ısı transferi çok ilgi çeken bir araştırma alanıdır. Mikro/minikanal kullanımı sayesinde gerçekleşen soğutma uygulamalarındaki ısı transferi artışı bu alanda önemli gelişmeler sağlamaktadır. Ayrıca deneysel çalışmaların, bu alandaki yeni gelişmeler ve araştırmalar için faydalı olan veritabanı oluşturmak için çok önemli olduğu bilinmektedir. Minikanallarda yürütülen iki fazlı akış deneyleri boyunca buzdolabı evaporatör koşulları olan düşük kütle debileri ve sabit duvar sıcaklığı yaklaşımı uygulanmıştır, çünkü bu çalışmanın amaçlarından biri test edilen minikanallar arasından buzdolabı evaporatör kısmında kullanıma en uygun olan minikanalı belirlemektir. R134a soğutkanıyla yürütülen iki fazlı akış deneyleri sırasıyla 1.69, 3.85 and 1.69 mm hidrolik çaplara sahip olan minikanallarda yapılmıştır. Diğerlerinden farklı olarak üçüncü minikanal pürüzlü iç yüzeye sahiptir. Üç minikanalın deneysel sonuçların karşılaştırlması sabit kütle akıları ve kuruluk derecelerinde zorlanmış konveksiyon ısı transfer katsayısı ve basınç düşümüne göre yapılmıştır. Deneylerin sonucunda test edilen minikanallar arasından buzdolaplarındaki evaporatör uygulamaları için en uygun minikanal tespit edilmiştir.

Anahtar kelimeler: Minikanallar, zorlanmış konveksiyonla ısı transferi, basınç düşmesi, soğutkan, R134a, iki fazlı akış, deneysel çalışma.

To My Parents

ACKNOWLEDGEMENTS

The author wants to express his sincere gratitude and appreciation to his supervisor Assoc. Prof. Dr. Almıla G. Yazıcıoğlu for her guidance, advices, constructive criticism, encouragements and perception throughout the research.

The author would also like to thank Dr. Hüsnü Kerpiççi, Mr. Aydın Çelik and Mr. Bilgehan Tekin for their support, suggestions and comments.

The technical assistance of Mr. Mustafa Yalçın and Mr. Fikri Çavuşoğlu are gratefully acknowledged.

This study was supported by The Scientific and Technological Research Council of Turkey (TÜBİTAK) Project No. 107M504, in which Arçelik provided technical and informative support as a project partner.

TABLE OF CONTENTS

LIST OF TABLES

LIST OF FIGURES

LIST OF SYMBOLS

A ..... surface area of the minichannels, m^2
Al ..... Aluminum
C ..... specific heat, kJ/kgK
d ..... diameter, m
D_h ..... hydraulic diameter, m
DP ..... differential pressure, bar
G ..... mass flux, kg/m^2s
$\bar{h}$ ..... average convective heat transfer coefficient of R134a, W/m^2K
h ..... enthalpy, kJ/kg
H ..... height, m
I ..... current, mA
j_g^* ..... non-dimensional mass flux
k ..... thermal conductivity, W/mK
L ..... length of the test section, m
$\dot{m}$ ..... mass flow rate, kg/s
P ..... pressure, Pa
P_h ..... heated perimeter, m
$\dot{Q}$ ..... heat transfer rate, W
Re ..... Reynolds Number
T ..... temperature, K
t ..... thickness, m
u ..... velocity, m/s
U ..... overall heat transfer coefficient, W/m^2K
$\dot{V}$ ..... volumetric flow rate, m^3/s
v ..... specific volume, kg/m^3
V ..... voltage input, Volt
w ..... width, m
X_{tt} ..... Lockhart-Martinelli parameter
x ..... quality

Greek letters

Δ.....difference

μ .....dynamic viscosity

ρ .....density

Subscripts

Al .....aluminum

c .....cross sectional

ch .....channel

ent ..... entered

he ..... pre-heater exit

hi ..... pre-heater inlet

i .....channel inner

ins..... insulation

inp .....insulation pipe

l .....liquid

LM ..... logarithmic mean

m ..... mean

R.....refrigerant

re .....refrigerant test exit

ri .....refrigerant test inlet

RI..... input to refrigerant

si.....shell inner

so .....shell outer

TP.....two-phase

v ..... vapor

V.....viscous heating

w..... test section wall

W..... water

W,loss.....water side loss to the surroundings

w,mean.....water mean

we..... water test exit

wi..... water test inlet

CHAPTER 1

INTRODUCTION

1.1 MICRO- AND MINICHANNEL HEAT TRANSFER

Nowadays the need for energy increases with developing technologies. The careful use of energy sources and efficiency issues in the transport of energy become more important issues. Heat transfer, being one of the major subjects in the area of energy, appears in our daily life and industrial applications frequently. One of the most common areas, in which heat transfer takes place, is cooling; in both industrial applications and household devices, such as refrigerators and air conditioners. For example, it is estimated that the energy consumption by refrigerators was approximately 13.7% in 2001 of the total domestic energy consumption in the USA [1]. In cooling systems and especially in refrigerators, evaporators with pipes are used. Evaporators in conventional refrigerators are produced by wrapping around a shell, which has a rectangular cross-section and formed by bending metal plates, with pipes. Heat transfer occurs with the help of natural convection.

Microtube and microchannel applications have started being used in many industries because of their compactness and the higher heat transfer coefficients they provide. Developments in manufacturing techniques cause microchannel applications to be applied in different sectors. In recent years, especially in heat exchangers used in automotive and air conditioner technology, microchannel applications appear more frequently. In automotive and air conditioner systems, mass flow rates are quite high. As a result, distributors and collectors are needed for a uniform distribution of the fluid used. In literature there are many studies on the design of distributors and collectors for microchannel applications. In

refrigerators, on the other hand, mass flow rates are much less than those in industrial cooling and air conditioning systems. Therefore, to prepare microchannel heat exchangers for refrigerators, there is no need to design a distributor or a collector; microchannels can be used in conventional and no-frost refrigerators, and evaporators with increased efficiencies can be designed.

Increase in performance of refrigerator cooling cycle provided by means of microchannel application in refrigerators decreases energy consumption of refrigerator. If it is thought that 2 million refrigerators are sold domestically, in the case of decrease in energy consumption about 10% with the help of microchannel application in aforementioned refrigerators annual average energy saving would be about 100 million kWh. This provides a saving about 0.63% of energy production of Keban Dam which generated 6.3 billion kWh [2]. Due to microchannel applications decrease in sizes of evaporators used provides an important increase in volume in refrigerators. Volume increase which is provided in refrigerators is an indicator increasing rivalry for refrigerator producer firms. Other than this, works done in this study serve to produce more compact and economic evaporators. Thus usage of cheaper evaporators having same efficiencies would be possible.

1.2 LITERATURE REVIEW

The issue of heat transfer in small scales is a relatively new area which attracts attention of researchers. When sizes are getting smaller, some different classification methods are suggested for tubes and channels. The most common method is the one suggested by Kandlikar [3]. In his definition, which classifies small tubes and channels according to their hydraulic diameters (D_h), the channels having hydraulic diameters larger than 3 mm are conventional (macro) channels, the ones with hydraulic diameters between 3 mm and 200 μm are called as minichannels, and if their hydraulic diameters are between 200 μm and 10 μm, they are called as microchannels. Although the Kandlikar's definition is the most common definition used to classify tubes and channels, it is known that there are also different definitions used for the same purpose and in some studies in literature and especially in industry there is a tendency to call the

channels in small sizes as microchannels. In this study, channel classification is made according to the Kandlikar's definition. While mentioning the studies which information is given about here, the channel categorizations made by the authors were not changed for the channels.

In the last 30 years many researches have been carried about the heat transfer in micro- and minichannels. The studies started with the purpose of CPU cooling in computers. The results of these studies led to many researches on this issue and heat transfer subject in micro- and minichannel has become quite widespread. Many studies were made on this issue by investigating micro- and minichannels for different flow conditions, fluid types, channel geometries and boundary conditions applied on them in terms of heat transfer coefficient and pressure drop. The study on cooling a chip exposed to high heat fluxes, up to 790 W/cm^2 with silicon wafer microchannel including laminar water flow, made by Tuckerman and Pease [4] in 1981 became the pioneer of the next studies on this area. In this study despite so high heat flux, the temperature of the chip could be kept under 110˚C. With this study importance of small scale channel for heat removal applications was showed up clearly. The article published by Kew and Cornwell [5] in 1997 showed that the correlations proposed until that year for the prediction of boiling heat transfer in the channels did not estimate the results in the channels having smaller diameters well by making flow boiling experiments with R141b in 500 mm long tubes whose diameters were 1.39 and 3.69 mm. Their study exhibited the need of more research on flow boiling heat transfer in narrow channels. Recently many important studies made with small scale channels are in the literature. Some of the investigated studies are presented in this section.

In 1998, Yan and Lin [6] conducted some experiments with R134a in a circular pipe whose diameter is 2 mm by using constant heat flux approach on the pipe. They investigated evaporation heat transfer and pressure drop. The results of the experiments showed that compared to the results obtained for the pipes with larger diameters, the pipe having smaller diameter caused 30-80% higher evaporation heat transfer coefficients and also it was observed that in the small pipe higher pressure drop occurs for the same amount of mass flux and heat flux

increases. As a result of their experiments they proposed evaporation heat transfer and friction factor correlations.

Yang and Shieh [7] studied experimentally on two-phase flow patterns for refrigerant R134a and air-water in the horizontally placed tubes having inner diameters of 1.0, 2.0 and 3.0 mm. Flow regime transitions were very sharp and clear in the experiments for R134a while not for water-air mixture. The results of the experiments with air-water were consistent with the correlations in the literature and transition slug to annular flow occurs depending on air mass velocity but not water mass velocity as stated in the literature. On the other hand the experiments made with R134a showed that in the smaller tube the transition from bubble to slug flow is affected by the refrigerant properties. Additionally, R134a flow caused bubble flow later than air-water flow due to its lower surface tension property. None of the flow patterns examined for comparison in the literature was not in a good consistency with the flows occurring in small tubes for both fluids.

For the purpose of investigation of thermohydrodynamic properties of two-phase capillary flow at the meniscus, two-phase laminar flow was examined for a heated microchannel by Yarin et al. [8]. Formulation of flow in a heated microchannel was carried out by using mass, momentum and energy equations for both phases and also balance conditions at the interphase. The flow problem in a heated microchannel was solved numerically by them. The authors proposed the classification of the flow regimes. They exhibited two stable states occurring because of dominancy of gravity and friction forces for meniscus. Also they proposed optimum microchannel diameter and length for the specified paramaters.

Agostini and Bontemps [9] made flow boiling experiments in mini-channels with refrigerant R134a. The mini-channel used in the experiments was made up of aluminum and had 11 parallel rectangular channels whose dimensions are 3.28 mm x 1.47 mm. Its hydraulic diameter was 2.01 mm. During the experiments mass fluxes changed in the range of 90-295 kg/m^2s, heat fluxes varied between 6.0 and 31.6 kW/m^2 while the working pressures were 405 and 608 kPa. Higher

heat transfer coefficients were obtained than the recorded ones for the conventional channels in the literature. Dry-out occurring at higher qualities than 0.4 caused decrease performance. This situation is compatible with the information about dry-out forming at medium qualities in mini-channels in the literature. Nucleate boiling was the dominant heat transfer mechanism for the heat fluxes higher than 14 kW/m^2 as stated in the study of Tran et al in 1997.

Harirchian and Garimella [10] investigated the effects of channel size, mass flux and heat flux on microchannel flow boiling regimes by conducting experiments with Flurinert FC-77. During mass fluxes varied between 225 and 1420 kg/m^2s. The flow boiling regimes (bubbly, slug, churn, wispy-annular, and annular flow) were observed with the help of high-speed photography. The widths of the six tested minichannels were between 100 and 5850 μm. Their depths were 400 μm. Instantaneous heat transfer coefficients could be found by means of visualization. The dominant heat transfer mechanism was nucleate boiling in the minichannels having width 400 μm and higher up to very high heat fluxes. In the channels having width less than 400 μm, lower heat fluxes made bubble nucleation at the walls suppress. Increase in the channel width caused replacement of bubbly flow with slug flow, intermittent churn/wispy-annular flow with intermittent churn/annular flow. As mass flux increases, the smaller and more elongated bubbles in the bubbly region, thinner liquid layer thickness in wispy-annular and annular regimes occurred. Comparison of the flow regimes observed in the experiments with those the literature showed that the flow regimes developing in microchannels cannot be estimated well by using the boiling regime predictions developed for large channels.

Cavalini et al. [11] set up a test apparatus to investigate heat transfer and fluid flow in single minichannels. In the single phase and flow boiling experiments R134a and R32 were used in the minitube having an inner diameter of 0.96 mm and rough surface. All experiments showed the surface roughness affect pressure losses in the case of turbulent single-phase flow and the two-phase flow in the minitube. The modals for predicting pressure losses in the single phase flow through channels gave satisfactory results and pressure drops in two-phase

flow in the minitube were estimated well by using the correlation proposed by Cavallini et al. with a simple modification.

Consolini and Thome [12] investigated flow boiling heat transfer in the micro-channels having diameters of 510 and 790 μm for R-134a, R-236fa and R-245fa. In the experiments mass velocities changed in the range of 300-2000 kg/m^{2}s, maximum heat flux was 200 kW/m^2. The experimental results showed that the heat transfer coefficients obtained for R-134a and R-236fa were dependent on heat flux and fluid properties in whole qualities. However the heat transfer coefficients in the experiments made for R-245fa were independent on heat flux in high qualities.

In et al. [13] carried out flow boiling experiments in a single circular stainless steel (Stainless steel 316) micro-channel with an inner diameter of 0.19 mm by using R123 and R134a. During the experiments heat fluxes were 10, 15 and 20 kW/m^2 and mass velocities were 314, 392 and 470 kg/m^{2}s. The vapor qualities occurred between 0.2 and 0.85. 158 and 208 kPa for R123, 900 and 1100 kPa for R134a were the saturation pressures. The experiments showed that the heat transfer coefficients of R123 were depended on mass velocity, heat flux and quality while the ones of R134a were dependent heat flux and saturation pressure except at high qualities. These results obtained for R134a is similar with the results of macro-channels in the literature. Therefore it was concluded that in the heat transfer for R123 evaporation of thin liquid film around bubbles played a significant role because of early suppression of nucleate boiling at low qualities, on the contrary in the heat transfer of R134a, nucleate boiling was the dominant mechanism till it was suppressed at high qualities then two-phase forced convection took its place. The correlations used for comparison were not consistent with the experimental results.

Ong and Thome [14] conducted flow boiling experiments by using R134a, R236fa and R245fa. The experiments were made in a 1.030 mm stainless steel (AISI 304) channel. In the experiments mass flux were in the range of 200-1600 kg/m^{2}s, heat fluxes were in the range of 2.3-250 kW/m^{2}s while saturation temperature was kept at 31˚C. The experimental results showed that heat

transfer coefficients were dependent on heat flux at low qualities while at higher qualities convective boiling was dominant heat transfer mechanism for all tested fluids. Among the tested fluids, the highest heat transfer coefficients were observed for R134a. Heat transfer was dependent on mass flux in the experiments with R134a and R236fa so it was said that increase in mass flux causes early inception of annular flow at lower qualities.

Li and Wu [15] proposed a general criterion by evaluating experimental results of saturated-flow boiling heat transfer in micro/mini-channels for both multi- and single-channel configurations in the literature. They investigated the respective accuracies of seven correlations by using the database including 4228 data points. It was concluded that none of the seven correlations satisfy the experimental data in wide ranges. The conventional to micro/mini criterion suggested by the authors were designated in terms of Bond and Reynolds number.

Kaew-on et al. [16] studied experimentally in a very similar way with the current study. Two different multiport minichannels were used in two-phase flow experiments. Firstly a counter flow-in-tube heat exchanger was designed to make these experiments using R134a flow through inner channel. The material of the minichannels was aluminum and the shell was constructed from a circular acrylic tube having a hydraulic diameter of 25.4 mm. One of the minichannels had a hydraulic diameter of 1.1 mm and 14 ports. Another one's hydraulic diameter was 1.2 mm and it had 8 ports. During the experiments mass flux varied between 300 and 800 kg/m^2s, heat fluxes which are between 15 and 65 kW/m^2 occurred in the saturation pressures changing between 4 and 6 bars. The boiling curves obtained by using the experimental data showed that nucleate boiling occurs along the minichannels, so increase in heat flux causes increase in the average heat transfer coefficients as being independent of mass flux. Also decrease in channel numbers from 14 to 8 resulted in an increase in the heat transfer coefficients by 50-70%. The authors showed consistency of the experimental results by comparing the results with the nine correlations proposed in the literature. The same authors published another article [17] investigating the pressure drop properties of the same minichannels. The experiments made for

pressure drop investigation were conducted at mass fluxes between 350 and 980 kg/m^{2}s, heat fluxes between 18 and 80 kW/m^2. During the experiments saturation pressure kept at 4, 5 and 6 bar. Also the inlet quality was 0.05 in the experiments. According to the results of the experiments, mass flux affects frictional pressure drop significantly. But compared with mass flux, increase in pressure drop with increasing heat flux was very slight. Also saturation pressure increase had a decreasing effect on the frictional pressure drop. The experimental results were again compared with the nine correlations proposed in the literature, and three correlations gave the satisfactorily close results to the experimental results.

Dall'Olio et al. [18] constructed a test device providing making flow visualization of R134a while flowing through the glass tube having a diameter of 4 mm and placed horizontally. The outer surface of the glass tube was covered by eight heaters which provided heat fluxes between 200 and 45000 W/m^2 along 320 mm length of the tube during the experiments. The experiments were conducted with mass fluxes between 20 and 122 kg/m^{2}s and saturation temperatures between 20 and 25˚C. The experiments were carried out for identifying the flow pattern inside the tube. The experimental results showed that other than the mass flux and the quality, also bubble coalescence and gravity affect the flow pattern appearance.

Ali et al. [19] investigated dryout characteristics of two-phase flow with R134a in vertical circular minichannels. They used minichannels having diameters of 1.22 and 1.70 mm with a length of 220 mm. The fluid flowing through the miichannels were R134a and during the experiments mass fluxes between 50 and 600 kg/m^{2}s and saturation temperatures between 27 and 32˚C occurred. The results of the experiments showed that there is a directly proportional relation between dryout heat flux and mass flux while increase in tube diameter causes decrease in dryout heat flux. Dryout started in the range of quality of 0.55-0.7 while quality fully dryout occurred changed with mass flux. Also any effect of system pressure was not observed. Finally when the experimental results were compared with some correlations in the literature, except one of the correlations used for comparison all showed good consistency with the experimental results.

Mahmoud et al. [20] made experiments to observe the surface effects on flow boiling heat transfer characteristics by using R134a in two microtubes. One of the microtubes was seamless cold drawn stainless steel with an inner diameter of 1.1 mm, another one was welded stainless steel with an inner diameter of 1.16 mm. Their heated lengths are same and 150 mm. and both of them were placed vertically. The experiments were made in a system pressure of 8 bars with mass flux of 300 kg/m^{2}s. At the inlet of the microtubes the fluid was in a sub-cooled state about 5 K and at the exit it reached up to a quality of 0.9. The experiments showed that nucleate boiling was the dominant mechanism for heat transfer in the seamless tube while a clear dominant mechanism was not observed in the welded tube. It had nucleate boiling only along some short lengths so it was understood that heat transfer coefficient is not uniform along the welded minitube although its inner surface seemed too smooth.

Costa-Patry et al. [21] studied on investigation of pressure drop characteristics of a silicon multi-microchannel evaporator. The evaporator consisted of 135 microchannels having width of 85 μm, height of 560 μm and length of 12.7 mm. The hydraulic diameter of it was 148 μm. The microchannels were separated by 46 μm wide fins. As working fluids, R236fa and R245fa were used. During the experiments mass flux varied between 499 and 1100 kg/m^{2}s, variation of heat flux was from 130 to 1400 kW/m^2. 30% of the total pressure drop occurred at the outlet of the minichannels so they were not neglected. The pressure drop measurements matched the predicted results by using Cioncolini et al. Pressure drop measurements showed almost linearly increase with increasing quality along the microchannels. R245fa had a larger pressure drops because of its higher density. In the second part of their study Costa-Patry et al. made experiments on the same evaporator to investigate its heat transfer specifications. This time there were 35 local heaters and temperatures were measured in a 5 x 7 array. Heat transfer coefficients occurred in the range of 5000-20000 W/m^{2}K for both fluids. At low heat fluxes heat transfer coefficients were not dependent on quality. For the heat fluxes higher than 45 kW/m^2, the heat transfer coefficients obtained in the experiments firstly decreased until bubbles were coalesced, then increased after annular flow region occurred.

Padovan et al. [22] made experiments with a 1400 mm long microfin copper tube by using R134a and R410A as refrigerant. The microfin tube having inner diameter of 7.69 mm had 0.23 mm high 60 fins. For the experiments the microfin tube was placed in a counter flow heat exchanger. During experiments saturation temperatures were between 30 and 40˚C, mass fluxes were between 80 and 600 kg/m^{2}s. Also reduced pressures were measured as between 0.19 and 0.49. Experimental results showed that when saturation temperature was 30˚C nucleate boiling and convective evaporation had an effect on heat transfer coefficient but when it was 40˚C, nucleate boiling caused an increase in heat transfer coefficient only at low quality. Heat transfer coefficient increased up to 200 kg/m^{2}s mass flux then showed a decrease. Heat transfer coefficients obtained for the microfin tube are higher than that in plain tube and dry-out starts at higher qualities. Also the results showed that mss flux increases cause shifting dry-out inception to higher qualities. Additionally comparison of the experimental results showed good compatibility with the results obtained by the correlations in the literature.

Maqbool et al. [23] investigated flow boiling heat transfer of ammonia in circular vertical mini channels which were made up of stainless steel (AISI 316) experimentally. The 245 mm long mini channels had internal diameters of 1.70 mm and 1.224 mm. Along their total length they were heated. In the experiments mass fluxes were changed between 100 and 500 kg/m^{2}s, heat fluxes were between 15 and 355 kW/m^2 while saturation temperatures were 23, 33 and 43 ˚C. The heat transfer coefficients obtained in the mini tube having 1.70 mm diameter and in the lower qualities of the mini tube having 1.224 mm diameter showed independency with mass flux and quality while they were dependent on heat flux. On the contrary the heat transfer coefficients were dependent on mass flux and quality and independent on heat flux at the higher qualities of 1.224 mm mini tube. The heat transfer coefficients were obtained in the experiments of the mini tube with lower diameter. Also higher heat transfer coefficients were obtained at higher saturation pressures at lower qualities while saturation pressure had no effect at higher qualities. In the comparison of the results with the correlations in the literature it was observed that the Copper's correlation is the most compatible correlation with the experimental results.

Copetti et al. [24] examined flow boiling of R134a in a horizontal tube having a inner diameter 2.6 mm experimentally. During the experiments heat flux varied between 10 and 100 kW/m^2, mass flux changed in the range of 240-930 kg/m^{2}s while saturation temperatures were 12 and 22˚C. They observed the significant heat flux effect in the heat transfer coefficient in the low qualities and the effect of mass velocity in the pressure drop. Also the mass flux had an effect in the heat transfer coefficient at low heat fluxes. The frictional pressure drop increased together with mass velocity and quality. When the experimental results were compared with the results obtained from the correlations in the literature, the correlations of Kandlikar and Balasubramanian were the best fitted ones but the statistical deviations were very large with respect to the desired accuracy value.

The studies investigated above lead to the conclusions below:

Saturation pressure has a very slight effect on heat transfer in flow boiling. Although some studies showed some increase in heat transfer coefficient with increasing saturation pressure, the general opinion on saturation pressure effect is that it has a negligible effect on heat transfer coefficient in flow boiling. Moreover in several studies it is mentioned that saturation pressure has an effect on heat transfer coefficient only at low qualities.

In many studies in the literature it is explained that for microchannels two phase flows with low qualities has an advantage in terms of heat transfer. But for high qualities, an increase in quality causes either a continuous increase or an increase up to a maximum (around a quality in the range of 20-50%), then a decrease in heat transfer coefficient. It should be considered that the experimental studies which concluded with this result may have experimental errors.

Some researchers propose some correlations at the end of their experimental or numerical studies. These correlations have a big significance in terms of constituting a database, making comparisons, and leading new researches. The correlations proposed are valid for their own experimental conditions.

Some studies emphasize the difficulty of obtaining high qualities.

When compared with liquid flows, it is observed that two-phase flows have higher pressure drops.

Especially in experimental studies constant heat flux boundary condition is mostly preferred rather than constant wall temperature boundary condition due to its easy applicability.

For all the fluids investigated, two-phase flow heat transfer coefficients are higher than those in single phase flow.

Some other points faced in the literature related to the current study are dry-out problems, horizontal or vertical placement of the channels, and need of high heat flux for obtaining high qualities.

1.3 MOTIVATION AND OBJECTIVES

Single phase laminar flow through a circular pipe is well known because it can be solved analytically. But this situation is not valid for two-phase flow. The studies in literature show that two-phase flow analyses are focused on numerical and experimental studies to build up a database and form an infrastructure in this area.

The main purpose of this study is to determine the most suitable minichannel for refrigerator applications among the three minichannels with different geometries, by comparing them experimentally for their two-phase flow heat transfer and pressure drop performance [25]. This study is a part of the TUBITAK 107M504 Project supported technically by Arçelik Inc. At the end of the project, determination and suggestion of the most suitable one among the three minichannels investigated for Arçelik Inc. are aimed. The technical drawings of the cross sectional views of these minichannels drawn in the same scale are given in Figure 1. The dimensions stated in Figure 1 are millimeters (mm). As it is seen the second minichannel is the larger channel with respect to the others and

the third minichannel has a rough inner surface. Respectively, 1st, 2nd and 3rd minichannels have 7, 5 and 7 ports.

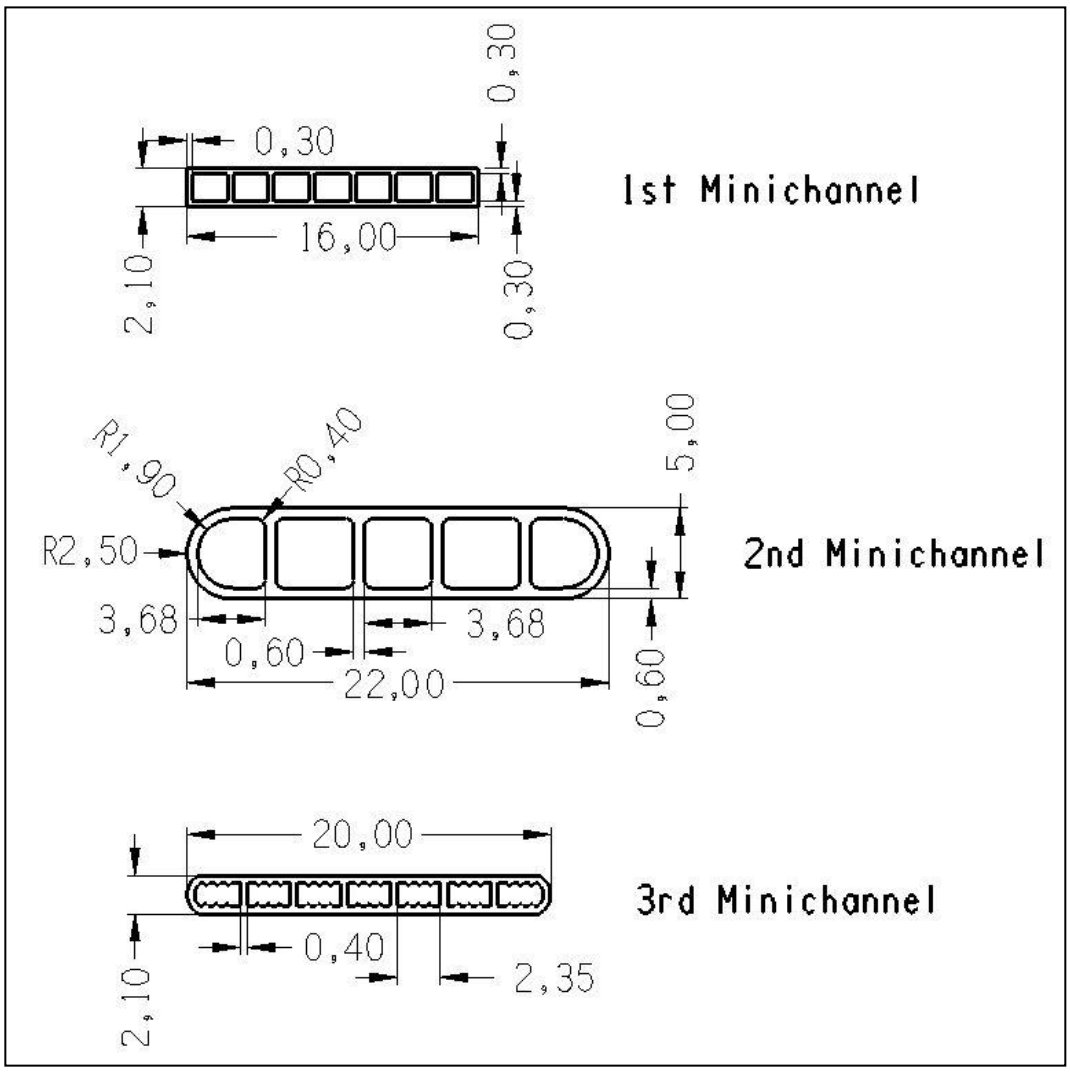

Figure 1: Technical drawings of the tested minichannels

In scope of the project, firstly an experimental setup was constructed and two-phase flow experiments were conducted with a 1.65 mm diameter copper minitube to verify the experimental setup by comparing its results with ones in literature before two-phase flow experiments with the minichannels. Construction of the experimental setup and verification of the setup by two-phase flow experiments with the minitube were realized by another graduate student,

Bilgehan Tekin [26]. Some brief information about his study is given in the following sections.

Literature review given in the previous section shows that the subject of forced convective heat transfer in two-phase refrigerant flow in micro and minichannels attract very much attention. However the contradictory and inadequate results which were come across frequently in these studies bring up the need for more research in this area. Therefore nowadays experimental, numerical and theoretical studies in this area are carried on and especially experimental studies lead numerical and theoretical studies; so for this study experimental studies are very valuable.

There are two approaches in modeling boundary conditions in experimental studies on microchannel heat transfer: Constant wall temperature and constant wall heat flux. Literature analysis shows that especially experimental studies head towards constant wall heat flux boundary condition predominantly. The main reason of this is the easiness of providing the constant wall heat flux boundary condition. On the other hand, the case faced in refrigerators (evaporators) is closer to a constant wall temperature boundary condition; so making experimental studies with this boundary condition is needed.

The investigations show that two-phase flow experimental studies were conducted generally at high refrigerant saturation pressures. The reason of this is that at room temperature, most refrigerants have high saturation pressures (6-7 bars) and experiments are made at room temperature. On the other hand refrigerants in refrigerators work at smaller saturation temperatures and pressures.

Lastly, a big part of the studies made so far were realized with higher flow rates than the ones used in refrigerators. Thus the results are not able to be used in the researches intended for refrigerator efficiently. However, in domestic refrigerators, refrigerant flow rates are about 1 g/s. Thus, making experiments at low flow rates are also important and necessary.

The factors summarized above constitute the motivation of the current study and form its purpose. If it is summarized one more time, the purpose of the current study is to compare three minichannels having different geometries by making two-phase flow experiments with the refrigerant (R134a) on the experimental setup verified by the experiments conducted with the circular minitube before this study and to determine the most suitable minichannel for use in the evaporators of the refrigerators by investigating the experimental results in terms of heat transfer and pressure drop performances.

In the following chapter, the experimental setup which was constructed for two-phase refrigerant flow tests by Tekin [26], and the modifications and calibrations made on the set-up for minichannel experiments are explained under the title “Experimental Set-up”. Chapter 3, titled “Two-phase Flow Experiments” includes the procedure followed, conditions, analyses and calculations related with the two-phase flow experiments conducted with the three minichannels. The experimental data collected during the two-phase flow experiments for the three minichannels, the results obtained with the help of the experimental data and discussions related with the experimental results are examined in Chapter 4. Finally in Chapter 5, titled “Summary, Conclusions and Future Work”, the thesis is concluded by giving a summary, comments on the conclusions and suggestions for possible future work.

CHAPTER 2

EXPERIMENTAL SET-UP

Towards the aim of this study two-phase flow experiments with the minichannels produced by Arçelik Inc. were conducted on the experimental set-up which was also used in two-phase flow experiments with the minitube before this study. Before the experiments with minichannels started, the experimental set-up was modified for the minichannel experiments and some calibrations for some devices of the set-up were carried out. In this section the previous work made before this study by Tekin [26] is introduced briefly. Also the modifications and calibrations which were made after his study are explained.

2.1 PREVIOUS WORK

2.1.1 Experimental Set-up Used in Minitube Experiments

As mentioned in the Introduction part, before two-phase flow experiments with the minichannels which are wanted to be investigated, an experimental set-up has been constructed and verification of the set-up has been realized using a 1.65 mm copper minitube by Bilgehan Tekin [26]. In this section the experimental set-up used for two-phase flow experiments in the copper minitube is explained briefly. This experimental set-up was used in two-phase flow experiments with the three minichannels by making some modifications on it.

2.1.1.1 Equipment

In this study to investigate the minichannels for use in evaporators of refrigerators, the condition which the evaporators have, constant wall temperature boundary condition, was tried to apply on the minichannels. Constant wall boundary condition was provided by using a concentric counter flow heat exchanger in the test section. Therefore two cycles were used in the set-up. These cycles are refrigerant (R134a) and water (water + ethylene glycol mixture) cycles.

To collect data in different experiment conditions, the states of the fluid used in the cycles are needed to be determined and arranged. So, two refrigerated circulating baths were used in these two cycles to condition the fluids by setting their temperatures. The refrigerated cooling bath used in the refrigeration cycle in the experimental setup is shown in Figure 2. Also in the water cycle the cooling bath having the same properties were used.

Figure 2: The refrigerated cooling bath used in the refrigerated cycle

For circulating the fluids in both cycles pumps were used in the set-up. These pumps provide the constant pressure and almost constant flow rates with very low oscillations at steady-state conditions. The water pump has a power of 373 Watts and can work with higher flow rates with respect to the refrigerant gear pump. The micro gear pump in the refrigerant cycle can work with low flow rates and its working speed can be controlled manually. The pumps used in the refrigerant and water cycle can be seen in Figure 3 and 4.

Figure 3: The micro gear pump used in the refrigerant cycle

Figure 4: The pump used in the water cycle

For data analyses and calculations some parameters are needed to be measured on the system. One of these parameters is flow rate. To determine the flow rate of the refrigerant, a micro flowmeter was used in the refrigerant cycle. In the water cycle, two rotameters were used instead of flowmeters because of liquid flow to arrange and measure the flow rates of the water and ethylene glycol mixture in the water cycle. The micro flowmeter in the refrigerant cycle is able to measure relatively low flow rates. The reason of use of this micro flowmeter in the refrigerant cycle is that to create conditions similar with those in evaporators, low flow rates are provided during the experiments in the refrigerant cycle. On the other hand, in water cycle low flow rates are not desirable property to approach constant wall temperature on the outer surface of the tested channels.

The test section is between the R134a cooling bath and the pre-heater. In the test section the refrigerant flows through the copper minitube. The test section includes a counter flow heat exchanger. The copper minitube was placed at the center of an aluminum shell designed for letting the water and ethylene glycol mixture flow around the minitube in the counter direction with respect to refrigerant flow inside the minitube. Around the shell to prevent the heat losses from the water side to the ambient there was an insulation material. There are two RTDs at the inlet and the outlet of the test section to know the temperature of the refrigerant at these points. For investigation of the pressure drop performance of the copper minitube a differential pressure transducer which measures the pressure drop between the inlet and exit of the test section was used. In Figure 5 the test section without the insulation material around the shell can be observed.

Just before the test section to determine the quality of the refrigerant, an electrical resistance heater with a maximum power of 150W was used by wrapping it around the copper tube before the test section as a pre-heater. Also a control box was used to control the pre-heater power. This control box was designed to control the power of the pre-heater manually or automatically. But due to not having a multiplexer card providing automatic control, during two-phase flow experiments with the copper minitube the pre-heater was used only manually. Also, a power transducer was used to take the power inputs from the pre-heater and to show the power value supplied by the pre-heater on the

computer. The pre-heater wrapped around the copper tube before the test section, the pre-heater and the power transducer can be seen in Figure 6.

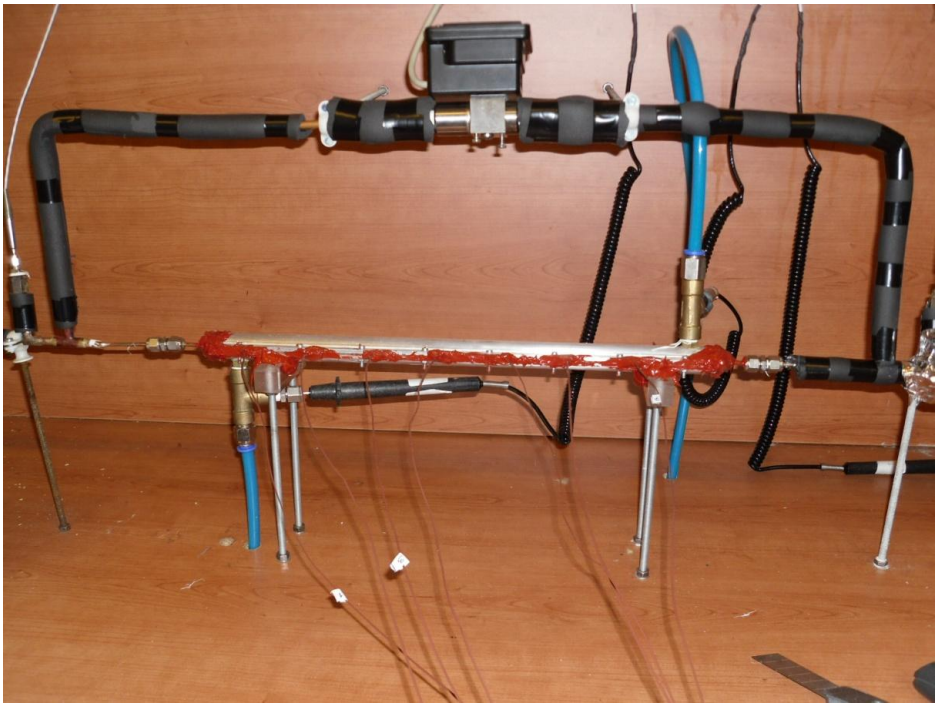

Figure 5: The test section with the copper minitube without the insulation around the shell

Figure 6: The pre-heater without the insulation, the control box and the power transducer

To determine the properties of the fluids in both cycles in the different sections of the experimental set-up, temperatures were measured by using RTD (Resistance Temperature Detector) probes and thermocouples. There were two types of RTD probes; thinner probe RTDs (having a diameter of 1.8 mm) and thicker probe RTDs (having a diameter of 2.36 mm). Thinner ones are more sensitive and take more accurate measurements so they were used in more critical locations on the set-up. These critical locations are inlet and outlet of the test section in the refrigerant side and the point near the flowmeter where obtaining fully liquid state is necessary. Thicker probe RTDs were used at the inlet and outlet of the test section in the water side and also at the exit of the cooling bath in the refrigerant cycle. Besides RTD probes, to measure the temperatures from the surfaces at different locations thermocouples were used. The most critical location which thermocouples were used on the set-up is the surface of the minitube tested in the test section. Totally 7 thermocouples were placed on the outer surface of the minitube to measure the outer surface temperature of the minitube. Moreover connector plugs were used to prevent shortening the length of the thermocouples when they were needed to cut to change their location.

Another parameter needed to determine in the system is pressure. Measurement of the system pressure was made by an identical pressure transducer in the each cycle. Additionally to determine the pressure drop in the refrigerant side along the minitube in the test section, a differential pressure transducer was used.

The voltage input needed by the pressure transducers was provided by a DC Power Supply.

Along the refrigerant cycle, copper tubes having an outside diameter of 1/4 inches (6.35 mm) were used for connecting the devices. The material of these tubes is copper because it is suitable for use in high pressure and low temperatures and it is a material not reacting with the refrigerant. Also many connecting parts were used to provide the transition between the devices and copper tubes. For water cycle to connect the devices a pneumatic hose being suitable for working temperature and pressure conditions in water cycle, not reacting with the fluid passing through it and providing an easy connection

between the devices, was used. The outer diameter of this hose was 6 mm and the inner one was 4 mm. Like the connecting parts in the refrigerant cycle, in the water cycle compatible fitting parts were used between the devices and the hose. To arrange the properties of the fluid at the particular areas by keeping it in a limited section and to provide the fluid flow through the desired lines, in both cycles the valves were located in different places.

To prevent any possible damages on the gears of the pumps, it is needed to provide the refrigerant in fully liquid phase through the pumps. So to be sure about the state of the refrigerant passing through the pump in the refrigerant cycle, a sight glass was placed before the pump to observe the refrigerant.

To hold all these devices together a structural frame was used. The devices belonging to the refrigerant cycle were placed on the upper part and the devices in the water cycle were placed on the lower part of this structural frame. The test section at which both of the cycles intersect was fixed a place on the upper part. More detailed information about the devices in the experimental set-up can be obtained from the thesis prepared by Tekin [26]. The specifications of the devices used in the experimental set-up can be seen in Appendix A.

2.1.1.2 Data Acquisition

One of the most important sections of this experimental set-up is data acquisition system. By using a data logger which having three slots for data acquisition cards the voltage and current inputs coming from the temperature measurement devices (RTD probes and thermocouples) and pressure measurement devices (identical and differential pressure transducers) are converted to the signals that can read by a computer which is used for collecting the experimental data. During the two-phase flow experiments with the copper minitube only two data acquisition cards were placed to the data logger. Also to gather and save the data in specific time intervals on a computer, HP VEE software programmed by Arçelik Inc. was used. This program collects the data in 15 seconds intervals and saves them in a format which can be read by Microsoft Excel software. The program also draws an instant graph of the temperature and pressure

measurements which are desired to see their change in time and this provides determining when the steady state condition is achieved during the experiments.

2.1.1.3 Refrigerant (R134a) Cycle

In the refrigerant cycle R134a is used as working fluid. To provide fully liquid refrigerant through the pump, the refrigerant is needed to be cooled to turn it to fully liquid phase before the pump. For this cooling process a refrigerated cooling bath is used. Due to being in gas state in the room conditions of the refrigerant R134a, the cooling bath is used by placing the copper tubes shaped like helical coils into the water and ethylene glycol mixture in the cooling bath. The cooling bath cools down the water and ethylene glycol mixture up to a desired temperature and the refrigerant flowing through the copper tubes loses heat and cools down while passing through the section in the cooling bath. The reason of use water and ethylene glycol mixture in the cooling bath is to be able to work at lower temperatures than both the freezing points of water and ethylene glycol. The proportion of the mixture in the refrigerated cooling bath was 66% ethylene glycol and 34% ionized water so the freezing point was decreased to a temperature between -45^{o}C and -50^{o}C.

At the exit of the cooling bath there is an RTD to determine the state of the refrigerant at that point by measuring the temperature of the refrigerant. If the flowing direction of the refrigerant is followed in the refrigerant cycle after the RTD at the exit of the refrigerated cooling bath, an accumulation vessel which helps providing liquid flow in the cycle and a charge valve are encountered. The refrigerant is injected via the charge valve and also when it is wanted the refrigerant can be taken out via the same valve. Because of this function of the charge valve, it can be used to arrange the system pressure inside the refrigerant cycle. To inject the refrigerant into the system any devices are not used like compressor. Injection process is realized by using a hose having an on/off valve between the charge valve and the R134a tank. The R134a tank has a higher pressure than the system pressure in the refrigerant cycle which is wanted to work in when it is full. Therefore by only opening the valve between the R134a tank and the charge valve R134a can be injected into the refrigerant cycle due to

the pressure difference. Being in liquid phase of the refrigerant at that point is important because after that point the refrigerant flows through the pump which can be damaged by a gas flow together with liquid flow passing through it. For the same purpose a sight glass is used to observe the refrigerant phase before the pump. After the sight glass, also before the R134a cooling bath there are on/off valves to cool down the refrigerant only near the cooling bath by closing it when necessary. The section between these two on/off valves in the refrigerant cycle can be seen in Figure 7.

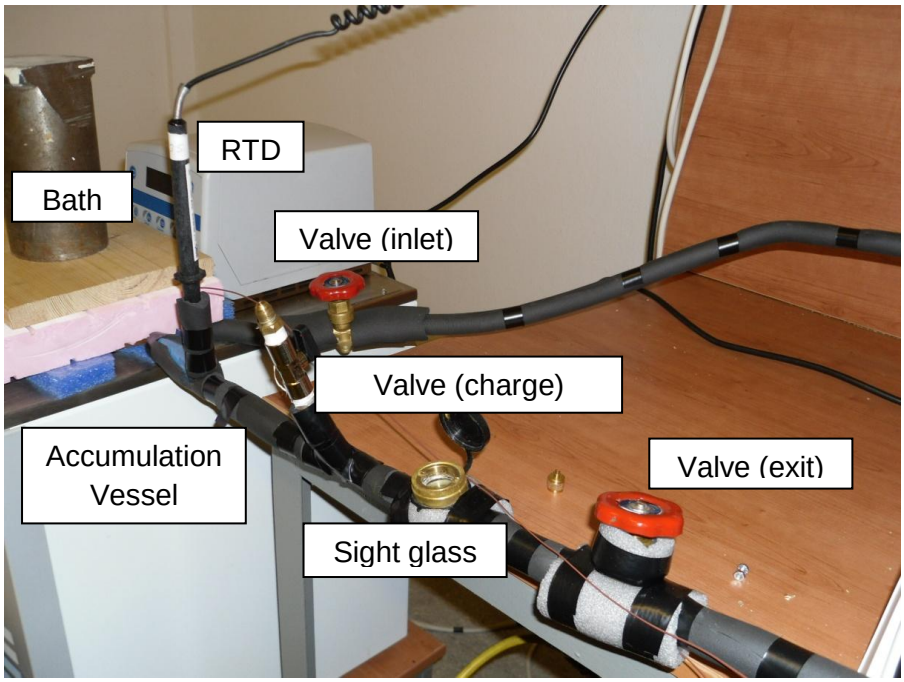

Figure 7: The section around the bath in the refrigerant cycle

Next, in the refrigerant cycle to provide the circulation of the refrigerant there is a pump that can provide the flow rates as low as the ones in refrigerators with very low oscillations. To measure the mass flow rate passing through the refrigerant cycle after the pump, a micro-flowmeter is used. When a gas flow together with liquid flow passes through the micro-flowmeter, it gives an error signal and so to sustain liquid flow through it there is a by-pass line between the inlet and exit of the micro-flowmeter to use it until fully liquid phase is obtained around it in the refrigerant cycle. Totally three valves are used at the inlet and exit of the micro-

flowmeter and the by-pass line to use these two lines preferably. The photo of the flowmeter and by-pass line is given in Figure 8.

Figure 8: The flowmeter and by-pass line

After the micro-flowmeter, before pre-heater there are an identical pressure transducer measuring the system pressure in the refrigerant cycle and an RTD reading the temperature at that point. During the minitube experiments the experimental data were always taken, when the subcooled refrigerant was obtained before the pre-heater. The reason of looking for only subcooled phase before the pre-heater is to be able to determine the enthalpy of the refrigerant at that point by knowing only the pressure and temperature there.

The pre-heater placed before the test section is used to determine the quality at the inlet of the test section. During the minitube experiments the power of the pre-heater was controlled manually by using its control box. The enthalpy of the refrigerant at the inlet of the test section which states the quality at this point is determined by knowing the heat transferred into the refrigerant from the pre-heater as a result of the calibrations made for the pre-heater. The photo of the pre-heater section is shown in Figure 6 in the previous section of the thesis.

To decrease the heat transfer occurring between the refrigerant cycle and the ambient, around the copper pipes connecting the devices along the refrigerant cycle insulation material was wrapped.

2.1.1.4 Water (Water + Ethylene Glycol Mixture) Cycle

In the experimental set-up there is a second cycle other than the refrigerant cycle. In this cycle as working fluid water and ethylene glycol mixture is used but for the simplicity in the thesis the name of this cycle is called as “the water cycle”. Also in the test section “the water side” is the definition used while mentioning the side of the water cycle. Just like the case in the cooling bath in the refrigerant cycle the reason of use of the water and ethylene glycol mixture in the water cycle is to provide working at lower temperatures than the freezing points of the both fluids in the water cycle by decreasing the freezing point up to a level between -35 and -40^{o}C. Water and ethylene glycol was used by mixing one to one in volume bases in the water cycle.

In the water cycle to arrange the temperature of the fluid a cooling bath is used. In the cooling bath the fluid flowing through the cycle is cooled down directly conversely to the case in the R134a cooling bath in the refrigerant cycle. After the cooling bath, there is a water pump circulating the water and ethylene glycol mixture in the cycle. To measure the flow rate in the water cycle a rotameter is used after the pump. The higher flow rates than the ones in the refrigerant cycle were sustained in the water cycle during the minitube experiments to decrease the temperature variation on the surface of the minitube. The flow rates were controlled by using the valve of the rotameter. In the cycle the fluid passing through the rotameter comes to the test section. In the test section the water and ethylene glycol mixture flows in the annular side inside a shell around the minitube. At the inlet and outlet of the test section and at the exit of the water cooling bath there are RTDs to measure the temperatures at these points. The system pressure in the water cycle is measured at the exit of the water pump by an identical pressure transducer.

Additionally there are two by-pass lines exiting from the point after the water pump and entering into the water cooling bath to decrease the pressure in the cycle causing overheating of the water pump. Also in the one of these two by-pass lines a rotameter is used to arrange the pressure in the water cycle and the flow rate going back into the cooling bath by using the valve on it. In the by-pass

line, which does not have the rotameter, a valve was used to deactivate the line when necessary. The photo of the water cycle is given in Figure 9.

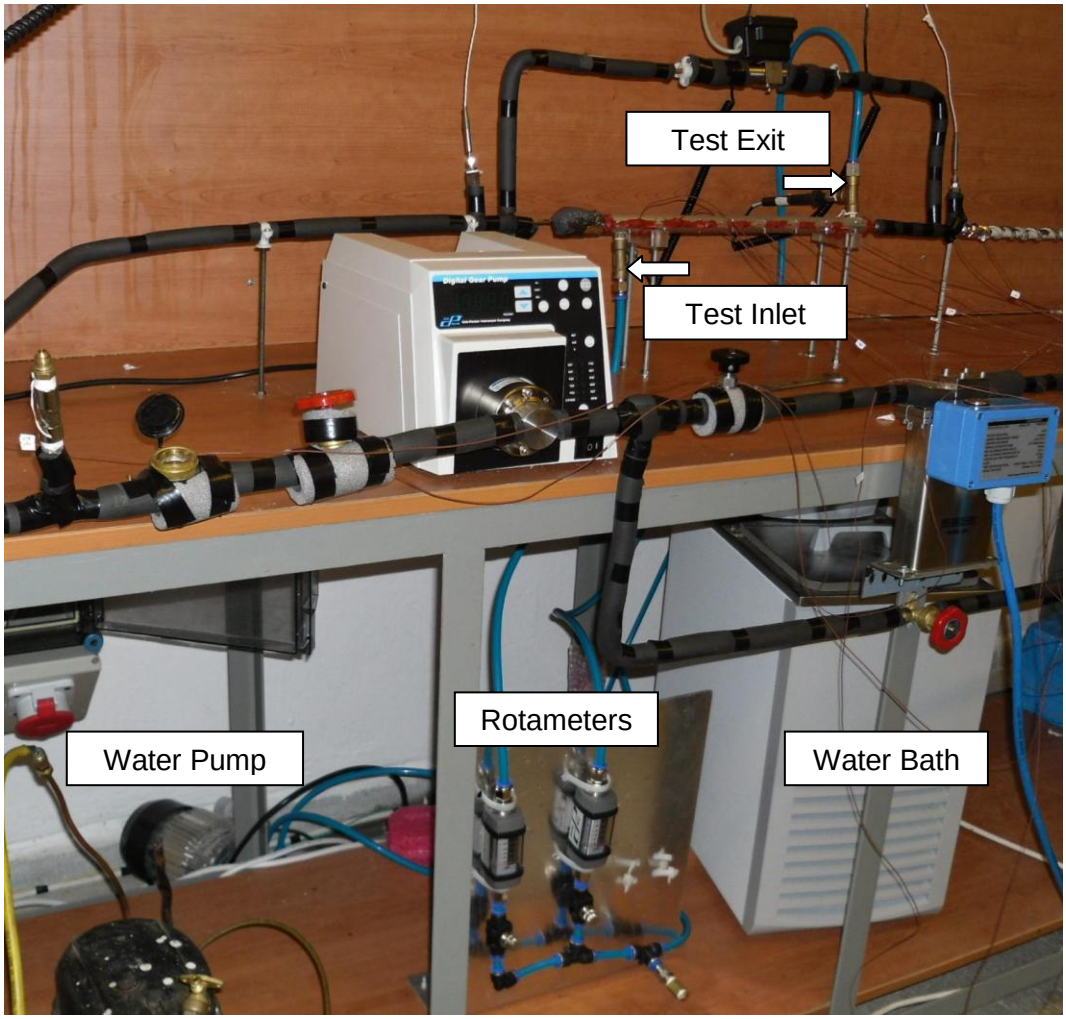

Figure 9: The water cycle

2.1.2 Two-phase Flow Experiments with the Minitube

Before all RTDs, thermocouples, pressure transducers were assembled to the experimental set-up, their calibrations were made by Arçelik Inc. and their calibration curves in their working ranges were entered to the program which provides collecting the data on the computer. Also the mass flowmeter used in the set-up was calibrated by the company that it was purchased from. After all

devices were assembled to the set-up, by giving air into the refrigerant cycle from the charge valve up to 6-7 bars and circulating the water and ethylene glycol mixture in the water cycle with the help of the pump a leakage was looked for. The point where the leakage occurred was determined by the bubble test when any pressure decrease occurred in the refrigerant cycle or by observation if there was a water leakage in the water cycle. After the leakage problem was solved in the experimental set-up, firstly to determine the heat transferred to the refrigerant from the pre-heater, corresponding to the voltage value supplied some single phase experiments were carried. When this calibration process made for the pre-heater was completed, the next process to be done was to determine the heat transferred to the refrigerant side from the water side in the test section. The theoretical calculations made for finding the heat loss from the water side to the ambient showed that the amount of heat transfer occurring between the water side and the ambient even in the maximum temperature difference which was worked during the experiments was only 2.5% of the amount of heat transfer from the water side to the refrigerant side. So the heat transferred through the insulation material around the shell was decided to neglect. Also to be able to determine the heat transferred to the refrigerant side from the water side with less error, viscous heating gaining importance in laminar flows having low speeds and low Re numbers was taken into consideration. Therefore while keeping the temperatures of the refrigerant side, the water side and the ambient equal by observing the measurements of the RTDs and thermocouples, the flow rate of the water side was adjusted to different values and for different Reynolds number (Re) values in the water side different viscous heating values were obtained and a linear graph was acquired. As a result of neglecting the heat loss from the water side and determination of the viscous heating depending on Re in the water side, the heat transferred to the refrigerant from the water side could be calculated. The calibrations made before two-phase flow experiments with the minitube are explained under the title “Calibrations” in detail.

In two-phase flow experiments with the minitube by arranging the temperatures and flow rate of the water cycle, constant wall temperature boundary condition was tried to achieve. Due to importance of the quality in the heat transfer coefficient in two-phase flow, the quality values were calculated at the inlet and

outlet of the test section. To be able to calculate the quality at these points during two-phase flow experiments fully liquid flow was provided around the point just after the micro-flowmeter and before the pre-heater, which the refrigerant temperature was detected at by an RTD. The reason of supplying always fully liquid flow at this point is that by only knowing the temperature and pressure of an fluid at a point the enthalpy value that the fluid has at that point can be determined if it is in single phase but not in two-phase. In other words in the two-phase case the temperature and pressure are not independent properties. To determine the quality of the refrigerant at the inlet of the test section, the refrigerant in liquid phase was pre-heated before the test section by the pre-heater and the refrigerant became two-phase at the inlet of the test section. The amount of the heat transferred by the pre-heater to the refrigerant could be found by using the calibration curve obtained for the pre-heater as a result of the calibration tests. By knowing the amount of the heat transferred from the pre-heater the enthalpy at the inlet of the test section was found and also using the pressure property at the same point the quality value was determined. Also the heat transferred to the refrigerant side from the water side in the test section could be determined by using the viscous heating correlation and the temperature values measured. So the enthalpy and then the quality of the refrigerant were calculated at the exit of the test section.

Information about the refrigerant and water side geometries in the test section and experimental conditions which occurred during two-phase flow experiments in the copper minitube can be achieved from the thesis of Tekin [26].

During two-phase flow experiments in the copper minitube the mass flow rate of the refrigerant changed between 0.34 and 0.94 g/s. The range of the mass flow rate was tried to vary in the working range of the refrigerants in the refrigerators. It is known that the operation flow rates of the refrigerants in the refrigerators are between 0.2 and 1.0 g/s.

When the water side parameters are investigated, it is seen that the pressure in the cycle was about 10-12 bars during the two-phase flow experiments with the minitube. Because of the almost incompressible flow in the water cycle the high

pressure in the water cycle did not affect the properties of the water and ethylene glycol mixture.

The maximum value of the volumetric flow rate in the water cycle was limited to 2.1 l/min due to the measurement range of the rotameter. During the experiments to provide more similar condition to the constant wall temperature boundary condition on the minitube surface the maximum flow rate value which was 2.1 l/min was tried to sustain in the water cycle. Also even in the maximum flow rate case there was a laminar flow in the water side in the test section. So in the calculations made for the heat loss of the water side developing laminar flow correlations were used.

As mentioned before, the purpose of the two-phase flow experiments with the copper minitube was to verify the experimental set-up constructed for the two-phase flow experiments with the different minichannels by comparing the experimental results of the minitube with the results in the literature. For this purpose firstly heat transfer coefficients and qualities were calculated for the data collected during two-phase flow experiments.

2.1.3 Verification of Experimental Set-up

To verify the experimental set-up heat transfer coefficients, qualities and mass fluxes were calculated, pressure drops and saturation pressures are measured for 28 acceptable two-phase flow experiments conducted. The data obtained at the end of these experiments were compared at constant mass fluxes and qualities with the results calculated by using the correlations given for the channels in the literature and the experimental results given in the literature. Another constant property is heat flux used in the literature for comparisons of channels but comparison is not made for constant heat flux because in this study constant surface temperature boundary condition was tried to apply and heat flux along the minitube was not kept constant. Heat transfer coefficients and pressure drops obtained were investigated by looking their changes with change in saturation pressure, mass flux and quality keeping either mass flux or quality constant.

For comparison Güngör and Winterton [27], Chen [27] and Bertsch [28] correlations and two experimental results [29, 30] were used.

The diagram showing the changes in the heat transfer coefficients with the changes in mass fluxes obtained by the experimental data and results obtained by using three different correlations in the literature at the constant quality of 18% is shown in Figure 10.

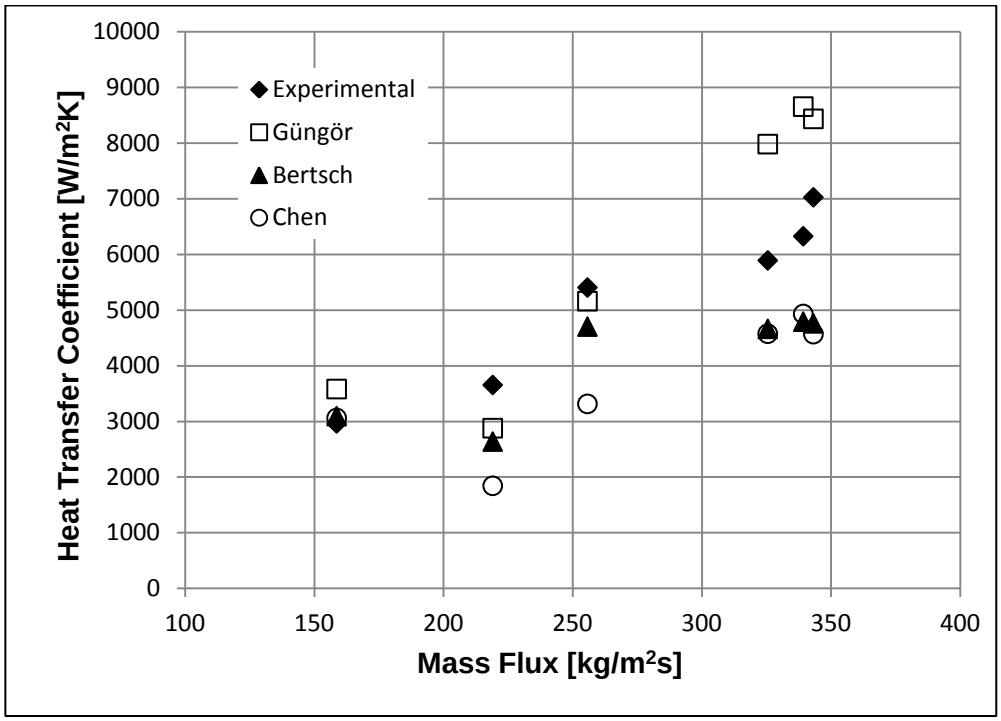

Figure 10: Comparison of experimental results and results of correlations in the literature for the heat transfer coefficient and mass flux, x = 18%. [26]

In Figure 10 it is seen that for all the results the mass flux effects are similar and increase in the mass flux values causes increase in the heat transfer coefficients. The results obtained at the end of the copper minitube experiments show a good consistency with the results calculated for the correlations in the literature.

When Figure 11 is investigated, it is understood that the experimental results and the results of Güngör and Winterton correlations and Bertsch correlation have the

maximum heat transfer coefficients at the quality of 40% at the higher quality level they have lower heat transfer coefficients.

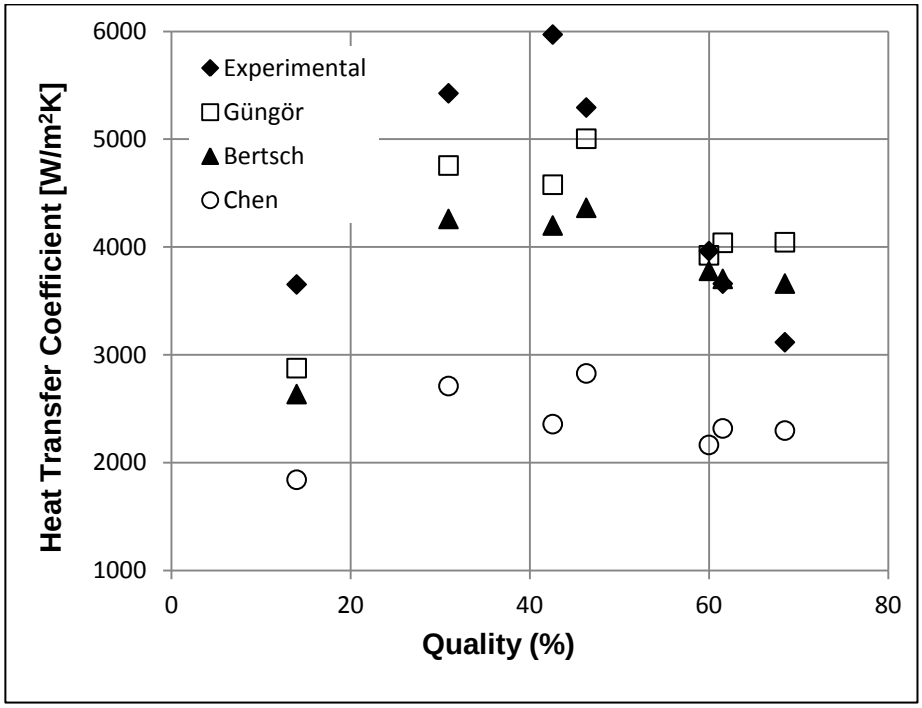

Figure 11: Comparison of experimental results and results of correlations in the literature for the heat transfer coefficient and quality. [26]

The graph obtained between pressure drops and mass fluxes in different qualities showed that increase in mass flux causes increase in pressure drop, which is an expected result.

As consistent with the studies in the literature, pressure drop versus quality graph at constant mass flux showed that with the quality increase the pressure drop also increases in the minitube.

The more detailed information about the two-phase flow copper minitube experiments is present in the thesis of Tekin [26]. The graphs shown for verification of the experimental set-up were taken from it. I was involved in the studies of Tekin [26] during the minitube experiments.

2.2 ADAPTATIONS AND MODIFICATIONS

In this section the adaptations and modifications which were made after the copper minitube experiments are explained.

2.2.1 Preparation of Test Section with the Minichannels

After two phase flow experiments in the copper minitube were completed, the copper minitube, shell and insulation around the shell in the test section of the experimental set-up were removed. Instead of these parts, the first minichannel which was produced by Arçelik Inc. and the shell, which was designed and produced in the suitable dimensions for being placed around the minichannel and which lets assembly of the hoses to its inlet and outlet allowing water-ethylene glycol mixture flow around the minichannel, were placed. The shell part consists of the insulation pipe whose dimensions were determined separately for the each minichannel and two lids which were assembled to the inlet and outlet of the insulation pipe by screws. To prevent leakage from any place of shell parts, silicon was applied to the places where leakage can occur. Before the minichannel was placed to the inside of the shell, 7 thermocouples were placed on the outer surface of the minichannel. During the process of removing the copper minitube from the set-up, no changes were made in the existing insulation of anywhere of the experimental set-up except the test section. After the new shell and the minichannel into the inside of the shell was placed, the outer surface of the test section was covered by glass wool to provide insulation of the test section. By following the same procedure for assembly of the second and third minichannels to the experimental set-up, the minichannel, whose two-phase flow experiments were completed, the shell designed for itself and the insulation covering the shell part were removed from the set-up then in place of them the new minichannel and shell were placed and covered by the insulation.

After each time when the channels were removed and replaced with the new one and all preparations were completed for the minichannel experiments, leakage tests were carried out by giving the refrigerant to the refrigerant cycle and pressure changes in the system were observed. If there were some changes in

the system pressure, the source of leakage was looked for by using bubbles and leakage was tried to prevent. Leakage tests were carried on until there was no leakage in the system.

The geometrical properties of the three minichannels in which two-phase flow experiments were conducted are given in Table 1.

Table 1: The geometrical properties of the three minichannels

Name	**Minichannel 1**	**Minichannel 2**	**Minichannel 3**
Width (mm)	16	22	20
Height (mm)	2.1	5	2.1
Wall thickness (mm)	0.3	0.6	0.4
Channel height (mm)	1.5	3.8	1.3
Channel width (mm)	1.94	3.68	2.35
Channel number (mm)	7	5	7
Channel length(mm)	465	440	525
Cross sectional area (mm^2)	20.4	66.27	21.84
Wetted parameter (mm)	48.2	68.79	51.8
Hydraulic diameter (mm)	1.69	3.85	1.69
Inner heat transfer area (mm^2)	22413	30268	27195

The cross sectional drawings of the 3 minichannels were shown in Figure 1. The geometrical properties of the shells whose dimensions were designed separately for the each minichannel to provide the water and ethylene glycol mixture flow over the minichannels are given in Table 2. The technical drawings of the flange and shell are given in Appendix B.1 and B.2 respectively.

Table 2: The geometrical properties of the shells

Name	**Shell 1**	**Shell 2**	**Shell 3**
Inner diameter (mm)	49.6	65.7	49.6
Outer diameter (mm)	65	75.7	65
Length (mm)	465	440	525
Cross sectional area (mm^2)	1898.61	3285.53	1890.21
Wetted parameter (mm)	192.02	256.11	200.02
Hydraulic diameter (mm)	39.55	51.31	37.80

The test sections prepared for the first and second minichannel experiments before covered with the insulation, and the test section prepared for the third minichannel experiments in the assembly level, with not completed connections in the water side, are shown in Figures 12, 13 and 14 respectively. In all of these figures the cables of the thermocouples which were placed on the outer surface of the minichannels, going out from the shells can be observed. Figures 15, 16 and 17 show the test sections which the minichannels were assembled in and whose insulations were completed.

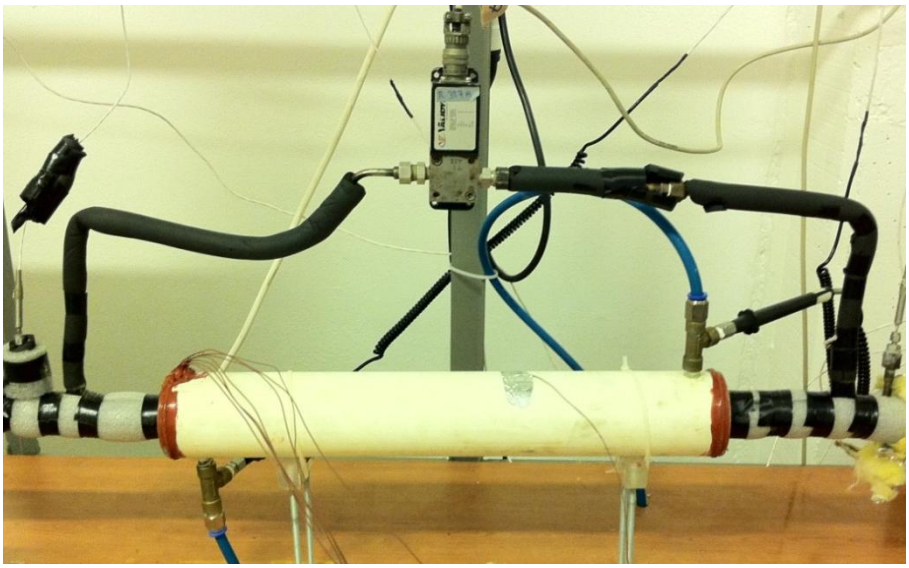

Figure 12: The test section in which the first minichannel and its shell are assembled

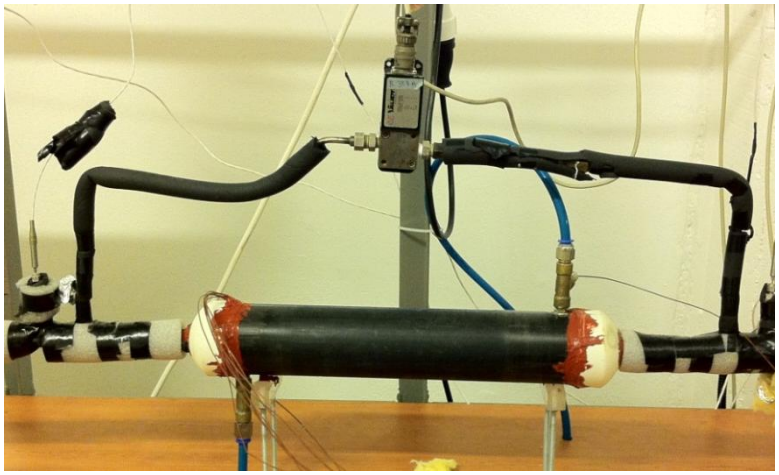

Figure 13: The test section in which the second minichannel and its shell are assembled

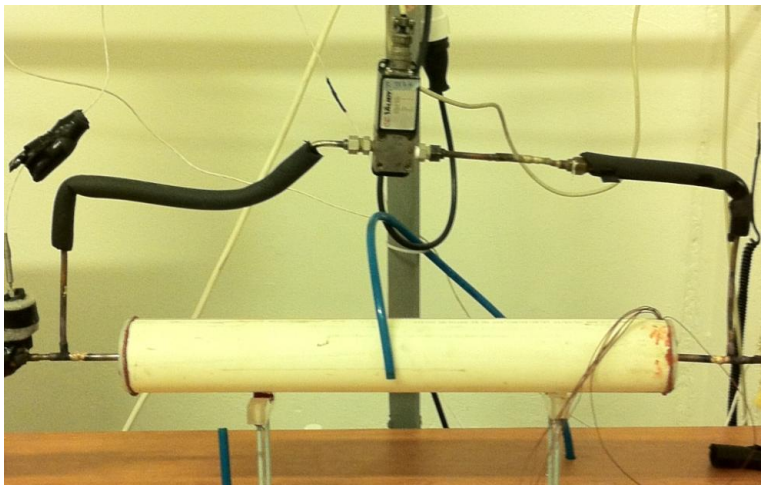

Figure 14: The test section in which the third minichannel and its shell are assembled, with not completed water side connections

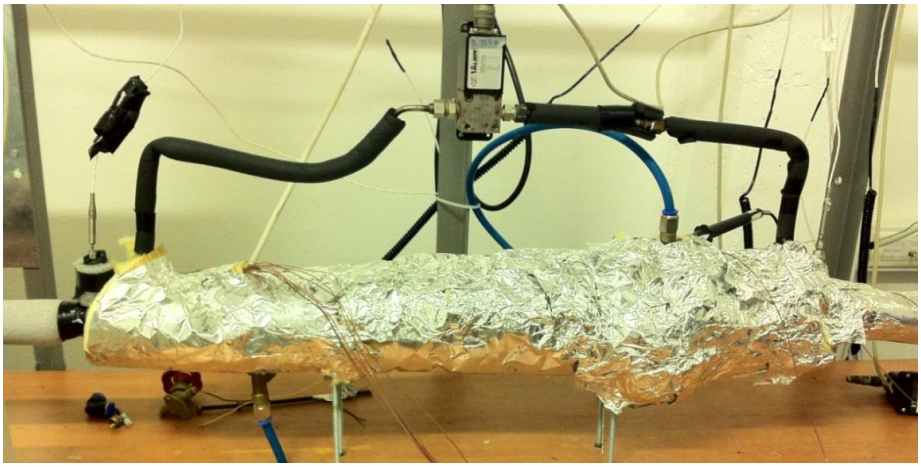

Figure 15: The test section with the completed insulation for the first minichannel experiments

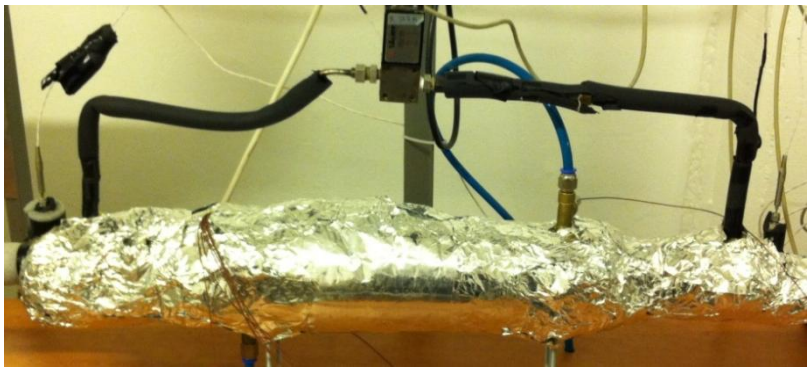

Figure 16: The test section with the completed insulation for the second minichannel experiments

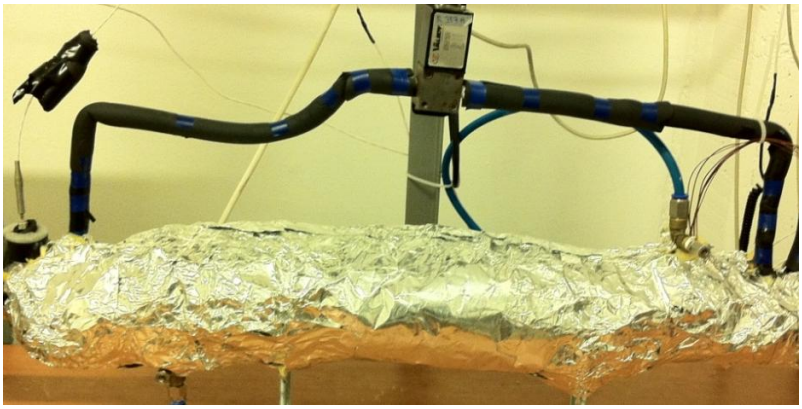

Figure 17: The test section with the completed insulation for the third minichannel experiments

2.2.2 Second Pump in the R-134a Cycle

During the experiments, the refrigerant passing through the refrigerant pump was tried to be kept in fully liquid phase to protect the gears of the pump from possible damages which two-phase flow passing through it can cause. However to obtain the refrigerant in liquid phase at the section around the pump decreasing the temperature of the refrigerant by using the refrigerant cooling bath is not enough. With the help of the refrigerant cooling bath it is possible to obtain the refrigerant in liquid phase only inside of the refrigerant cooling bath and at the areas near it. Also increasing the pressure of the refrigerant by adding more refrigerant to the system and turning the refrigerant in the whole system into liquid phase are considered but this process could not be applied in case that the refrigerant tank has lower pressures than the system pressure. Because transfer of the refrigerant in the refrigerant tank into the system is not carried out by a compressor or pump, it is only provided by a valve with the help of the pressure difference between the refrigerant tank and the refrigerant cycle. For this reason in addition to the system, placing a second pump to the system which is connected parallel to the existing pump was decided. A pump which works in higher flow rates was acquired. So by operating this pump before operating the micro pump which is used in two-phase flow experiments the refrigerant flow was provided in the system and temperature decrease occurring in the refrigerant

cooling bath was spread to the whole areas in the refrigerant cycle. Decrease in temperature resulted in decrease in the system pressure. This situation provided an ability of liquefaction of the refrigerant by transferring refrigerant from the R134a tank to the system in case that temperature decrease provided by the refrigerant cooling bath was not enough to make the refrigerant liquid in the desired areas. It is not worried about the damages occurring in the second pump due to the two-phase flow passing through inside it because it has more stronger gears than the micro pump used in the experiments and also despite the losses in its performance it can provide a circulation of refrigerant in the refrigerant cycle in a sufficient level for decreasing the temperature of the whole system. Additionally it should be noted that this second pump is not used during the two-phase flow experiments, it is used only before the experiments to be able to start the experiments by not damaging the micro pump which is used in the experiments.

2.2.3 Miscellaneous Parts

During the two-phase flow experiments to be able to determine the quality at the inlet of the test section thus to determine the enthalpy value at the area just before the pre-heater, after the micro flowmeter by using only temperature and pressure measurements at that point, the refrigerant flow at the area before the pre-heater was kept in fully liquid phase. Due to importance of providing liquid refrigerant flow at this section, a sight glass was placed just before that section to be sure about the phase of the refrigerant by observation in addition to measurements.

As mentioned before, whole air inside the refrigerant cycle was tried to take out to the ambient by vacuuming, then the refrigerant cycle is filled by the refrigerant. However, removing 100% of air in the refrigerant cannot be achieved so a little amount of air remains inside the system. The moisture in the air which may possibly remain in the system can damage the devices which the refrigerant flows through at the temperatures of the freezing point of water. For this reason a dryer was placed to the refrigerant cycle at the exit of the refrigerant cooling bath.

While replacing the first minichannel with the second one, the RTDs in the water side at the inlet and outlet of the test section were damaged. So instead of the RTDs, two thermocouples which are in touch with the water-ethylene glycol mixture in the water cycle were assembled to the same places.

To prevent heating problems in the water pump occurring due to the high pressure in the water cycle the flow path of the water cycle was modified and the water pressure was decreased. Although this operation reduced the water flow rate pumped by the water pump into the test section, it did not cause any problem because of the higher flow rate in the existing conditions than the maximum limit which the rotameter in the water cycle can measure.

Lastly, a multiplexer card was acquired to control the pre-heater automatically by means of HP VEE software in the computer instead of manual control used during the minitube experiments.

The experimental set-up constructed after these adaptations and modifications mentioned above is shown in Figure 18 schematically and in Figure 19 in a photograph.

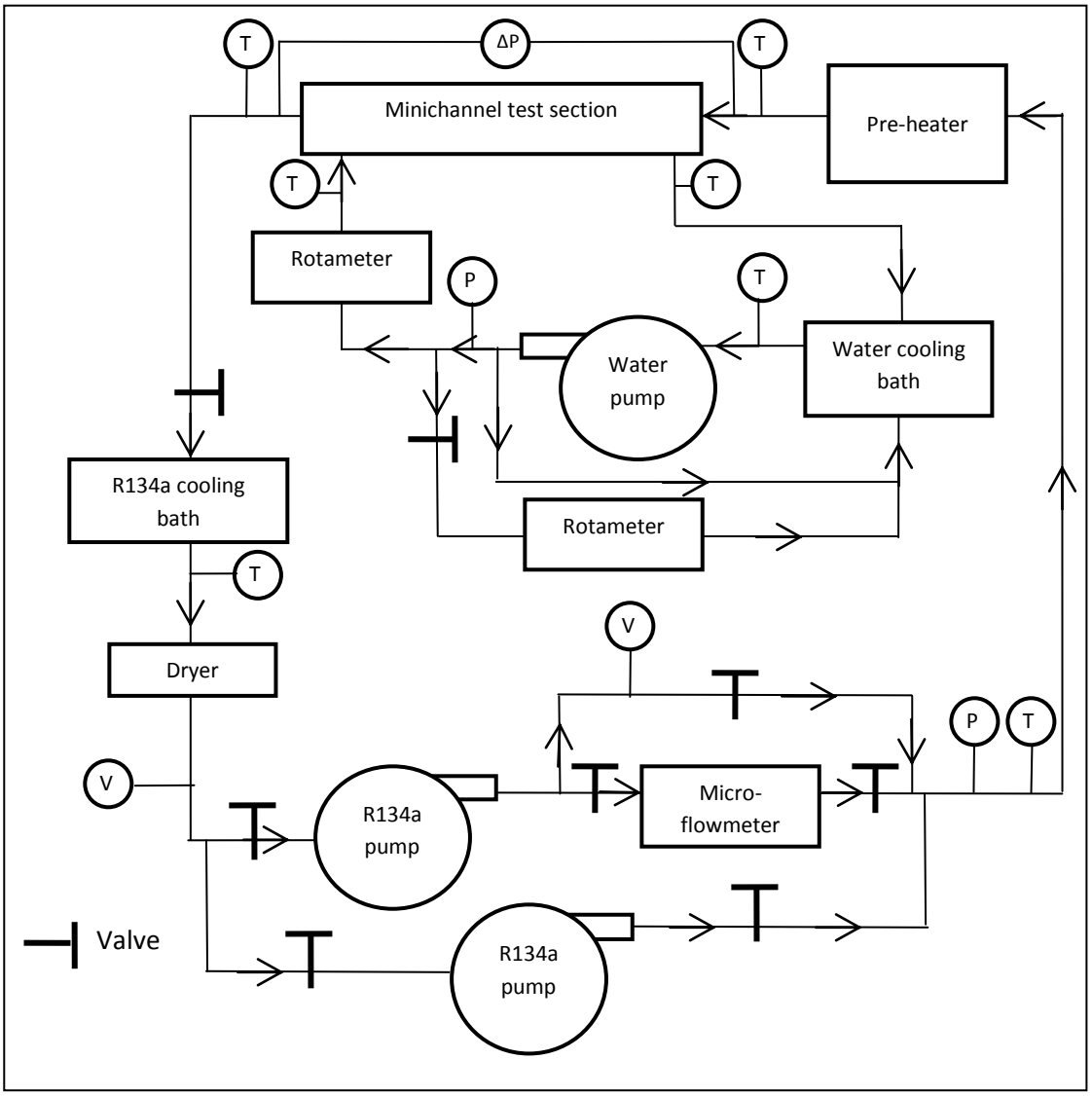

Figure 18: The schematic view of the experimental setup in which two-phase flow minichannel experiments were conducted

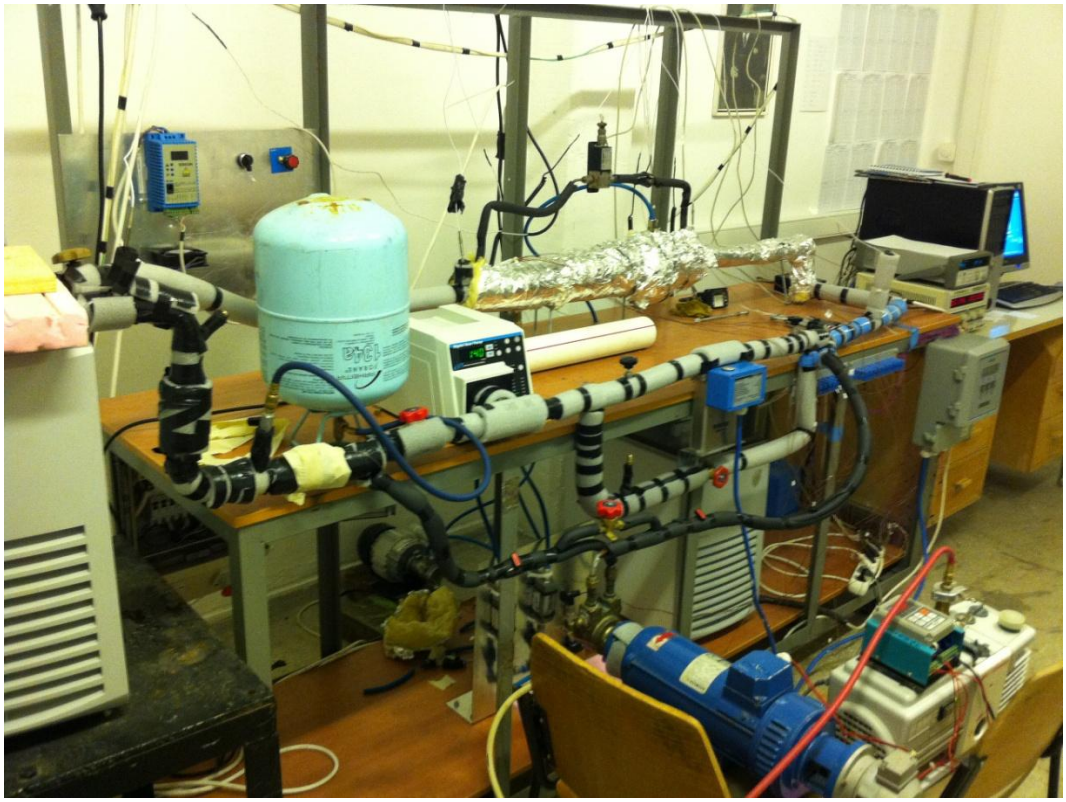

Figure 19: The experimental set-up after the changes made for two phase flow experiments in the minichannels

The detailed information of the devices in the experimental set-up is given in Appendix A.

2.3 CALIBRATIONS

The calibrations which were carried out are the calibration of the measurement devices and the determination of the losses from the parts affecting the experimental results. Some of the calibrations were applied before the copper minitube experiments and some of them were at the beginning of the minichannel experiments.

2.3.1 Previous Calibrations

The calibration of the micro-flowmeter in the refrigerant cycle was provided by its producer company and there was no need to calibrate it again. Only using the menu on its monitor, g/s was selected as the unit which the measurements were wanted to be in. Any operation to read its measurements on the computer was not made and the measurements were read from its monitor manually.

Also the rotameters in the water cycle are manually operating devices and there was no calibration made for them. They show the volumetric flow rate of the water passing through them in the unit of l/min.

The thermocouples and RTDs which were used in the different sections of the experimental set-up were calibrated by Arçelik Inc. laboratories by taking measurements in different ambient temperatures together with a reference temperature measurement device whose measurements are considered as exactly true. Then a calibration curve was determined at the end of these measurements. The constants of the calibration curve were entered to the computer software (HP VEE) which was used in collection of the data from the devices in the experimental set-up.

In a similar procedure with the calibration of the thermocouples and RTDs, two identical pressure transducers and one differential pressure transducer which were used in the set-up were calibrated by Arçelik Inc. and their calibration curve data were sent us to enter to the software providing to collect data. The identical pressure transducers have an output range of 0-10V and they make measurements in the range of 0-1000W. They were calibrated for the pressures between 0-200 psi by using it with the valves which are used to control the pressurized nitrogen gas in pipes. Also instead taking voltage outputs from them obtaining current output, which is changing between 4 - 20 mA, was provided by making necessary connections on the cards inserted to the data logger by the researches of Arçelik Inc. The calibration lines obtained for the identical pressure transducers used in the refrigerant cycle and the water cycle are given in Eq. (1) and Eq. (2) respectively.

$$P[psi] = 12682 * I[mA] - 50.417 \quad (1)$$

$$P[psi] = 12705 * I[mA] - 50.520 \quad (2)$$

Additionally for the differential pressure transducer used in the test section in the refrigerant cycle, a calibration curve was obtained in a similar way with the identical pressure transducer calibration.

The calibration results and curves obtained for RTDs and the compact pressure transducers can be seen in Appendix C.1 – 4. Information about the calibration of the differential pressure transducer is given in the thesis of Tekin [26].

The purpose of usage of the pre-heater in the experimental set-up is to be able to determine the refrigerant quality at the inlet of the test section. Determination of the quality is made by supplying liquid refrigerant just before the pre-heater firstly and then by knowing the temperature and pressure at that point, enthalpy of the refrigerant can be found at that point. To calculate the quality of the refrigerant at the inlet of the test section the heat transferred to the refrigerant along the pre-heater placed before the test section must be known accurately. To determine the heat transferred to the refrigerant from the pre-heater the heat transferred to the ambient from the pre-heater must be taken into consideration.

The calibration of the pre-heater was carried out by providing liquid refrigerant along whole refrigerant cycle. As mentioned before, just before the pre-heater and after the pre-heater, before the test section there were RTDs to measure the temperatures of the refrigerant at these points. Also there was an identical pressure transducer before the pre-heater section measuring the refrigerant pressure. The pressure of the refrigerant at the exit of the pre-heater section was not measured but it is assumed that along the pre-heater section pressure change is negligible. By considering the pre-heater section as a control volume like shown in Figure 20, the first law of thermodynamics was applied to the control volume. So this analysis gives us the relation in Eq. (3).

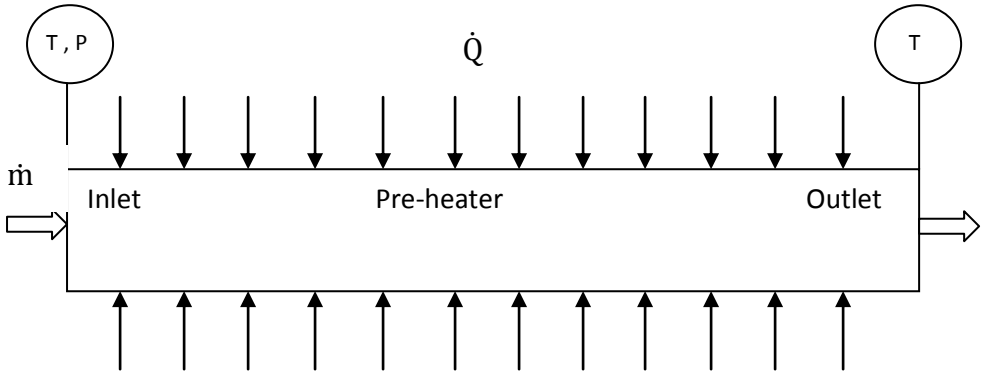

Figure 20: The analysis of the pre-heater section as a control volume

$$\dot{Q}_{RI} = \dot{m}_R(h_{he} - h_{hi}) \quad (3)$$

where $\dot{Q}_{RI}$ is the heat transferred to the refrigerant from the pre-heater, $\dot{m}_R$ is the mass flow rate of the refrigerant, h_{he} is the enthalpy of the refrigerant at the exit of the pre-heater section, and h_{hi} is the enthalpy of the refrigerant at the inlet of the pre-heater section. The measurements and the negligible pressure change assumption along the pre-heater section provide to be able calculate the heat transferred to the refrigerant from the pre-heater by using Eq. (3). The power supplied to the pre-heater was observed on the computer. By means of the single phase flow experiments repeated for different pre-heater powers, different amounts of heat transferred to the refrigerant from the pre-heater corresponding to different pre-heater powers were obtained and a relation was obtained between them.

Beside the pre-heater calibration, to determine the refrigerant quality at the exit of the test section the heat losses from the test section and the heat transferred to the refrigerant in the test section were other issues which must be considered. Due to being dependent properties of temperature and pressure in two-phase flow, the heat transferred to the refrigerant from the water side in the test section is calculated by making calculations for the water side. Firstly, by considering that in the water side of the test section heat is transferred to the refrigerant from the water side, there is heat loss to the ambient and viscous heating occurs due to

laminar water flow in the water side, the energy equilibrium is formulated as in Eq. (4).

$$\dot{Q}_W = \dot{V}_W \rho_W (h_{wi} - h_{we}) + \dot{Q}_V - \dot{Q}_{W,loss} \quad (4)$$

where $\dot{Q}_W$ is the net heat transfer to the refrigerant from the water side in the test section, $\dot{V}_W$ is the volumetric flow rate of the water-ethylene glycol mixture in the water side, ρ_W is the density of the water-ethylene glycol mixture used in the water side, h_{wi} and h_{we} are the enthalpies of water-ethylene glycol mixture at the inlet and exit of the test section, $\dot{Q}_V$ is the viscous heating and $\dot{Q}_{W,loss}$ is the heat loss to the ambient from the water side in the test section.

During the experiments there was always fully liquid flow in the water side, for calculation of enthalpy difference of the fluid Eq. (5) was used by assuming the liquid flowing in the water side is incompressible and its specific volume is very small which provides a negligible $v_W(P_{wi} - P_{we})$ term [31].

$$h_{wi} - h_{we} = C\ (T_{wi} - T_{we}) \quad (5)$$

where C is the specific heat of the water-ethylene glycol mixture in the water side, T_{wi} and T_{we} are the temperatures of the water-ethylene glycol mixture at the inlet and exit of the test section.

To find the properties of the water-ethylene glycol mixture in the water side, curves were fitted to the data known for some specified mixture proportions. These curves are given in Appendix D.1 – 4.

To find the viscous heating some experiments for different water flow rates were conducted in the conditions which the temperatures of ambient, water-ethylene glycol mixture and refrigerant in test section are almost same. During the viscous heating experiments only the cooling bath in the water cycle was turned on, the cooling bath in the refrigerant cycle was not operated. The reason of operating the cooling bath in the water cycle is that this cooling bath is used in parallel

connection with the water pump and the water pump cannot be operated without operating the cooling bath in the water cycle. There was no flow in the refrigerant cycle, but to determine the viscous heating values in different flow rates in the water cycle the flow of the water-ethylene glycol mixture was provided by running the water pump. As the result of the experiments a linear relation was obtained between the viscous heating and Reynolds number.

Also the heat loss calculation was carried out by considering the properties of the aluminum shell and the insulation around the counter flow heat exchanger in the test section and the equation used for this purpose is given in Eq. (6).

$$\dot{Q}_{W,loss}[W] = \frac{\Delta T}{\frac{1}{\pi d_{si} L h_W} + \frac{ln(d_{so}/d_{si})}{2\pi k_{Al} L} + \frac{ln(d_{ins}/d_{so})}{2\pi k_{ins} L} + \frac{1}{\pi d_{ins} L h_{air}}} \quad (6)$$

where d_{si}, d_{so} and d_{ins} are the inner, outer shell and outer insulation diameters, L is the length of the counter flow heat exchanger in the test section, k_{Al} and k_{ins} are the thermal conductivities of aluminum and insulation material, h_W and h_{air} are the convective heat transfer coefficients of water-ethylene glycol mixture and air, ΔT is the temperature difference between the water side and ambient. The heat loss to the ambient from the test section was calculated by dividing the temperature difference between inside and outside of the counter flow heat exchanger in the test section by thermal resistances between them. h_W and h_{air} in Eq. (6) were calculated by using different correlations suggested for laminar flows in thermally developing region. These correlations are the ones suggested by Gnielinski, Hausen, Pohlhausen and the correlation called as “The asymptotic mean Nusselt numbers in circular ducts” in the book of Kakaç [27].

As the result of the calculation of the heat loss from the water side to the ambient and the heat transferred to the refrigerant from the water side, even for the maximum temperature difference case the heat loss was calculated as being only 2.5% of the heat transferred to the refrigerant so it was decided that the heat loss term in Eq. (6) can be neglected.

The calibrations of the measurement devices, mentioned in this section, made before the minitube experiments are also valid for the minichannel experiments. The calibration processes made for determination of the heat transferred to the refrigerant from the water side in the test section were conducted also before the each minichannels' two-phase flow experiments in similar way.

2.3.2 Calibrations for Minichannel Experiments

In this section the calibrations made on the experimental set-up after the minitube experiments are explained.

2.3.2.1 Pressure Transducer

During the first two-phase flow experiments of the second minichannel made after the second minichannel was placed to the experimental set-up, a deviation from the true values was determined on the values which were given by the differential pressure transducer. Additionally, the pressure drops occurring along the test section was very lower than the working range of the existing differential pressure transducer. Therefore a new differential pressure transducer which works between the pressures of 0 – 5kPa (=0 – 0.05bar) was acquired from Arçelik Inc. This device was calibrated in the laboratories of Arçelik Inc. After the calibration process was completed, two phase flow experiments were sustained by using the calibration curve obtained. The calibration curve of this differential pressure transducer is given in Appendix C.6.

2.3.2.2 Pre-heater

As mentioned before, after the minitube experiments were completed, to be able to control the pre-heater by means of the computer in the laboratory a multiplexer card was obtained and inserted to the data logger. So, the power wanted to supply to the pre-heater was able to be provided by entering voltage values with the help of the HP VEE software on the computer. Due to the purpose of usage of the pre-heater in the experimental setup, knowing the heat transferred to the

refrigerant from the pre-heater is necessary to determine the refrigerant quality at the inlet of the test section.

To determine the heat transferred to the refrigerant from the pre-heater corresponding to the voltage values entered on the computer, some single phase flow experiments were conducted. Due to being independent properties of temperature and pressure in single phase flows, providing single phase flow was important during these experiments to determine the enthalpy of the refrigerant at the points whose temperature and pressure values are known. Calibration of the pre-heater was carried out in a similar way with the one made before the minitube experiments. Again the control volume analysis shown in Figure 20 was gone through with and Eq. (3) was used to find the heat received by the refrigerant from the pre-heater.

During these single phase flow experiments different voltage values were entered on the computer and steady state conditions were waited to achieve for. Then using the temperature readings obtained from the RTDs at the inlet and exit of the pre-heater section and mass flow rate values read from the micro-flow meter in the refrigerant cycle, the heat transferred to the refrigerant from the pre-heater was calculated. The experiments were repeated for different voltage values. The properties of the refrigerant at the inlet and exit of the pre-heater section in the steady state conditions for the different voltage values entered in the range of 1-4V are given in Table 3. The calibration of the pre-heater was carried out in the range of 1-4V firstly before the experiments of the first minichannel, but after the experiments of the first minichannel were completed, it was decided that to be able to obtain higher refrigerant qualities at the inlet of the test section the calibration of the pre-heater was made in the range of 4-7V too. The properties belonging to the calibration of the pre-heater in the range of 4-7V are given in Table 4.

Table 3: The refrigerant properties for the pre-heater calibration (1-4V)

Name	**Unit**	**Exp. 1**	**Exp. 2**	**Exp. 3**	**Exp. 4**
Mass flow rate	g/s	7.37	7.35	7.24	7.27
R134a pressure	bar	5.38	5.39	5.4	5.4
Pre-heater inlet temperature	ºC	5.52	5.55	5.58	5.6
Inlet enthalpy	kJ/kg	207.49	207.53	207.58	207.6
Pre-heater exit temperature	ºC	6.35	6.82	7.43	8.14
Exit enthalpy	kJ/kg	208.62	209.26	210.09	211.06
Voltage value entered	V	1	1.5	2	2.5
Heat transferred to the refrigerant	W	8.33	12.72	18.16	25.15
Name	**Unit**	**Exp. 5**	**Exp. 6**	**Exp. 7**	
Mass flow rate	g/s	7.24	7.21	7.25	
R134a pressure	bar	5.43	5.46	5.45	
Pre-heater inlet temperature	ºC	5.64	5.68	6.48	
Inlet enthalpy	kJ/kg	207.66	207.71	208.8	
Pre-heater exit temperature	ºC	9.05	10.16	11.62	
Exit enthalpy	kJ/kg	212.3	213.82	215.82	
Voltage value entered	V	3	3.5	4	
Heat transferred to the refrigerant	W	33.59	44.05	50.87	

Table 4: The refrigerant properties for the pre-heater calibration (4-7V)

Name	**Unit**	**Exp. 1**	**Exp. 2**	**Exp. 3**	**Exp. 4**
Mass flow rate	g/s	7.45	7.06	7.44	7.4
R134a pressure	bar	5.61	5.45	5.49	5.59
Pre-heater inlet temperature	ºC	6.05	6.08	6.07	6.1
Inlet enthalpy	kJ/kg	208.22	208.25	208.24	208.29
Pre-heater exit temperature	ºC	11.74	13.17	14.49	15.94
Exit enthalpy	kJ/kg	215.99	217.95	219.78	221.79
Voltage value entered	V	4	4.5	5	5.5
Heat transferred to the refrigerant	W	57.89	68.52	85.82	99.90
Name	**Unit**	**Exp. 5**	**Exp. 6**	**Exp. 7**	**Exp. 8**
Mass flow rate	g/s	7.39	7.39	7.38	7.51
R134a pressure	bar	5.71	6.17	6.11	4.34
Pre-heater inlet temperature	ºC	6.12	6.23	6.27	1.92
Inlet enthalpy	kJ/kg	208.32	208.47	208.53	202.61
Pre-heater exit temperature	ºC	17.17	18.42	19.46	8.86
Exit enthalpy	kJ/kg	223.51	225.26	226.71	212.02
Voltage value entered	V	6	6.5	7	4.5
Heat transferred to the refrigerant	W	112.3	124.08	134.25	70.70

When the values of heat transferred to the refrigerant were obtained for 4V in both calibration ranges shown in Table 3 and 4, it was seen that heat transferred to the refrigerant is higher for 4V in the calibration made in the range of 4-7V. The reason of this difference is that the pre-heater calibration experiments were conducted at different ambient and refrigerant conditions. The changes in pre-heater calibration in different conditions such as different temperature differences between the refrigerant and ambient, varying resistance of the pre-heater with different temperature conditions were assumed as small and the calibration curves obtained in the conditions shown in Table 3 and 4 were used for during all two-phase flow experiments. Additionally the heat transferred to the refrigerant corresponding to 4V was calculated by using the calibration curve obtained in the range of 4-7V for the 2^{nd} and 3^{rd} minichannels while it was calculated by using the calibration curve in the range of 1-4V for the 1^{st} minichannel.

The calibration curves obtained by using the values shown in Tables 3 and 4 are shown in Figure 21 and 22 respectively. Linear curves were fitted to the data obtained as the result of the pre-heater calibration experiments although it is known that the electrical power is proportional with the square of the voltage value. However the voltage values entered on the computer are not the exact voltages supplied to the pre-heater and when the pre-heater calibration curves were investigated, it is seen that the linear curves were fitted with very small deviations to the experimental pre-heater calibration data.

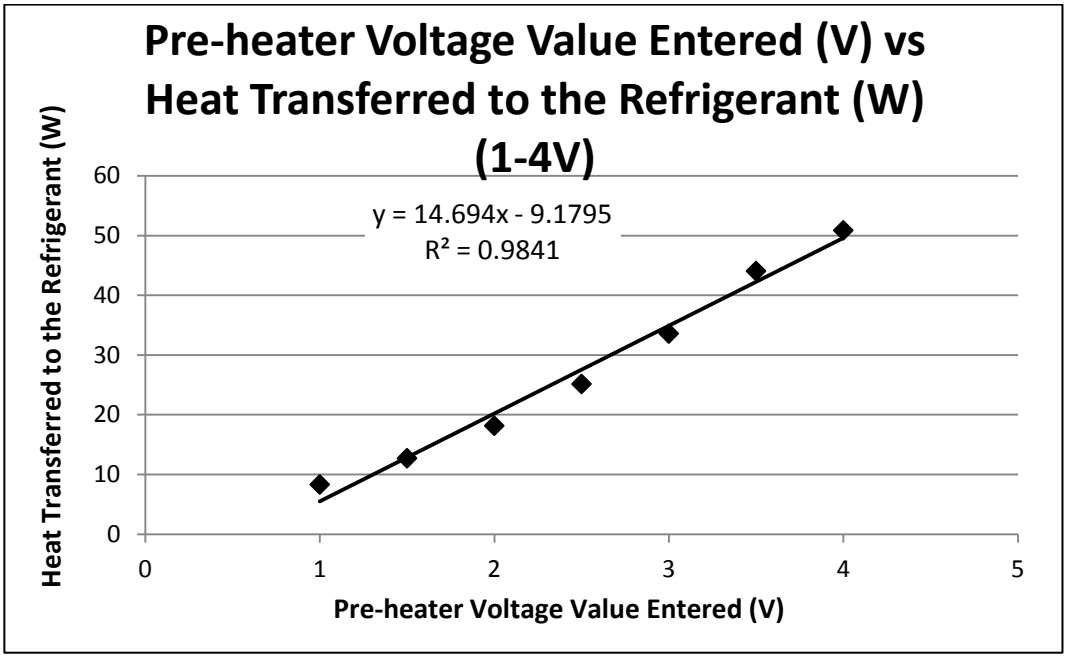

Figure 21: The relation between the voltage value entered for the pre-heater and the corresponding heat transfer to the refrigerant (1-4V)

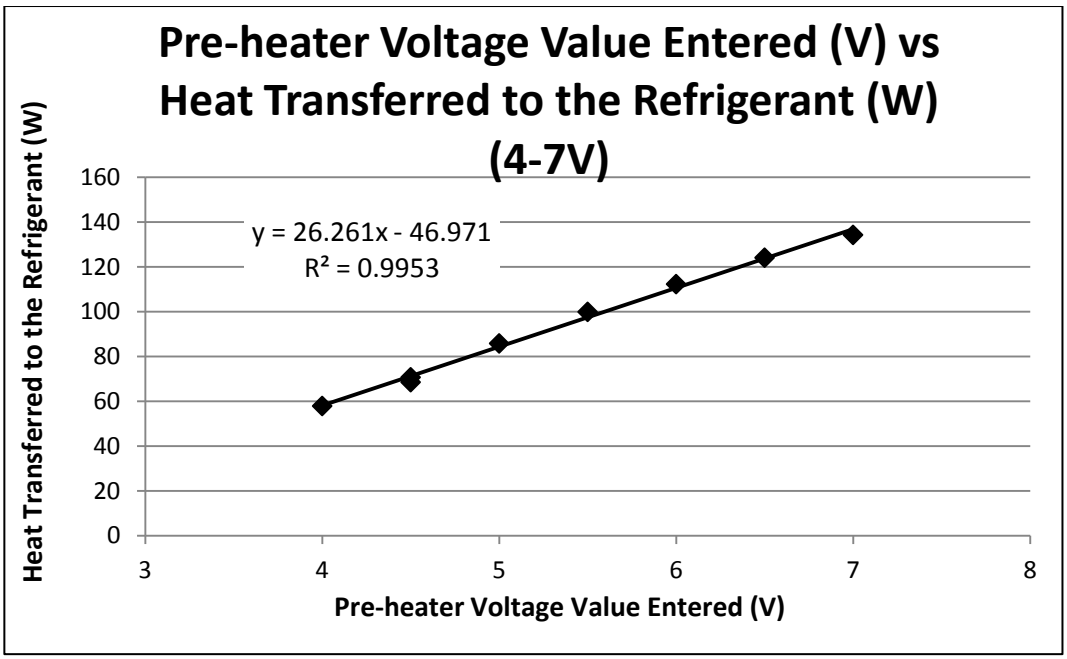

Figure 22: The relation between the voltage value entered for the pre-heater and the corresponding heat transfer to the refrigerant (4-7V)

The correlations obtained for the calibration curves in the voltage ranges of 1-4V and 4-7V are given in Eq. (7) and (8) respectively.
For the voltage range of 1-4V:

$$\dot{Q}_{RI}(W) = 14.694 * V_{ent}(V) - 9.1795 \quad (7)$$

For the voltage range of 4-7V:

$$\dot{Q}_{RI}(W) = 26.261 * V_{ent}(V) - 46.971 \quad (8)$$

where $\dot{\mathrm{Q}}_{\mathrm{RI}}$ is the heat input to the refrigerant coming from the pre-heater, $\mathrm{V}_{\mathrm{ent}}$ is the voltage value entered on the computer for the pre-heater.

2.3.2.3 Test Section

Similarly to the approach used in the two phase flow minitube experiments, the heat loss from the test section was neglected considering that it is very small compared to the heat transferred to the refrigerant from the water side in test section for the maximum temperature difference condition among the data collected during two-phase flow experiments. Before making this assumption, heat losses were calculated in the cases of the maximum temperature difference between the water side of the test section and the ambient for each minichannel. The water side parameters used in the heat loss calculations are given in Table 5.

Table 5: The water side parameters for the heat loss calculations

Name	Unit	Minichannel 1	Minichannel 2	Minichannel 3
Outer diameter	mm	49.6	65.7	49.6
Inner perimeter	mm	36.2	49.71	42.00
Outer perimeter	mm	155.82	206.40	155.82
Cross-sectional area	mm^2	1898.61	3285.53	1890.21
Wetted parameter	mm	192.02	256.11	200.02
Hydraulic diameter	mm	39.55	51.31	37.80
Test section length	mm	465	440	525

As the results of the calculations made for determination of heat loss from the water side to the ambient by using Eq. (9) being similar with Eq. (9) it was decided that the heat loss which was at most 5.92% of the heat transferred to the refrigerant can be neglected for simplicity of the calculations made for the minichannels.

$$\dot{Q}_{W,loss}[W] = \frac{\Delta T}{\frac{1}{\pi d_{si} L h_W} + \frac{ln(d_{so}/d_{si})}{2\pi k_{inp} L} + \frac{ln(d_{ins}/d_{so})}{2\pi k_{ins} L} + \frac{1}{\pi d_{ins} L h_{air}}} \quad (9)$$

where d_{si}, d_{so} and d_{ins} are the inner, outer shell and outer insulation diameters, L is the length of the counter flow heat exchanger in the test section, k_{inp} and k_{ins} are the thermal conductivities of the material of the insulation pipe (polypropylene random copolymer) used as shell in the test section and the insulation material, h_W and h_{air} are the convective heat transfer coefficients of water-ethylene glycol mixture and air, ΔT is the temperature difference between the water side and ambient. The geometrical properties, thermodynamic properties and heat loss calculation results are given in Table 6.

Table 6: The results for the water side in the case of the maximum heat loss to the ambient

Name	**Unit**	**Minichannel 1**	**Minichannel 2**	**Minichannel 3**
d_{si}	mm	49.6	65.7	49.6
d_{so}	mm	65.0	75.7	65.0
t_{ins}	mm	35	35	35
d_{ins}	mm	135	145.7	135
k_{inp}	W/mK	0.23	0.23	0.23
k_{ins}	W/mK	0.04	0.04	0.04
h_W	W/m²K	1000	1000	1000
h_{air}	W/m²K	10	10	10
L	mm	465	440	525
ΔT	K	14.78	18.81	9.40
Q	W	4.01	5.92	3.11
Q/Qr	%	5.77	5.92	5.41

In the maximum temperature cases of the each minichannel, the rate of the heat loss to the heat transferred to the refrigerant was found as about 5.5%. So to ease the heat transfer calculations, the heat loss term was neglected in Eq. (4).

Firstly the viscous heating experiments were conducted with the first minichannel by providing single phase flow in the same way with applied in minitube viscous heating experiments mentioned under the title of “Previous Calibrations”. At the end of the viscous heating experiments made for the first minichannel the correlation which is given in Eq. (11) was obtained between Reynolds number (Re_w) and the viscous heating ($\dot{Q}_V$). By keeping the difference between the mean refrigerant and water temperatures under 0.36˚C the heat transfer between these two fluids was decreased to a negligible level. The heat losses were also neglected as mentioned. So the only heating was considered to be viscous heating in the water side of the test section during the experiments. Therefore Eq. (4) was simplified to the Eq. (10) which can be easily calculated by using the measurements taken in the experiments.

$$\dot{Q}_V = \dot{V}_W \rho_W (h_{we} - h_{wi}) \tag{10}$$

The experimental data obtained as the result of the viscous heating experiments made for the first minichannel are given in Table 7. The curve showing the relation between Reynolds number (Re_w) and viscous heating in the water side of the test section and the correlation between them are shown in Figure 23 and Eq. (11) respectively.

Table 7: The experimental data obtained the viscous heating experiments

Name	**Unit**	**Exp. 1**	**Exp. 2**	**Exp. 3**	**Exp. 4**
P_w	bar	0.93	5.00	4.70	4.73
V_w	l/dk	0.5	0.61	0.9	1.05
$T_{w,\,mean}$	°C	25.26	25.39	25.48	25.67
ρ_w	kg/m^3	1077.97	1077.91	1077.86	1077.77
m_w	kg/s	0.0089	0.0110	0.0162	0.0189
C	J/kgK	3404.58	3405.03	3405.33	3405.94
μ	kg/ms	0.0027	0.0027	0.0027	0.0027
k	W/mK	0.4027	0.4027	0.4027	0.4026
V	m/s	0.0044	0.0054	0.0079	0.0092
Re_W	-	69.19	84.12	123.80	143.68
Q_V	W	1.53	3.58	6.68	7.94
$T_w - T_{R\text{-}134a}$	°C	0.28	-0.18	-0.30	-0.22
Name	**Unit**	**Exp. 5**	**Exp. 6**	**Exp. 7**	**Exp. 8**
P_w	bar	4.70	4.80	4.66	4.45
V_w	l/dk	1.15	1.55	1.9	1.35
$T_{w,\,mean}$	°C	25.72	25.72	24.56	24.99
ρ_w	kg/m^3	1077.74	1077.74	1078.32	1078.11
m_w	kg/s	0.0207	0.0278	0.0341	0.0243
C_p	J/kgK	3406.13	3406.13	3402.29	3403.69
μ	kg/ms	0.0027	0.0027	0.0027	0.0027
k	W/mK	0.4026	0.4026	0.4027	0.4027
V	m/s	0.0101	0.0136	0.0167	0.0119
Re_w	-	157.10	211.74	267.08	188.06
Q_V	W	8.76	12.51	13.40	11.63
$T_w - T_{R\text{-}134a}$	°C	-0.25	-0.27	-0.30	-0.35

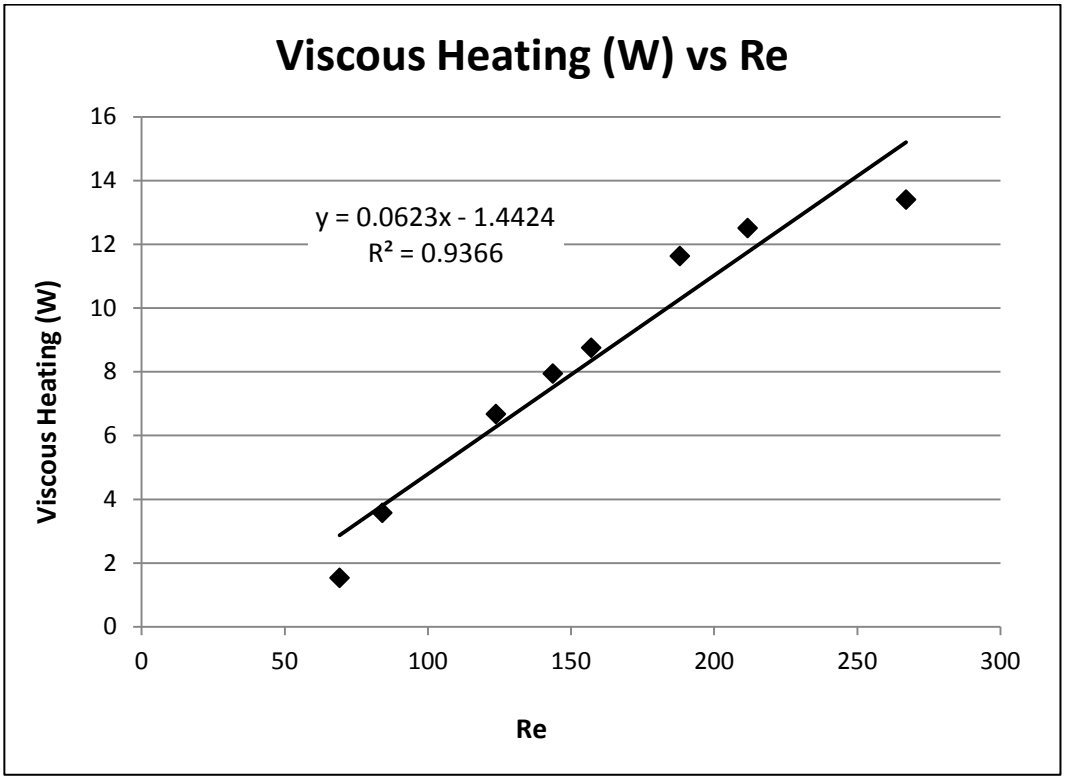

Figure 23: The relation between the viscous heating and Reynolds number in the waterside of the test section

$$\dot{Q}_V[W] = 0.0623 * Re_w - 1.4424 \quad (11)$$

The viscous heating experiments which were carried out for the first minichannel were not repeated for the other two minichannels. The changes which possibly occur in the relation between the viscous heating and Reynolds number for the other two minichannels were neglected and the viscous heating correlation shown in Eq. (11) was used to find the viscous heatings occurring in the water side of the test section during the experiments of the second and third minichannels.

CHAPTER 3

TWO-PHASE FLOW EXPERIMENTS

In this chapter, the approach in the two-phase flow experiments of the minichannels, the conditions existing during these experiments, the procedure followed in the experiments, the analysis of the data collected as the result of the experiments and the calculations made by using the data are explained.

3.1 APPROACH

Obtaining two-phase refrigerant flow in the test section was aimed during the experiments. To create a condition like the evaporator section of the refrigerators, the constant temperature approach was preferred instead of constant heat flux approach commonly preferred in the literature due to its easy application. For providing constant temperature condition around the minichannels in the test section, a counter flow heat exchanger was used. The parameters which are important for the heat transfer coefficient in the two-phase flow experiments were especially quality variation along the minichannels and heat flux in the test section. Mass flux of the refrigerant flowing through the minichannels, saturation temperature and pressure are other parameters to be examined.

By means of pre-heater calibration, the refrigerant quality at the inlet of the test section was found. In the test section there was a heat transfer from the water side to the refrigerant. Determination of the amount of heat transfer to the refrigerant in the test section and measurement of the mass flow rate of the refrigerant provided to find the enthalpy of the refrigerant at the exit of the test section. As distinct from the common knowledge about the constant saturation temperature in phase change, there are fluctuations on the saturation temperature and the average temperature is assumed as the saturation

temperature. So to designate the refrigerant state at the exit of the test section the pressure at that point was decided to use. As mentioned before, the system pressure was measured before the pre-heater in the refrigerant cycle. Pressure drop along the pre-heater section was neglected due to single phase flow which causes low pressure drops. The system pressure measured before the pre-heater section was accepted as the same with the pressure at the inlet of the test section. With the help of the differential pressure transducer in the test section, pressure drop occurring along the minichannels was measured and therefore the pressure at the exit of the test section was able to be calculated. The enthalpy and pressure values which are independent parameters in phase change were enough to designate the quality of the refrigerant at the exit of the test section. As common procedure applied in the studies in the literature, the average of the qualities at the inlet and exit of the test section was considered as the quality of the experiment.

Beside the constant wall temperature approach, providing low mass flow rates was another issue which was tried to apply. The refrigerant flow rates used in the refrigerators are between 0.2 and 1 g/s. In the two-phase flow experiments low mass flow rates were tried to use as much as possible.

3.2 EXPERIMENTAL CONDITIONS

The parameters in the two-phase flow experiments conducted in the minichannels were examined in three parts: the refrigerant side, the water side and the pre-heater power input.

The minimum and maximum values of the parameters of mass flow rate, inlet and exit pressures, inlet and exit qualities, and pressure drop in the refrigerant side which are varying with the flow conditions in two-phase in the test section are given in Table 8. The software “REFPROP 7” and the graphs prepared according to saturation pressure which are used to find the refrigerant properties are same with the ones used in minitube experiments and the graphs are presented in Appendix E by using the data given in the tables in the books of Kakaç [27] and Incropera [45].

As seen in Table 8, the flow rates worked with in the refrigerant cycle were higher than 1 g/s. The reason of this is that the micro-flowmeter used in the two-phase flow minichannel experiments did not allow to take any flow rate measurements under 1 g/s after a while. Although it is known that in the refrigerators the refrigerant mass flow rates are between 0.2 and 1 g/s, the experiments could not be carried out in this range, the experimental data were tried to collect with the mass flow rates as low as possible in the range which the micro-flowmeter allowed to take measurements. To observe the tendency of the refrigerant properties for which the minichannels were examined with changing parameters, the mass flow rates were changed starting from the minimum levels which can be measured up to 5.60, 6.40 and 4.88 g/s respectively for the 1st, 2nd and 3rd minichannel.

Table 8: The refrigerant conditions in the test section in the two-phase flow experiments

		Minichnl. 1		**Minichnl. 2**		**Minichnl. 3**	
Parameter	**unit**	**min**	**max**	**min**	**max**	**min**	**max**
Mass flow rate	g/s	1.04	5.60	1.33	6.40	1.08	4.88
Inlet pressure	bar	3.01	4.74	2.50	6.49	2.97	4.81
Inlet temp.	ºC	0.72	15.04	-4.30	24.15	0.36	14.55
Inlet quality	-	%0.00	%20.05	%0.00	%42.14	%4.11	%54.36
Pressure drop	bar	0.0003	0.0570	0.0025	0.0269	0.0039	0.0312
Exit pressure	bar	2.95	4.87	2.49	6.48	2.94	4.81
Exit temp.	ºC	0.25	14.90	-4.42	24.10	0.09	25.64
Exit quality	-	%8.82	%45.17	%2.33	%58.19	%20.94	%100

Like in the minitube experiments, in the two-phase flow experiments of the minichannels due to inability of obtaining sufficiently low temperatures to condensate the refrigerant in the refrigerant cooling bath, the pressure of the refrigerant at the inlet of the test section was in the higher levels than the ones in the refrigerator application which are about 1 bar [32]. In the light of the studies in the literature, it is known that saturation pressure has a negligible effect on the heat transfer in two-phase flow. The minimum and maximum values of the pressures obtained in the two-phase flow minichannel experiments are about 2.5 and 6.5 bars respectively as it is seen in Table 8. According to the minimum and

maximum pressure drop values presented for the each minichannel, the lowest and highest values were obtained for the first minichannel and they are determined as 0.0003 and 0.0570 bars respectively. For this reason it is understood that there was not significant pressure drops between the inlet and exit of the test section and the averages of the pressures at the inlet and exit of the test section were accepted as saturation pressures in the experiments.

It should be noted that the quality in the test section was accepted as the average of the refrigerant qualities at the inlet and exit of the test section as similarly accepted in the heat transfer coefficient calculations in the minitube experiments and the studies in the literature. The deviations of the trends followed by the data on the graphs drawn depending on the average quality values, which possibly caused by big variations occurring especially in the third minichannel on the quality along the channel was taken into consideration. The quality was calculated as between 0% and 20.05% at the inlet of the test section, and between 8.82% and 45.17% at the exit of the test section for the first minichannel. Before the experiments of the second minichannel were started, although higher refrigerant quality values were obtained at the inlet of the test section by means of the calibration of the pre-heater for the higher voltage range (4-7V), during the experiments of the second minichannel which has a bigger hydraulic diameter compared with the other minichannels, high mass flow rates, which cause low quality increase along the minichannel, were provided to obtain similar mass fluxes in the experiments for comparison of the minichannels. So the highest quality value obtained at the inlet of the test section in the experiments of the second minichannel was limited with 42%. In case of the experiments of the third minichannel, due to the high amount of heat transferred to the refrigerant from the water side in the test section, big differences between the quality values at the inlet and exit of the test section occurred and to prevent from the single phase flow which possibly can take the place of the two-phase flow at the exit of the test section as much as possible the quality value at the inlet of the test section was not increased over the value of 54.36%. Also in order not to go away too much from the mass flow rate values in the refrigerator applications very high mass flow rates which cause low quality change along the minichannels were not implemented. The experimental data which have the

quality value of 0% at the inlet of the test section were included among the two-phase flow experimental data examined because when investigated the conditions of these experiments it was seen that the refrigerant enthalpy at the inlet of the test section was very close to the enthalpy of the saturated liquid in the saturation pressure and it is known that single phase flow at the inlet of the test section turns into the two-phase flow in a very short distance in the minichannel. Similarly, the experimental data having the quality value of 100% at the exit of the test section in the experiments of the third minichannel were included among the two-phase flow experimental data examined because when investigated the conditions of these experiments it was seen that the refrigerant enthalpy at the exit of the test section was very close to the enthalpy of the saturated vapor in the saturation pressure and it is known that single phase flow at the exit of the test section is formed in a very short distance to the exit of the minichannel.

The minimum and maximum values of the two-phase experiment conditions of the each minichannel are shown in Table 9. Refrigerant pressure drop values show the average refrigerant pressure in the test section.

Table 9: The average refrigerant side parameters for two-phase flow experiments

		Minichannel 1		**Minichannel 2**		**Minichannel 3**	
Parameter	**unit**	**min**	**max**	**min**	**max**	**min**	**max**
Saturation pressure	bar	2.98	4.88	2.49	6.48	2.95	4.81
Saturation temperature	ºC	0.49	14.97	-4.36	24.12	0.22	20.02
Average quality	-	4.41%	32.61%	5.29%	50.17%	%14.48	%69.10

Some of the data having minimum and maximum values given in Table 8 and 9 were not used in the investigations of the minichannels for comparison because of few amounts of the data in the similar conditions.

As similar with the minitube experiments, the minichannel experiments were also conducted by changing the temperature and flow rate in the water side according to the changes of the refrigerant properties in the two-phase flow experiments. After the changes made on the lines followed by the water-ethylene glycol

mixture in the water cycle, the pressure in this cycle changed between 3 and 5.5 bars. Due to almost incompressibility of the liquid water-ethylene glycol mixture, the pressure had no effects on the properties of this mixture. The parameter ranges which occurred during the two-phase flow minichannel experiments in the water cycle are given in Table 10.

Table 10: The range of the parameters in the water side of the test section during the two-phase flow experiments

		Minichannel 1		**Minichannel 2**		**Minichannel 3**	
Parameter	**unit**	**min**	**max**	**min**	**max**	**min**	**max**
Volumetric flow rate	l/min	1.30	1.88	1.68	2.1	1.51	2
Mass flow rate	g/s	23.50	34.04	30.52	37.78	27.17	36.00
Reynolds number	-	127.87	266.77	60.50	226.27	149.66	273.42
Inlet temperature	ºC	8.70	20.87	1.68	30.20	10.95	23.18
Exit temperature	ºC	8.15	20.51	1.09	29.52	9.97	21.99

During the two-phase flow experiments made with the minichannels, the flow rate in the water side was controlled by means of the valves on the rotameters and the flow rate values were read from the rotameter manually. To obtain almost constant wall temperature on the minichannels the volumetric flow rates close to the maximum value, 2.1 l/min, which can be measured by the rotameter were provided in the water side. As it is seen in Table 10 during the minichannel experiments Reynolds number in the test section in the water side did not exceed 274, so in the heat loss calculation in the test section in the water side the thermally developing laminar flow correlations were used. Additionally it is seen that the flow rate in the water cycle of the first minichannel which has the lowest mass flow rate in the water side is about 5 times the highest mass flow rate the same minichannel has in the refrigerant cycle. When the other minichannels are examined it is observed that this ratio is close or higher than this level. When the mean flow rates are handled, it is understood that even the first minichannel having the lowest flow rate in the water side has 8.66 times its refrigerant flow rate for this case. The reason of these high flow rates in the water cycle is being tried to increase the validity of the constant wall temperature approach on the

minichannel surface by decreasing the temperature variation on the surface along the minichannel.

The same approach was pursued in the minichannel experiments for the pre-heater with the one in the minitube experiments. To acquire different quality values along the minichannel in the test section the pre-heater was used by entering the different voltage values in the different experiments. The ranges of the voltage values entered, the heat transferred to the refrigerant from the pre-heater corresponding to the voltage values entered, the viscous heating in the water side in the test section and the heat transferred to the refrigerant from the water side in the test section are shown in Table 11 for the three minichannels.

Table 11: The amount of heat transferred in the test and pre-heater section for the two-phase flow experiments

		Minichannel 1		**Minichannel 2**		**Minichannel 3**	
Parameter	**unit**	**min**	**max**	**min**	**max**	**min**	**max**
Voltage value entered for pre-heater	V	2	6	3	7	2	7
Net power transferred to refrigerant by pre-heater	W	20.21	78.98	34.90	136.86	20.21	136.86
Viscous heating	W	6.52	15.18	2.33	12.65	7.88	15.59
Net heat transferred to refrigerant	W	31.97	125.17	28.67	109.72	105.90	216.61

3.3 FLOW CHART

In this part the way followed during the two-phase flow minichannel experiments after the modifications and adaptations at the end of the copper minitube experiments is shown in a flow order in Table 12 and 13.

Table 12 shows the steps followed until the refrigerant pump is turned on at the beginning of the experiments.

Table 12: Minichannel flow chart (1st part)

1		Turn on the computer, DC power supply, and the data logger.
2		Start the data acquisition program on the computer.
3		Be sure that all valves in the system are open.
4		Check the refrigerant pressure.
5		Is the refrigerant pressure zero?
	YES	Charge the cycle with R-134a. Go back to step 4.
	NO	Continue with step 6.
6		Is the refrigerant in liquid phase* ** ***?
	YES	Continue with step 8.
	NO	Turn on the bath to decrease the temperature. Close the valves before the refrigerant pump and after the micro-flowmeter. Turn on the second pump in the refrigerant cycle. Continue with step 7.
7		Is the refrigerant in liquid phase* ** ***?
	YES	Continue with step 8.
	NO	Charge the refrigerant cycle more with R-134a. Decrease the bath temperature. Increase the flow rate of the second pump. Go back to step 7.
8		Turn off the second pump.
9		Close the valves before and after the second pump.
10		Open the valves before the refrigerant pump and after the micro-flowmeter.
11		Set the refrigerant pump speed to a desired value.
12		Is the refrigerant in liquid phase for the whole cycle* ** ***?
	YES	Continue with step 13.
	NO	Go back to step 6.
	*****	Check from the computer.
	******	Check the sight glass after the refrigerant cooling bath.
	*******	Check the sight glass before the pre-heater.

Table 13 shows the steps followed since the refrigerant pump is turned on until the end of the experiments, including the arrangements of the devices to constitute the desired conditions during the two-phase flow minichannel experiments.

Table 13: Minichannel flow chart (2nd part)

13		Turn on the flowmeter.
14		Turn on the water bath and pump.
15		Turn on the pre-heater and adjust a small power input value.
16		Increase the power input of the pre-heater.
17		Adjust water temperature w.r.t. R-134a saturation temperature.
18		Check the steady-state conditions****.
19		Is the water temperature close to and higher than the refrigerant
	YES	Continue with step 20.
	NO	Go back to step 17.
20		Does the water temperature decrease in the test section?
	YES	Continue with step 21.
	NO	Go back to step 17.
21		Is the constant wall-temperature acquired at the test section?
	YES	Continue with step 22.
	NO	Adjust the flow rate in the water cycle. Go back to step 17.
22		Record the flow rate of the refrigerant (50 readings minimum).
23		Is the refrigerant in two-phase at the inlet* *****?
	YES	Continue with step 24.
	NO	Go back to step 16.
24		Note down the time and record the flow rate in the water cycle.
25		Is the experiment finished for the specified saturation pressure?
	YES	Continue with step 26.
	NO	Go back to step 11 (to change the flow rate)
26		Are the experiments finished for all saturation temperatures?
	YES	**END**
	NO	Change the saturation pressure by charging or discharging the refrigerant. Go back to step 11.
	*****	Check from the computer.
	******	Check the sight glass after the refrigerant cooling bath.
	*******	Check the sight glass before the pre-heater.
	********	50 successful consecutive readings in the range of device accuracy.
	*********	Apply the calculations.

This flow chart was constituted by taking as the model of the flow order chart in the thesis of Tekin [26].

3.4 DATA ANALYSIS

The two-phase flow experiments of the each minichannel were completed by following the flow order stated in Table 12 and 13 and the analysis of the experimental data was made after the experiments. As similar with the procedure applied in the copper minitube experiments, the analysis of the experimental data made for the minichannels can be investigated in the two parts: the analyses of manual measurements and the measurements recorded by the computer.

The manual measurements were made for the flow rates of the refrigerant in the refrigerant cycle and the water-ethylene glycol mixture in the water cycle and the pre-heater power supplied. The flow rates values were read directly from the flowmeters in both cycles during minichannel experiments because they were not recorded by the computer. These measurements were realized about 15 minutes after the steady state conditions were achieved. During the experiments the temperature and pressure measurements were drawn on the graph time dependently by the HP VEE software in the computer and so it was easy to observe on this graph whether the steady state conditions were achieved or not. The monitor of the micro-flowmeter in the refrigerant cycle showed the refrigerant flow rates instantly and there were very small oscillations on the flow rate measurements even in the steady state conditions. So, the refrigerant flow rate was determined by taking the average of at least 50 measurements showed by the flowmeter consecutively. For the flow rate in the water cycle the value read from the rotameter working mechanically was noted down for the each experiment. The flow rates read from the rotameter were stable in the steady state conditions and averaging process was not applied for this measurement in the water cycle.

The pre-heater power was controlled by entering the voltage values in the computer. This voltage value was used to determine the power supplied to the pre-heater. For the each experiment conducted with the minichannels, the

voltage value entered for the pre-heater was recorded manually together with the flow rates and experiment time.

Besides the manual measurements, temperature and pressure measurements were made by the data acquisition system in the experimental set-up automatically. The temperature values were measured by the thermocouples and RTDs placed in different places in the experimental set-up. The pressure values were measured by the pressure transducers. The temperature and pressure values were recorded on the computer. The data logger in the data acquisition system was arranged to collect the data from the temperature and pressure measurement devices in each 15 seconds. When the steady state conditions were achieved, by using the necessary measurement data the quality values in the test section was determined and when two-phase flow was obtained in the test section, the experiment time was recorded and the two-phase flow experiments were repeated for the different mass fluxes and qualities. At the same time with the recorded experiment time, the mass flow rates in the both cycle and the voltage value entered for the pre-heater were recorded for the each experiment. The analyses of the collected data were made at the end of the each experiment day by using the data sheet created by the HP VEE software in the computer. The temperature and pressure values of the each experiment were determined by taking the average values of at least 50 data points after the time at which the steady state conditions were obtained.

3.5 CALCULATIONS

The purpose of the experimental calculation depending on the experimental measurements is to calculate the heat transfer coefficients at different refrigerant qualities in the test section of the refrigerant cycle. To provide two-phase flow along the minichannels, the pre-heater was placed just before the test section. The heat transferred to the refrigerant from the pre-heater was calculated by using Eq. (7) and (8). The quality at the exit of the pre-heater section is the quality at the inlet of the test section as shown in Eq. (12) and the quality at the exit of the pre-heater section was calculated with the help of Eq. (3).

$$h_{he} = h_{ri} \tag{12}$$

where h_{ri} is the refrigerant quality at the inlet of the test section.

The heat transfer from the water side to the refrigerant in the test section was calculated by Eq. (4) including the enthalpy change and viscous heating calculated in Eq. (5) and (11) with the negligible heat loss assumption. The quality of the refrigerant at the exit of the test section was calculated by adding the enthalpy change caused by the heat transferred to the refrigerant from the water side in the test section on to the refrigerant quality at the inlet of the test section as shown in Eq. (13).

$$h_{re} = \frac{\dot{Q}_W}{\dot{m}_R} + h_{ri} \tag{13}$$

where $\dot{m}_R$ is the refrigerant mass flux, h_{re} is the refrigerant enthalpy at the exit of the test section. The temperature of the refrigerant at the exit of the test section was considered as the one calculated by using the pressure and enthalpy value at that point. Due to oscillations on temperatures in two-phase, instead of temperature pressure was taken in to consideration as mentioned before. Additionally the refrigerant quality at the exit of the test section was calculated with the help of the known pressure and enthalpy values at that point.

For calculation of the average heat transfer coefficient in the minichannels, knowing the wall temperature was needed. The data having at most 0.5°C wall temperature difference along the minichannel were investigated in the calculations. 0.5°C was selected as the maximum allowable temperature difference because 0.5°C is the measurement sensibility of the seven thermocouples placed on the outer surface of the minichannels with the equal distances to designate the wall temperature. The wall temperature was determined by taking average of the measurements of these seven thermocouples. The temperature difference occurring between the inlet and exit of the test section due to pressure drop along the minichannel led to using the logarithmic mean temperature difference method in the calculations as shown in Eq. (14).

$$\Delta T_{LM} = \frac{(T_w - T_{ri}) - (T_w - T_{re})}{ln\left(\frac{T_w - T_{ri}}{T_w - T_{re}}\right)} \quad (14)$$

where T_w is the wall temperature, T_{ri} is the refrigerant temperature at the inlet of the test section, and T_{re} is the refrigerant temperature at the exit of the test section.

The inner heat transfer area for the minichannels was calculated using Eq. (15).

$$A_i = P_h L \quad (15)$$

where A_i is the inner heat transfer area, P_h is the heated perimeter inside the minichannels and L is the length of the minichannels. In the calculation of the heated perimeter inside the minichannels, it was assumed that the heated perimeter inside the minichannels is same with the wetted perimeter inside the minichannels because of their very small heights compared to their widths. The overall heat transfer coefficient for the minichannels was designated in terms of the inner heat transfer area as stated in Eq. (16).

$$U_i = \frac{\dot{Q}_W}{A_i \Delta T_{LM}} \quad (16)$$

where U_i is the overall heat transfer coefficient.
For each minichannel by considering the walls of the minichannels as flat plate the average heat transfer coefficient was calculated. The equation used for this purpose is given in Eq. (17).

$$\bar{h}_{TP} = \left(\frac{1}{U_i} - \frac{t}{k_{Al}}\right)^{-1} \quad (17)$$

where $\bar{h}_{TP}$ is the average heat transfer coefficient for the two-phase flow in the test section, t is the thickness of the minichannel wall and k_{Al} is the thermal conductivity of aluminum which the minichannels were made up of.

CHAPTER 4

EXPERIMENTAL DATA, RESULTS AND DISCUSSION

In this section the experimental findings of the 3 minichannels having different geometries (see Figure 1 and Table 1 for geometries) provided by Arcelik Inc., are presented. The analyses regarding the heat transfer coefficient and the pressure drop for the each minichannel are indicated separately and a comparison is made by evaluating the 3 minichannels together. Each minichannel is investigated at constant mass flux and constant quality in terms of heat transfer coefficient and pressure drop on four graphs. The numbers of the minichannels in the parentheses near the values held constant indicate which minichannel they belong to.

4.1 HEAT TRANSFER COEFFICIENT

In accordance with the purpose of the project the two phase flow experiments have been done and the experimental data for the each minichannel are evaluated considering the heat transfer coefficient and the pressure drop at constant quality and constant mass flux. In this section the heat transfer coefficient is discussed. No comparison is made at constant wall heat flux values due to the constant wall temperature approach followed in the experiments.

4.1.1 Constant Quality

Similar to the copper minitube experiments made by Tekin [26] also in the minichannel experiments the flow in the minichannel could not be conditioned at a constant quality value. Providing that within the limits of a definite error margin the constant quality value is decided based on the average of the approximate

quality values. The quality value of the refrigerant calculated for an experiment is the average of the quality values at the inlet and the exit of the test section.

Minichannel 1

In this section, 2 different constant qualities are determined regarding to the analysis of the data obtained in the two-phase flow experiments done with the first minichannel. The relationship between the mass flux and heat transfer coefficient is examined at the constant quality values. In Table 14, the experimental data and calculations can be found of the 7% and 12% which are the constant refrigerant quality values of the first minichannel. In Figure 24, the change in the heat transfer coefficient by the mass flux at the constant quality values is presented on the graph.

Due to the pre-heater calibration implemented within 1-4 V before the two phase experiments done for the first minichannel the pre-heater has been used within this calibration interval throughout the experiments carried out with this minichannel. Resulting from the flow meter not being able to measure the flow rate less than 1 g/s the flow rate being more than stated rate were carried out. The quality could not be increased over 32.61% due to the high mass flux and the inadequacy of the maximum heat input provided by the pre-heater in its calibration interval. When the qualities obtained were investigated, 12% was determined as the highest quality which can be evaluated as a constant quality value.

In Figure 24, between the mass fluxes of 175-275 kg/m^{2}s, it is seen that the heat transfer coefficient values change around 1750 W/m^{2}K in a very narrow range, even remain almost constant with the increase in mass flux analyzing the data at the refrigerant quality of 7%. The data at 12% constant quality are obtained between the mass fluxes of 90-151 kg/m^{2}s on the same graph and the invariable heat transfer coefficient tendency with increasing mass flux derived at 7% constant quality is also observed at 12% constant quality. The heat transfer coefficient being approximately constant is calculated as 2020 W/m^{2}K at 12% constant quality by using the data given in Table 14.

It is remarked that at 7% and 12% qualities, the heat transfer coefficient at the highest values in the stated mass flux intervals increased a little.

Table 14: Heat transfer coefficient and mass flux values for constant refrigerant qualities (Minichannel 1)

7%			**12%**		
x	**G**	**h_{exp}**	**x**	**G**	**h_{exp}**
%	**kg/m²s**	**W/m²K**	**%**	**kg/m²s**	**W/m²K**
6.58	175.65	1689.09	10.21	90.11	1996.45
6.71	274.63	2038.76	11.35	156.33	2147.28
7.87	241.52	1598.73	11.54	125.99	1963.23
8.08	231.30	1619.69	11.81	130.42	1813.99
			12.92	151.01	2244.56
			13.95	115.54	1968.26

It is remarkable that the qualities at which the test data are evaluated are the average of the inlet and outlet qualities of the minichannel in the test section. It should be noted that in spite of the handled data, which have the same or very close quality values, the data having different inlet-outlet qualities have an effect on the differences in the heat transfer coefficients, which are obtained at the same quality and approximately the same mass flux.

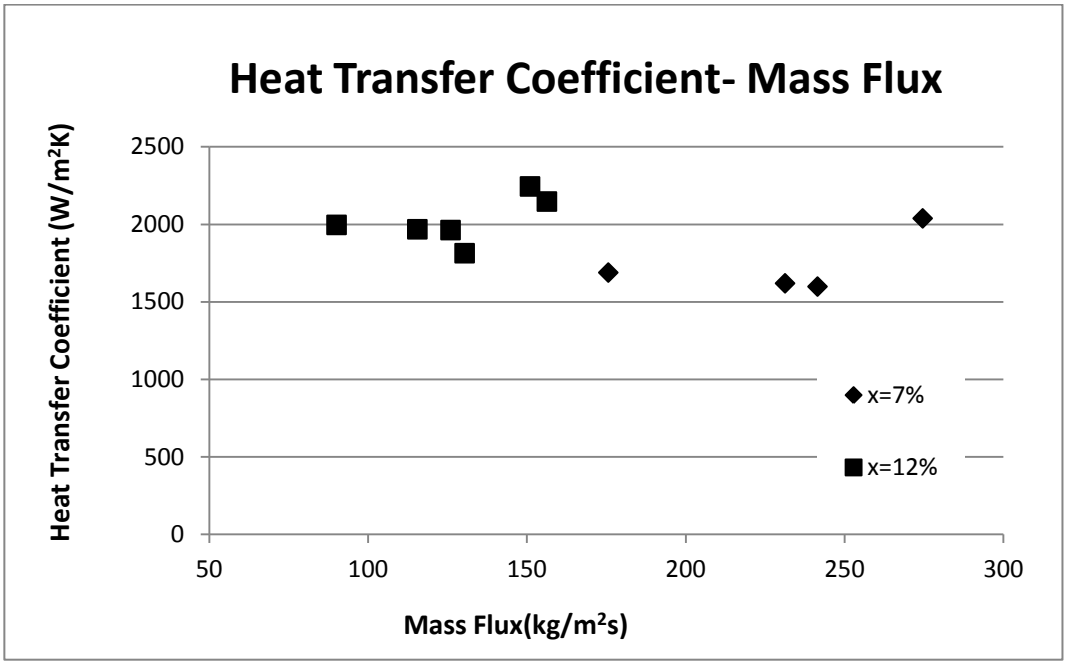

Figure 24: Change in heat transfer coefficient by mass flux for constant refrigerant quality (Minichannel 1)

Minichannel 2

In this section, the two-phase experimental data gathered from the second minichannel are evaluated at the constant qualities. Table 15 shows the test data undertaken for 3 different qualities at 2.2%, 4.6% and 12% for the minichannel 2 as the change in the heat transfer coefficient values by the mass flux is presented in Figure 25.

The pre-heater is calibrated at between 4-7 V before the two-phase flow experiments is implemented for the second minichannel, thereby the peak power becomes 150 W that is energized by the pre-heater so this enables the heat transfer which is from the pre-heater to the refrigerant to reach high levels. In order to obtain the mass flux values at the same level which are gained from the other minichannel experiments the flow rate of the refrigerant passing through the second minichannel is held as high flow rate comparing to the flow rates of other minichannels due to the bigger hydraulic diameter of the second minichannel

(see Table 1). In spite of the heat quantity transferred from the pre-heater to the refrigerant the increase in the flow rate of the refrigerant enables the quality taken along the minichannel to reach at 50.17%. The highest quality is determined as 12% at the constant quality regarding to the given data.

Table 15: Heat transfer coefficient and mass flux values for constant refrigerant quality (Minichannel 2)

2.2%			**4.6%**			**12%**		
x	**G**	**h_{exp}**	**x**	**G**	**h_{exp}**	**x**	**G**	**h_{exp}**
%	**kg/m²s**	**W/m²K**	**%**	**kg/m²s**	**W/m²K**	**%**	**kg/m²s**	**W/m²K**
1.16	69.73	6802.53	3.44	75.19	2206.53	11.25	96.06	5088.30
1.39	68.61	1686.62	3.49	78.26	1943.29	11.26	95.55	4498.53
1.57	64.41	4415.55	3.84	79.55	9048.98	12.53	95.85	5749.79
1.68	63.74	1950.35	4.01	82.34	3507.62	12.87	47.77	1699.02
1.85	65.70	2006.47	4.13	79.36	5796.61	12.93	47.64	2293.00
1.89	58.25	2877.86	4.46	79.65	4448.53	12.94	93.59	7667.86
2.00	59.94	1439.85	4.49	78.21	3876.96	13.07	92.94	8409.95
2.32	66.04	1381.14	4.50	78.45	3115.36	13.44	90.76	5846.00
2.50	67.32	2223.84	4.84	49.39	1441.25	13.48	93.26	3743.00
2.81	68.77	2218.03	5.18	79.58	2190.02	13.51	91.03	5364.61
2.99	78.48	2498.07	5.29	51.04	2001.26			
3.11	60.98	3126.86	5.42	51.19	5909.28			
3.22	77.10	3160.54	5.68	49.11	4300.21			
3.25	74.07	4903.24	5.72	48.77	6428.41			

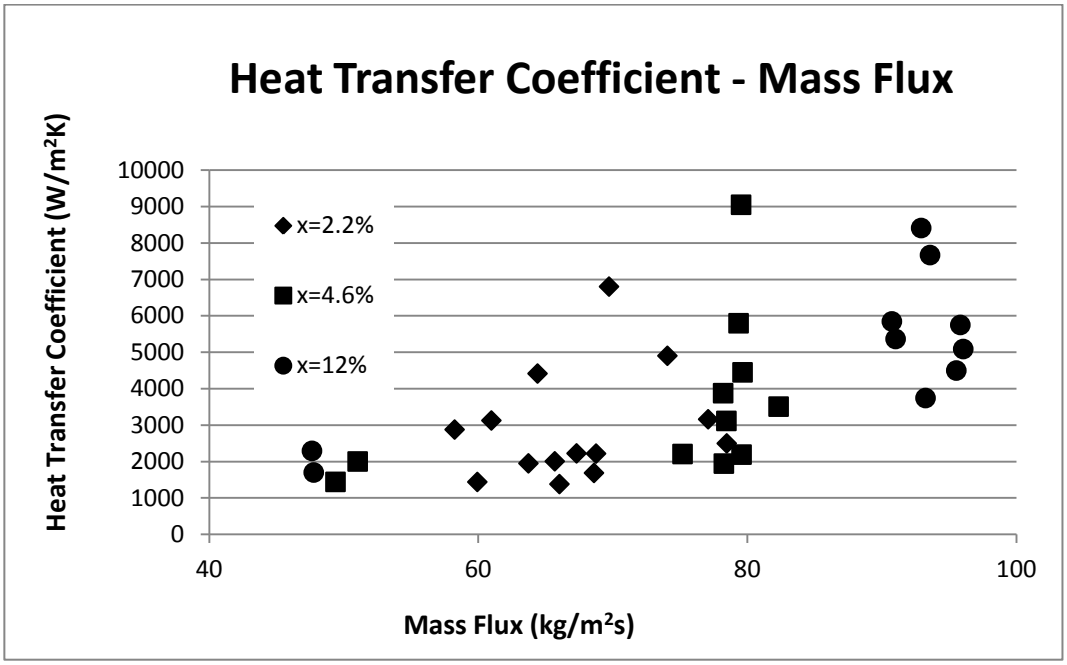

Figure 25: Change in heat transfer coefficient by mass flux for constant refrigerant quality (Minichannel 2)

There might be a couple of reasons for the big differences in the heat transfer coefficient at the close mass fluxes for all quality values in Figure 25. Primarily in the calculation of the average quality some data having “0” value for the inlet quality averaged with the outlet quality value indicates that the average value may not be the real average value. Furthermore, it is emphasized in many researches in the literature that small differences in the quality leads to bigger differences in the heat transfer coefficient value due to the frequent changes in the flow boiling regime at the lower qualities. However it is not possible to determine the flow regimes and their effects on the heat transfer without implementing flow visualization. For instance due to the small and multiple channels it should be conceivable that in the nucleate boiling regime at the lower qualities the sizes of the bubbles are close to the dimensions of the channel and with the effect of the laminar flow the bubbles which cannot strip off the wall may lead to sharp decreases in the heat transfer. Therefore it is plausible to explain the bigger changes in the heat transfer coefficient value at the same mass flux and approximately the same average qualities by the stated above. Likewise the

experimental measuring errors and the assumptions in the calculations and investigations might be effective too. Nevertheless it might be stated that there is a tendency for increase in the heat transfer coefficient value considering the increasing mass flux in the whole given data.

Minichannel 3

Due to the experiments held for the third minichannel being distinctive from the first minichannel and similar to the second minichannel higher heat transfer was reached by using the pre-heater at the calibration range of 4-7 V. The large hydraulic diameter caused by the geometry of the second minichannel is different from the diameter of the third minichannel rather the third minichannel has the same hydraulic diameter as the first minichannel. (see Table 1) Obtaining the quality at the larger interval was enabled due to the higher heat transfer achievement from the pre-heater to the refrigerant and the appropriate arrangement of the refrigerant flow rate for the hydraulic diameter of the third minichannel.

It is significant to notice the grooved structures in the interior surface of the minichannel. This kind of surface roughness results in a bigger real heat transfer surface comparing to the calculated heat transfer surface. This states that the calculated heat transfer coefficient value is bigger than the real heat transfer coefficient value arising from the real heat transfer surface being bigger than the calculated heat transfer surface.

The data from the two phase flow experiments implemented for the third minichannel are evaluated at 28%, 35%, 43% and 57% being 4 different constant quality values. It is found out that in the two-phase flow experiments of the third minichannel the significant changes in the refrigerant quality value comparing to the ones taken in the other minichannels and the bigger qualities comparing to the ones provided in the other minichannels were obtained in spite of implementing the flow rate being closer to the highest flow rates had in other minichannel experiments due to the positive effect on the heat transfer by the grooved interior surface which will be evaluated in the subsequent sections.

Table 16 shows the experimental data and calculation results evaluated at the constant qualities and the graph displaying these values are presented in Figure 26.

Table 16: Heat transfer coefficient and mass flux values for constant refrigerant quality (Minichannel 3)

28%			**35%**		
x	**G**	**h_{exp}**	**x**	**G**	**h_{exp}**
%	**kg/m²s**	**W/m²K**	**%**	**kg/m²s**	**W/m²K**
27.39	102.8	7850.5	32.40	111.6	11678.7
29.61	81.9	16925.5	34.23	69.3	8400.9
29.78	100.4	7604.8	34.69	108.5	12730.1
30.34	95.8	6921.3	34.78	93.7	8075.8
30.42	98.6	17645.5	37.59	63.9	9088.0
			38.16	79.8	16597.5
43%			**57%**		
x	**G**	**h_{exp}**	**x**	**G**	**h_{exp}**
%	**kg/m²s**	**W/m²K**	**%**	**kg/m²s**	**W/m²K**
41.63	85.1	8052.3	56.14	76.0	10767.7
41.87	101.7	12597.7	56.17	61.0	9888.7
41.91	74.8	9497.4	56.18	69.9	8419.7
45.43	91.1	8400.8	57.93	91.5	11310.5
46.00	97.8	6374.4			

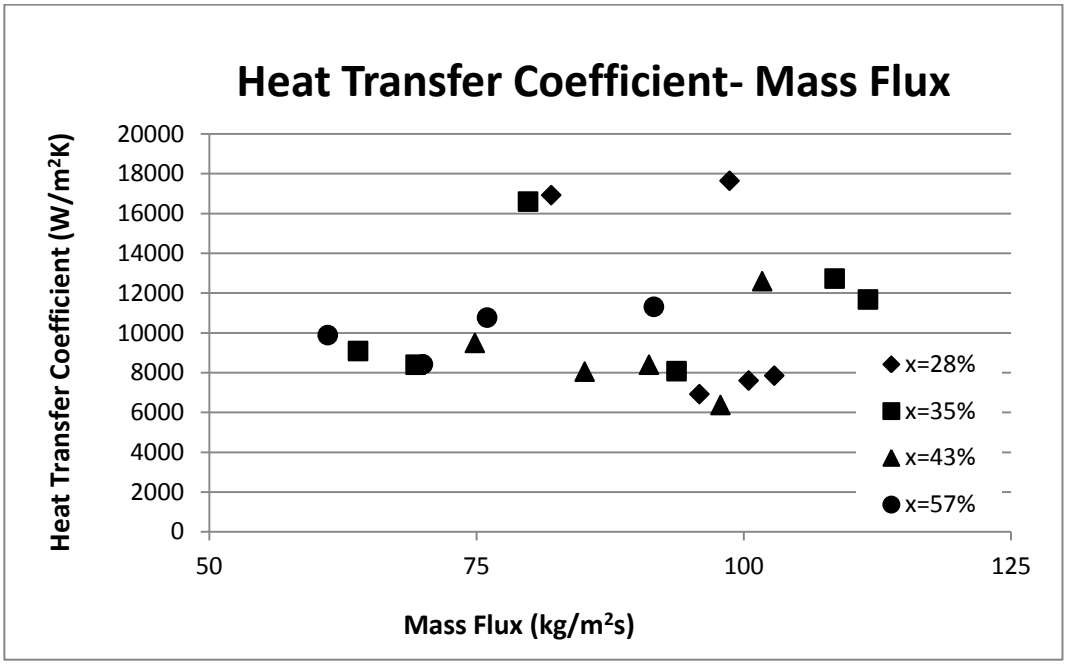

Figure 26: Change in heat transfer coefficient by mass flux for constant refrigerant quality (Minichannel 3)

Among the data evaluated for the constant quality it cannot be shown a significant tendency regarding to the relation between the mass flux and heat transfer coefficient resulting from a major change at the refrigerant quality along the channel and the studied quality's being the average of the inlet and outlet quality values. Similar statements like the explanations about the flow boiling regimes for the second minichannel might also be given for this part too. For this minichannel the qualities which are more different than each other (the quality values in the wider range) were determined as the constant quality values with respect to the qualities determined as constant in the other minichannel experiments. For example, as it can be seen in Table 16 the data analyzed at 28% quality vary from 24.42% to 30.42% quality values. This stated situation is also effective on the weak tendency among the studied parameters.

When 28% quality value is investigated, again the different heat transfer coefficient values are obtained at the same quality and approximately the same mass flux (averagely 96 kg/m^{2}s). In this mass flux the average heat transfer

coefficient value is calculated approximately as 11390 W/m^{2}K. Still there cannot be shown an obvious tendency at 35% and 43% quality values, there can be established an increasing heat transfer coefficient tendency in response to an increasing mass flux when a trendline is drawn among the given data. It is observed that the increase in the heat transfer coefficient by the increase in mass flux with 4 studied data at 57% quality.

Comparison of the Minichannels

In this section, the relation between the mass flux and heat transfer coefficient is evaluated by determining the constant refrigerant quality values enabling to make a comparison among them for the each minichannel from the experimental data of 3 analyzed minichannels. The comparison is made by selecting the qualities such as 12% from the first minichannel, 12% from the second minichannel, 28% and 35% from the third minichannel. In Table 17 and Figure 27 the relation between the mass flux and heat transfer coefficient at the stated qualities can be found.

The third minichannel is analyzed at least 28% quality yet it could not be reached the qualities being at the stated (28%) quality level averagely for the other minichannels. The difficulty for obtaining higher qualities has been stated in the literature too [33]. In the comparison of the second and third minichannels it can be seen that the whole heat transfer coefficients gathered from the third minichannel experiments are higher than the coefficients gathered from the second minichannel experiments. It should be noticed that this comparison is made at a lower mass flux in the second minichannel.

It is found out that the second minichannel has a higher heat transfer coefficient at approximately 92 kg/m^{2}s mass flux when the first and second minichannel are analyzed at 12% quality. Furthermore, it is seen that the increase in the heat transfer coefficient of the second minichannel is larger in response to the same level increase in the mass flux at the stated quality. This tendency at the stated quality might indicate to obtain the larger heat transfer coefficients for the second minichannel comparing to the first one at the mass fluxes more than 50 kg/m^{2}s.

Particularly, at the mass flux interval consisting of 64-112 kg/m^{2}s the heat transfer coefficient of the third minichannel is significantly higher than the other two minichannels' when the data of 3 minichannels are evaluated together. This might be because of the grooved internal structure of the third minichannel. It should also be noted that the quality of the third minichannel is more than the other two minichannels'.

Table 17: Heat transfer coefficient and mass flux values for constant refrigerant quality (Minichannels 1, 2, 3)

12%	Minichannel 1		12%	Minichannel 2	
x	G	h_{exp}	x	G	h_{exp}
%	kg/m²s	W/m²K	%	kg/m²s	W/m²K
10.21	90.1	1996.4	11.25	96.0	5088.3
11.35	156.3	2147.2	11.26	95.5	4498.5
11.54	125.9	1963.2	12.53	95.8	5749.7
11.81	130.4	1813.9	12.87	47.7	1699.0
12.92	151.0	2244.5	12.93	47.6	2293.0
13.95	115.5	1968.2	12.94	93.5	7667.8
			13.07	92.94	8409.9
			13.44	90.76	5846.0
			13.48	93.26	3743.0
			13.51	91.03	5364.6

28%	Minichannel 3		35%	Minichannel 3	
x	G	h_{exp}	x	G	h_{exp}
%	kg/m²s	W/m²K	%	kg/m²s	W/m²K
27.39	102.8	7850.5	32.40	111.6	11678.7
29.61	81.9	16925.5	34.23	69.3	8400.9
29.78	100.4	7604.8	34.69	108.5	12730.1
30.34	95.8	6921.3	34.78	93.7	8075.8
30.42	98.6	17645.5	37.59	63.9	9088.0
			38.16	79.8	16597.5

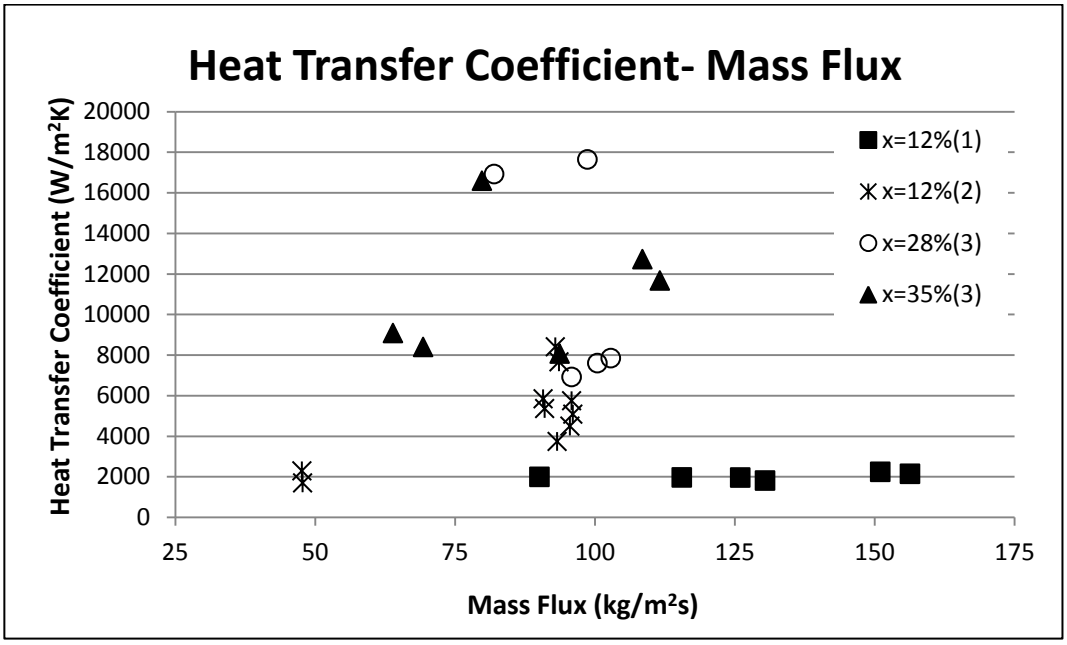

Figure 27: Change in heat transfer coefficient by mass flux for constant refrigerant quality (Minichannels 1, 2, 3)

4.1.2 Constant Mass Flux

In this section the experimental data, which were obtained with the two phase flow experiments, of the three minichannels having different geometries are evaluated by the qualities and heat transfer coefficients at the constant mass flux. During the experiments, although it was tried to keep the flow rate values constant by adjusting the pump power, the same flow rate could not be obtained in every experiment set due to the different temperature and pressure conditions. Similar to the determination of the constant quality case in order to analyze the data, the mass flux values taking as constant are selected to be established from the experimental data having closer mass fluxes at the constant mass flux condition. There is an important point to be taken into account while analyzing the experimental findings. Although the change in the heat transfer coefficient by the quality is given at a constant mass flux value (kg/m^2s) in the figures nevertheless this change does not bring the change in the heat transfer coefficient by the increase in the quality along the flow through the minichannel.

In order to make an evaluation like this, it requires a flow visualization to be done as stated before.

Minichannel 1

67, 94 and 137 kg/m^{2}s being the constant mass fluxes from the experimental data of the two phase flow experiments are determined for the first minichannel and the evaluations on this channel are implemented at the stated mass fluxes. Table 18 presents the experimental data which would be analyzed for the constant mass fluxes and calculation findings. Figure 28 shows the graph of the heat transfer coefficient - quality belonging to the stated values.

Table 18: Heat transfer coefficients and qualities for constant mass fluxes (Minichannel 1)

G			**G**			**G**		
67	**x**	**h_{exp}**	**94**	**x**	**h_{exp}**	**137**	**x**	**h_{exp}**
kg/m²s	**%**	**W/m²K**	**kg/m²s**	**%**	**W/m²K**	**kg/m²s**	**%**	**W/m²K**
51.19	32.61	2840.50	90.11	10.21	1996.45	121.26	14.46	1771.13
58.63	15.62	5440.21	90.67	14.07	3949.19	125.99	11.54	1963.23
63.40	29.43	2153.47	91.55	17.48	2181.20	130.42	11.81	1813.99
74.86	21.33	3162.56	92.12	9.60	2833.15	151.01	12.92	2244.56
79.96	6.52	4959.18	94.78	19.16	1885.95	156.33	11.35	2147.28
80.63	22.60	1943.86	96.59	16.49	1515.51			
			98.31	21.93	2896.33			

Discussing the graph in Figure 28 at 67 kg/m^{2}s mass flux value, it is seen that with the increasing quality there is a decline till 22.60% quality value at the heat transfer coefficient and then there is a slower increase comparing to the decline in the quality. In the same graph the data is gathered from a narrower quality interval at 94 kg/m^{2}s mass flux comparing to the interval at 67 kg/m^{2}s mass flux. The need for the data in a larger quality interval occurs due to not having a clear tendency for the stated data. At 137 kg/m^{2}s mass flux it is found out that the whole data are obtained almost at the same quality. At this point the calculated

average heat transfer coefficient is approximately 1990 W/m^{2}K and quality is 12.41%.

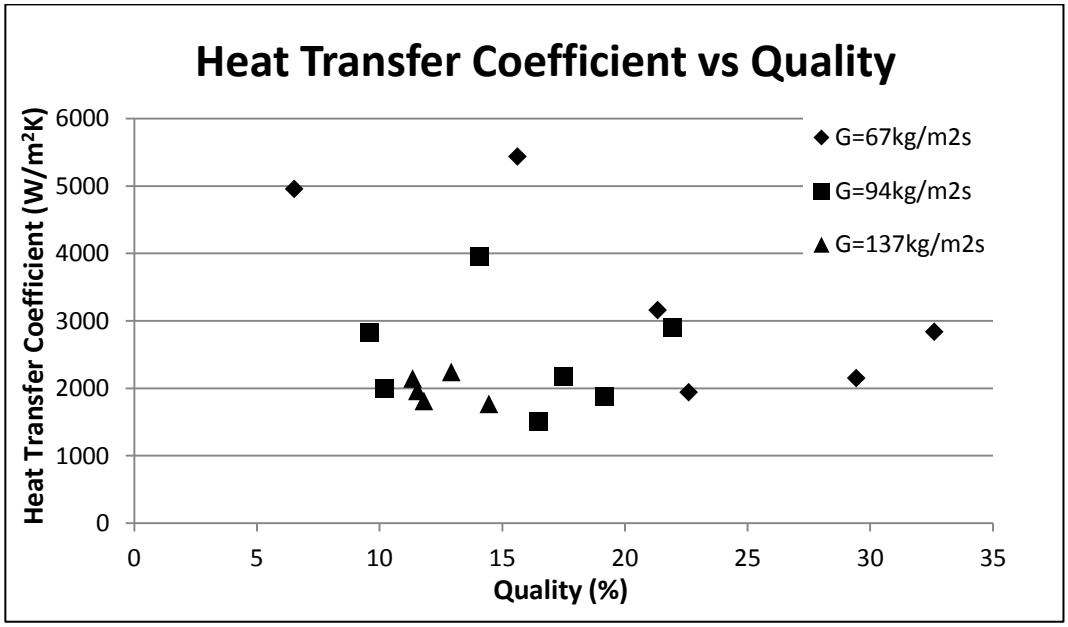

Figure 28: Change in heat transfer coefficient by quality for constant mass fluxes (Minichannel 1)

Analyzing the 3 different mass fluxes together it is shown that the increasing mass flux leads to a narrowing in the quality interval which can be obtained from the experiments. At 12.42% quality value where the data gathered at 137 kg/m^{2}s mass flux it is observed that the decrease in the mass flux leads to an increase in the heat transfer coefficient.

Local quality impacts the heat transfer coefficient value during internal flow boiling. Oscillations occur notably at the inlet of the tubes/channels, in the bubbles on the walls and at the lower qualities. These oscillations lead to the change in the heat transfer coefficient and instability. There would be sharp increases and declines in the heat transfer coefficient. On the other hand as the quality increases the growing bubbles establish a vapor layer by merging. These bubbles cause declines in the heat transfer coefficient value acting as an insulation partly due to the lower heat transfer coefficient of the vapor.

Accordingly the bubble dynamics plays an important role at flow boiling in the tubes/channels. Especially because bubble dimensions in micro/minichannels are comparable to the characteristic dimensions of the channels, the importance of the subject grows. Therefore in order to explain the change in the heat transfer by the quality it is important to determine the flow visualization and flow regime as stated before.

Minichannel 2

The experimental data acquired with the experiments of the second minichannel are evaluated at 48, 60 and 94 kg/m^{2}s constant mass fluxes. Table 19 shows the test data and calculation results taken at the stated mass fluxes. In Figure 29 calculated values are shown as a diagram.

Table 19: Heat transfer coefficients and qualities for constant mass fluxes (Minichannel 2)

G			G			G		
48	**x**	**h_{exp}**	**60**	**x**	**h_{exp}**	**94**	**x**	**h_{exp}**
kg/m²s	**%**	**W/m²K**	**kg/m²s**	**%**	**W/m²K**	**kg/m²s**	**%**	**W/m²K**
46.18	25.99	3567.75	58.25	1.89	2877.86	90.76	13.44	5846.00
46.94	27.18	4078.10	59.67	15.33	5685.61	91.03	13.51	5364.61
47.32	27.72	4894.79	59.94	2.00	1439.85	93.26	13.48	3743.00
47.64	12.93	2293.00	60.49	18.58	6365.46	94.45	10.43	4716.92
47.77	12.87	1699.02	60.98	3.11	3126.86	95.55	11.26	4498.53
49.01	10.18	2845.13	61.44	16.76	4783.45	95.79	9.41	4047.35
49.39	4.84	1441.25				95.85	12.53	5749.79
51.04	5.29	2001.26				96.00	8.64	3373.13
						96.06	11.25	5088.30
						96.58	7.49	3383.63

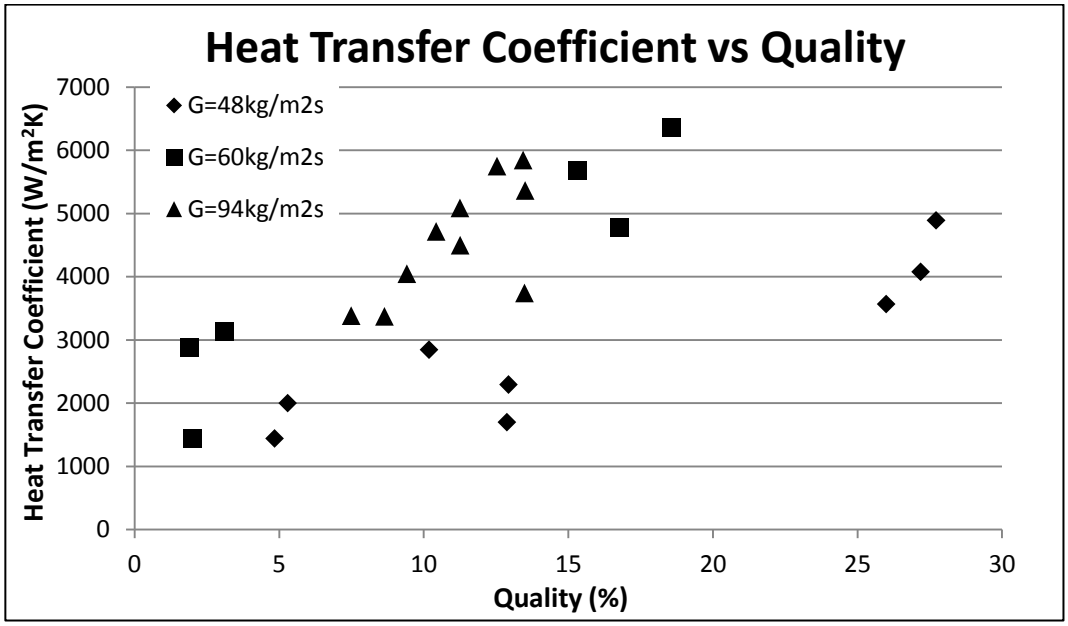

Figure 29: Change in heat transfer coefficient and quality for constant mass fluxes (Minichannel 2)

In Figure 29 it is observed that there is an increase in the heat transfer coefficient from (approximately) 5% quality to 28% quality value when the data are analyzed at 48 kg/m^{2}s mass flux. It is found out that the data can only be taken at the quality interval from 2% to 19% for 60 kg/m^{2}s mass flux. Again at this quality interval it is shown that there is an increase in the heat transfer with the increasing quality. Similar to the tendency realized at 60 kg/m^{2}s mass flux the increase in the heat transfer coefficient is followed by the increase in the quality at 94 kg/m^{2}s mass flux however the data are gathered from a narrower quality interval for this time. Predominantly, the lowest heat transfer coefficients are obtained at the lowest mass fluxes.

Minichannel 3

The data of the two phase flow experiments implemented for the third minichannel are evaluated at 65, 95 and 104 kg/m^{2}s mass fluxes. The information about the parameters of the data belonging to these experiments is shown on Table 20. The data given on the stated table are shown on Figure 30 as a diagram.

Experimental data of the third minichannel at 65 kg/m^{2}s mass flux are acquired at the quality interval from 34% to 77%. The increase in the quality is followed by the increase in the heat transfer coefficient at the stated quality interval. The data at 95 kg/m^{2}s constant mass flux are obtained at 30-60% quality interval. Comparing to the quality interval at 65 kg/m^{2}s mass flux, it is seen that there is an increase tendency in heat transfer coefficient with the increasing quality at a narrower quality interval. With the decline in the quality interval that can be analyzed it is seen that the increase in the heat transfer coefficient is caused by the increase in the quality in this narrower quality interval while holding the experiment with 104 kg/m^{2}s mass flux. There is compatibility between the experimental results at the different mass flux values.

Table 20: Heat transfer coefficients and qualities for constant mass fluxes (Minichannel 3)

65			**95**			**104**		
G	**x**	**h_{exp}**	**G**	**x**	**h_{exp}**	**G**	**x**	**h_{exp}**
kg/m²s	**%**	**W/m²K**	**kg/m²s**	**%**	**W/m²K**	**kg/m²s**	**%**	**W/m²K**
60.02	77.18	14626.07	91.14	45.43	8400.82	100.46	29.78	7604.82
61.09	56.17	9888.75	91.59	57.93	11310.56	101.72	41.87	12597.79
63.92	37.59	9088.05	93.72	34.78	8075.86	102.85	27.39	7850.58
64.14	49.66	9859.70	95.85	30.34	6921.38	108.50	34.69	12730.17
69.31	34.23	8400.94	97.82	46.00	6374.44			
69.99	56.18	8419.71						

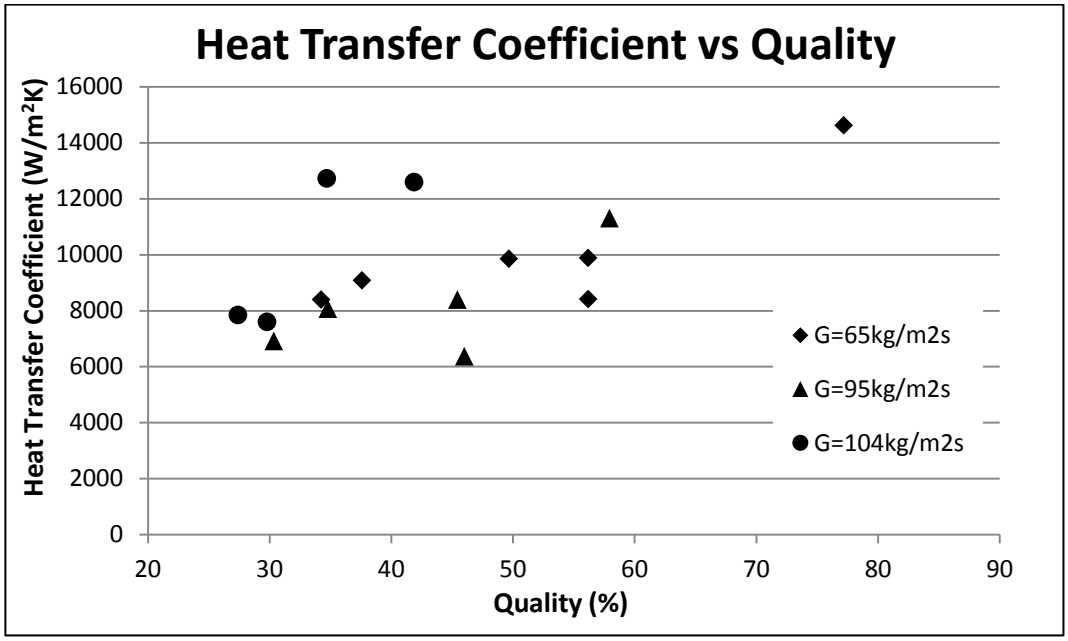

Figure 30: Heat transfer coefficient vs quality for constant mass flux diagram (Minichannel 3)

Comparison of the Minichannels

The comparison between 3 minichannels made at the constant mass flux is implemented at 67 and 94 kg/m^{2}s, 60 and 94 kg/m^{2}s and lastly 65 and 95 kg/m^{2}s mass fluxes respectively for the first, second and third minichannel. The relation between the heat transfer coefficient and quality taken for the experimental data at the stated constant mass flux values can be seen in Table 21 and Figure 31.

In the analysis of the minichannels respectively first, second and third tested at respectively 67 kg/m^{2}s, 60 kg/m^{2}s and 65 kg/m^{2}s mass fluxes it is found out that the data lower than 33% quality can be taken from the first and second minichannels however the data related to third minichannel are bigger than 34% quality value. Due to the third micro channel's providing a higher heat transfer comparing to the other channels' heat transfer and its having big difference between the inlet and outlet refrigerant qualities resulting in a failure to lower down the values at the average quality calculated along the channel, the test data cannot be acquired for the third micro channel at lower qualities and the

same mass flux. The pre-heater power limited with the upper value of the calibration is the reason that there are no values at higher qualities for the data belonging to the first minichannel. For the second minichannel in spite of the use of the pre-heater at larger calibration interval, the amount of the heat needed to be transferred from the pre-heater to the refrigerant is increased to more than 150 W which is the highest value that the pre-heater standing in the testing apparatus can supply concretely and the data at higher qualities cannot be obtained due to the high flow rates worked with during the experiments because of its larger hydraulic diameter.

Table 21: Heat transfer coefficients and qualities for constant mass fluxes (Minichannel 1, 2, 3)

67	**Minichannel 1**		**94**	**Minichannel 1**		**60**	**Minichannel 2**	
G	**x**	**h_{exp}**	**G**	**x**	**h_{exp}**	**G**	**x**	**h_{exp}**
kg/m²s	**%**	**W/m²K**	**kg/m²s**	**%**	**W/m²K**	**kg/m²s**	**%**	**W/m²K**
51.19	32.61	2840.50	90.11	10.21	1996.45	58.25	1.89	2877.86
58.63	15.62	5440.21	90.67	14.07	3949.19	59.67	15.33	5685.61
63.40	29.43	2153.47	91.55	17.48	2181.20	59.94	2.00	1439.85
74.86	21.33	3162.56	92.12	9.60	2833.15	60.49	18.58	6365.46
79.96	6.52	4959.18	94.78	19.16	1885.95	60.98	3.11	3126.86
80.63	22.60	1943.86	96.59	16.49	1515.51	61.44	16.76	4783.45
			98.31	21.93	2896.33			

94	**Minichannel 2**		**65**	**Minichannel 3**		**95**	**Minichannel 3**	
G	**x**	**h_{exp}**	**G**	**x**	**h_{exp}**	**G**	**x**	**h_{exp}**
kg/m²s	**%**	**W/m²K**	**kg/m²s**	**%**	**W/m²K**	**kg/m²s**	**%**	**W/m²K**
90.76	13.44	5846.00	60.02	77.18	14626.07	91.14	45.43	8400.82
91.03	13.51	5364.61	61.09	56.17	9888.75	91.59	57.93	11310.56
93.26	13.48	3743.00	63.92	37.59	9088.05	93.72	34.78	8075.86
94.45	10.43	4716.92	64.14	49.66	9859.70	95.85	30.34	6921.38
95.55	11.26	4498.53	69.31	34.23	8400.94	97.82	46.00	6374.44
95.79	9.41	4047.35	69.99	56.18	8419.71			
95.85	12.53	5749.79						
96.00	8.64	3373.13						
96.06	11.25	5088.30						
96.58	7.49	3383.63						

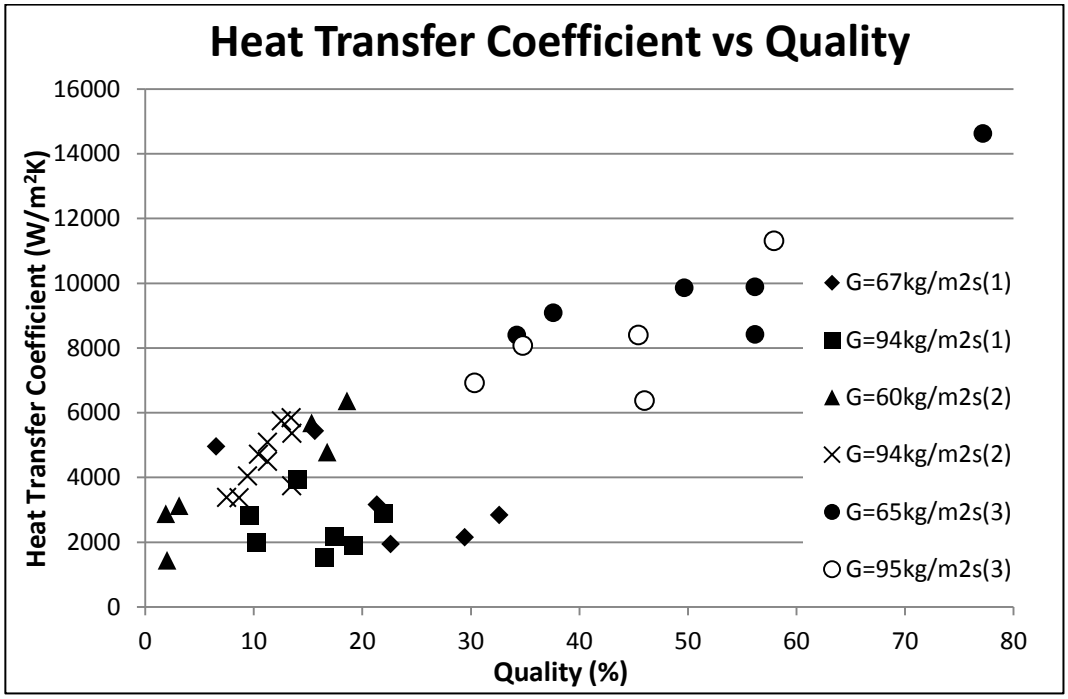

Figure 31: Change in heat transfer coefficient by quality value for constant mass fluxes (Minichannel 1, 2, 3)

As the first and second minichannels being analyzed at 67 and 60 kg/m^{2}s mass fluxes, respectively and quality interval between 0-10% it is observed that the heat transfer coefficient of the only datum taken from this interval at the stated mass flux interval values for the first minichannel is higher than the average value of the data gained from the second minichannel.

Considering the data on Figure 31 it is possible to make a better comparison at 94-95 kg/m^{2}s mass fluxes. The higher heat transfer coefficient values are obtained at 7%-22% quality interval for the second minichannel comparing to the values taken from the first minichannel. Similar to other observations, 95 kg/m^{2}s mass flux value at which the third minichannel is analyzed, enables to acquire the data at higher qualities comparing to the values taken from the experiments of other minichannels. Likewise the data of the third minichannel is higher regarding to the heat transfer coefficient. However in the analysis of the whole values on the diagram it is observed that the change in the average quality of the third minichannel cannot be compared to other two minichannels sturdily. Considering

the need for the complete evaporation in the applications of refrigerators it is noticed that the third minichannel holding higher outlet quality and average quality value would be the best choice regarding to its heat transfer performance in the whole analyzed minichannels. It is required to analyze the pressure drop values of the minichannels in order to make a substantial decision. The following section presents the findings and discussions related to the mentioned subject.

As mentioned before the flow regime plays an important role in the heat transfer during the two phase flow. Despite the fact that the flow visualization cannot be implemented for the current experiment the flow regimes can be estimated roughly based on some analyses. The Lockhart–Martinelli parameter (X_{tt}) given in the Eq. (18) and non-dimensional mass flux defined in Eq. (19) are needed to estimate the flow regime in two phase flow.

$$X_{tt} = \left(\frac{1-x}{x}\right)^{0.9} \left(\frac{\rho_v}{\rho_l}\right)^{0.5} \left(\frac{\mu_l}{\mu_v}\right)^{0.1} \tag{18}$$

$$j_g^* = \frac{xG}{[gD_h\rho_l(\rho_l-\rho_v)]^{1/2}} \tag{19}$$

G is mass flux, ρ is density and μ is viscosity. l and v are subscripts for liquid and vapor. The definition related to the flow regimes can be made by these two values. According to the general definition the flow regimes vary as slug flow for j_g^* < 0.5 and X_{tt} > 1.5, stratified and wavy flow for j_g^* < 0.5 and X_{tt} < 1.0, bubble flow for j_g^* > 1.5 and X_{tt} > 1.5 and annular flow for j_g^* > 1.5 and X_{tt} < 1.0 [27]. Different flow regimes are defined in some studies but the mentioned ones are generally acceptable flow regimes. During flow boiling the heat transfer coefficient is relatively lower in stratified and wavy flow and higher in annular flow.

Sample experimental data are chosen for the whole three minichannels and the flow regimes are estimated by using Eq. (18) and (19). Table 22 presents the results obtained through calculations.

Table 22: Test data and calculations for flow regime estimate in minichannels

	Parameter	Unit	Exp. 1	Exp. 2	Exp. 3	Exp. 4	Exp. 5
Minichannel 1	T_{sat}	ºC	9.37	4.60	12.77	9.76	11.25
	x (%)	-	15.62	17.22	6.52	13.95	17.48
	X_{tt}	-	0.78	0.65	1.97	0.88	0.71
	j_g^*	-	0.45	0.80	0.25	0.79	0.77
	Flow regime	-	Stratified & wavy		slug		
Minichannel 2	T_{sat}	ºC	8.92	12.71	3.03	4.03	21.85
	x (%)	-	1.68	1.89	4.84	3.44	11.26
	X_{tt}	-	6.60	6.29	2.24	3.13	1.33
	j_g^*	-	0.04	0.03	0.09	0.09	0.30
	Flow regime	-	slug	slug	slug	slug	slug
Minichannel 3	T_{sat}	ºC	13.50	0.95	8.31	35.46	11.92
	x (%)	-	41.87	24.42	34.69	77.18	57.93
	X_{tt}	-	0.24	0.41	0.30	0.08	0.13
	j_g^*	-	1.99	2.53	1.89	1.62	2.53
	Flow regime	-	slug	slug	slug	slug	slug

When examining the values in the Table 22 it is observed that the flow regime for the whole current experiments is the annular flow in the third micro channel while supporting the evidence for a higher heat transfer coefficient. It is detected that there are stratified and wavy flow and slug flow regimes according to the classification mentioned above for two experiments in the first minichannel. Low X_{tt} and the values being approximately to 1 indicate the undetermined flow regime in other three data sets studied for the first minichannel is close to stratified and wavy flow regime. Likewise these results support the experimental data of the first minichannel holding relatively lower heat transfer coefficient

values. At last in the analysis of the second minichannel it is expected to acquire a medium level heat transfer coefficient due to the slug flow occurred in whole current experiments furthermore the experimental data indicates that this minichannel has a medium heat transfer performance.

4.2 PRESSURE DROP

Following the comparison between the heat transfer coefficients the minichannels are also evaluated for the pressure drop. The pressure drop values are measured with the differential pressure transducer detecting the pressure drop between the inlet and outlet pressure values in the tested minichannel. Similar to other analysis the pressure drop is also evaluated in two different parts such as constant quality and constant mass flux. While comparing the minichannels, pressure drop values per length of minichannel, instead of pressure drop values directly, are presented because the minichannels which are examined have different lengths which affect pressure drop values direct proportionally.

4.2.1 Constant Quality

The pressure drop values handled in this section are evaluated by using the experimental data analyzed for the heat transfer coefficient.

Minichannel 1

For the first minichannel the experimental data are evaluated at 7% and 12% constant quality values. With the analysis of the data obtained at the mentioned qualities in Table 23 primarily it is seen that the increasing quality enhances the quality interval in which the data are selected. In this case the handled data at lower quality reflect the real-like characteristics of the determined constant quality.

Table 23: Pressure drop and mass flux values at constant refrigerant qualities (Minichannel 1)

%7			%12		
x	G	ΔP	x	G	ΔP
%	kg/m²s	bar	%	kg/m²s	bar
6.52	79.96	0.0003	10.21	90.11	0.0074
6.58	175.65	0.0170	11.35	156.33	0.0350
6.71	274.63	0.0570	11.54	125.99	0.0201
7.87	241.52	0.0561	11.81	130.42	0.0274
8.08	231.30	0.0508	12.92	151.01	0.0380
			13.95	115.54	0.0240

In the analysis of Figure 32 for the first minichannel it is observed that there is an increase in the pressure drop by mass flux at constant qualities. This result is an expected result and compatible with the literature. The same increase in the mass flux leads to more increase in the pressure drop at higher quality values selected as constant.

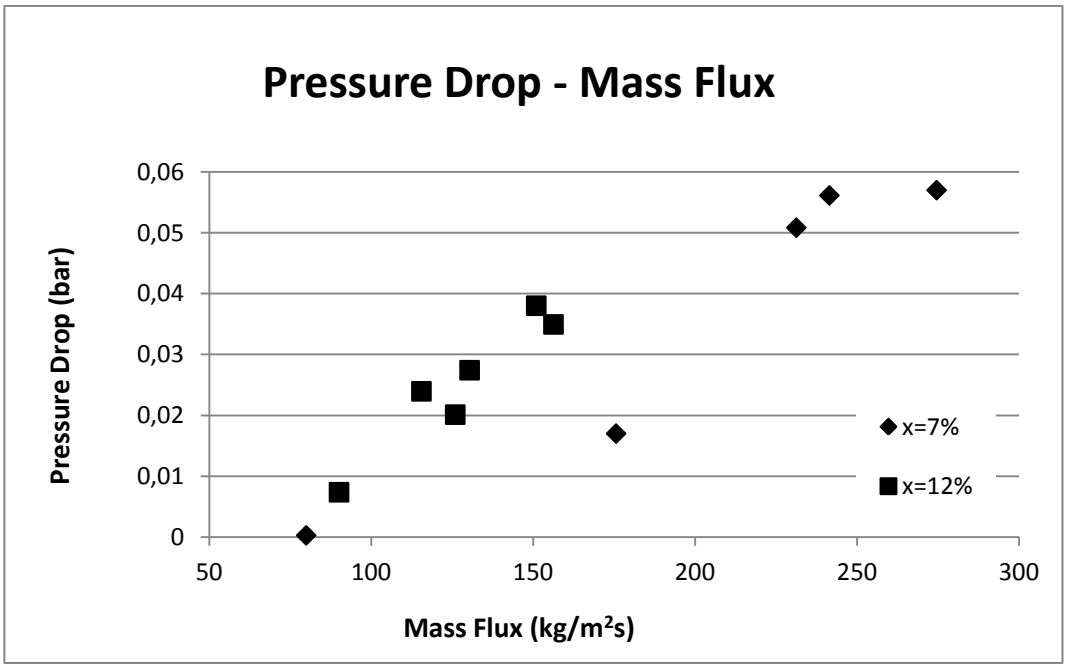

Figure 32: Pressure drop vs mass flux for constant refrigerant quality diagram (Minichannel 1)

Minichannel 2

For the second minichannel the data of two flow phase experiments are evaluated at 2.2%, 4.6% and 12% quality values. Table 24 shows the mass flux and pressure drop values of the experimental data at the stated qualities. In Figure 33 the change in the pressure drop with respect to the mass flux in the experiments at these 5 different qualities are shown as a diagram.

Increase in the mass flux results in increase in the pressure drop at 2.2% quality. The same tendency is also observed at 4.6% and 12% qualities by evaluating the data obtained for these quality values; however the experimental data are not sufficient to show the tendency clearly because the mass fluxes at which the experiments were conducted for this minichannel are far away from each other. It is also realized that a higher pressure drop occurs at higher qualities in the same mass fluxes in Figure 33 by observing the quality tendencies.

Table 24: Mass flux and pressure drop values at constant refrigerant qualities (Minichannel 2)

%2.2			**%4.6**			**%12**		
x	**G**	**ΔP**	**x**	**G**	**ΔP**	**x**	**G**	**ΔP**
%	**kg/m²s**	**bar**	**%**	**kg/m²s**	**bar**	**%**	**kg/m²s**	**bar**
1.16	69.73	0.0029	3.44	75.19	0.0090	11.25	96.06	0.0246
1.39	68.61	0.0035	3.49	78.26	0.0097	11.26	95.55	0.0211
1.57	64.41	0.0027	3.84	79.55	0.0094	12.53	95.85	0.0251
1.68	63.74	0.0029	4.01	82.34	0.0116	12.87	47.77	0.0083
1.85	65.70	0.0038	4.13	79.36	0.0104	12.93	47.64	0.0050
1.89	58.25	0.0028	4.46	79.65	0.0142	12.94	93.59	0.0247
2.00	59.94	0.0029	4.49	78.21	0.0130	13.07	92.94	0.0254
2.32	66.04	0.0044	4.50	78.45	0.0119	13.44	90.76	0.0239
2.50	67.32	0.0051	4.84	49.39	0.0047	13.48	93.26	0.0269
2.81	68.77	0.0056	5.18	79.58	0.0147	13.51	91.03	0.0256
2.99	78.48	0.0086	5.29	51.04	0.0025			
3.11	60.98	0.0046	5.42	51.19	0.0033			
3.22	77.10	0.0082	5.68	49.11	0.0029			
3.25	74.07	0.0078	5.72	48.77	0.0033			

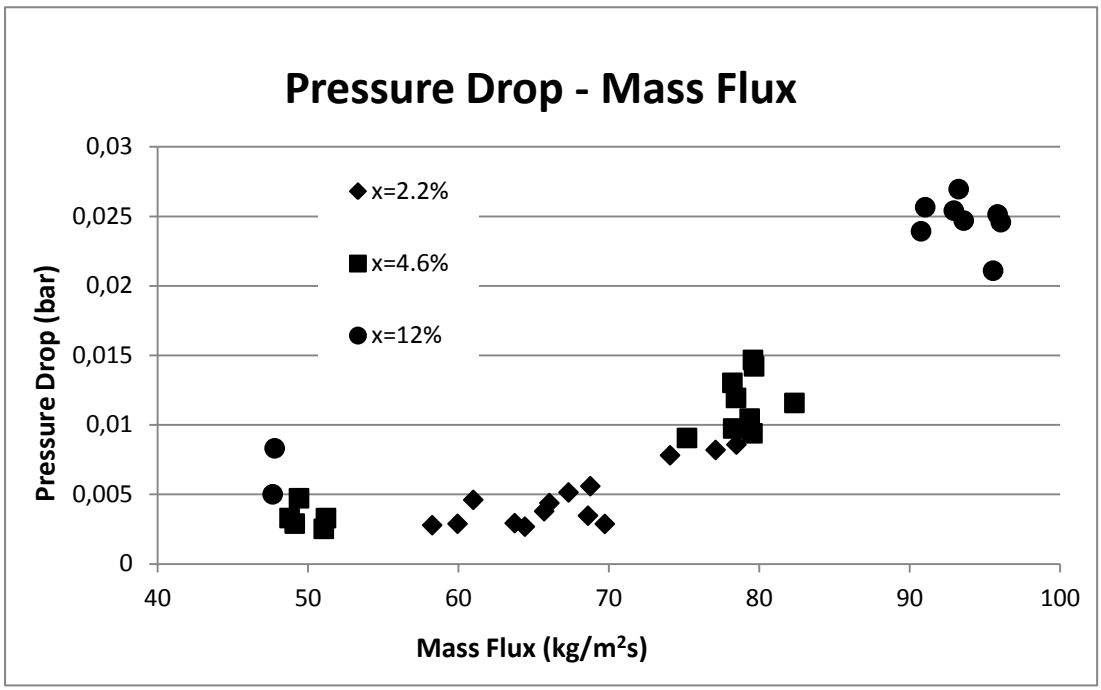

Figure 33: Change in pressure drop by mass flux for constant refrigerant qualities (Minichannel 2)

Minichannel 3

In this part the experimental data of the third minichannel are evaluated for 28%, 35%, 43% and 57% qualities. The corresponding specifications of these experiments which are analyzed for the pressure drop are shown in Table 25. In Figure 34 the pressure drop connected with the mass flux for the mentioned qualities is shown as a diagram.

For every 4 quality values presented in Figure 34 it is observed that there is an increase tendency in pressure drop connected with the increase in the mass flux. As the evaluated quality value is increased it is remarkable that the increase in the mass flux catches up the same tendency at higher pressure drops.

Table 25: Mass flux and pressure drop values at constant refrigerant qualities (Minichannel 3)

%28			%35		
x	G	ΔP	x	G	ΔP
%	kg/m²s	bar	%	kg/m²s	bar
27.39	102.85	0.0071	32.40	111.62	0.0078
29.61	81.99	0.0054	34.23	69.31	0.0039
29.78	100.46	0.0076	34.69	108.50	0.0087
30.34	95.85	0.0072	34.78	93.72	0.0076
30.42	98.67	0.0074	37.59	63.92	0.0039
			38.16	79.82	0.0047
%43			%57		
x	G	ΔP	x	G	ΔP
%	kg/m²s	bar	%	kg/m²s	bar
41.63	85.12	0.0073	56.14	76.00	0.0067
41.87	101.72	0.0073	56.17	61.09	0.0047
41.91	74.85	0.0052	56.18	69.99	0.0062
45.43	91.14	0.0082	57.93	91.59	0.0092
46.00	97.82	0.0098			

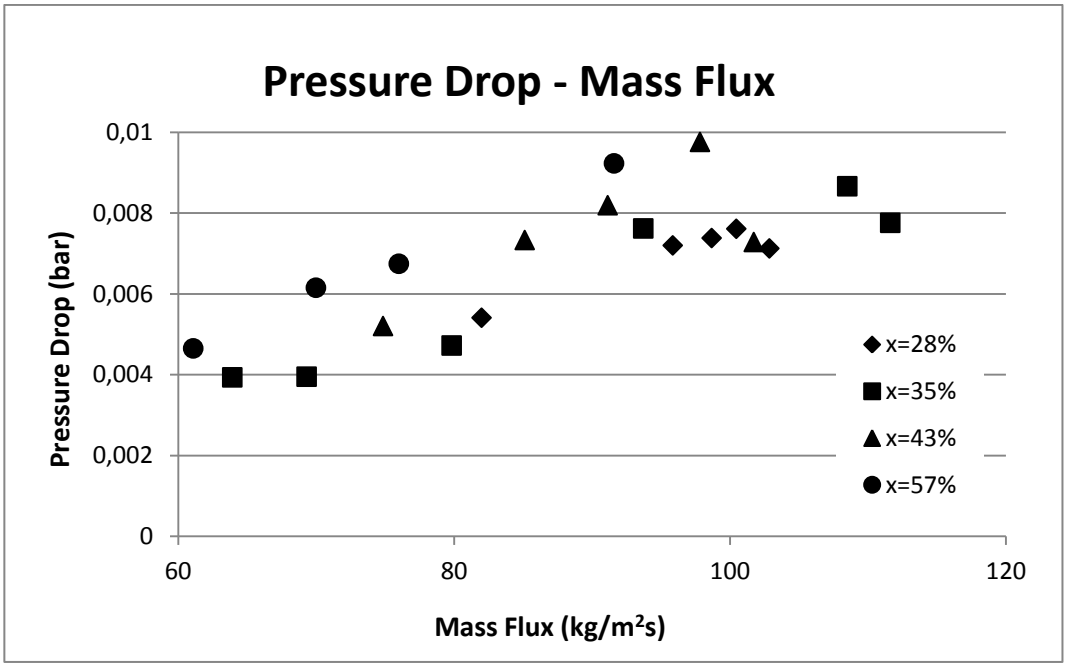

Figure 34: Change in pressure drop by mass flux for constant refrigerant qualities (Minichannel 3)

Comparison of the Minichannels

In this section for the each minichannel constant quality values which can be used to compare the minichannels in terms of pressure drop are determined and mass flux and pressure drop properties depending on these quality values are presented in Table 26 and Figure 35. Pressure drop properties are evaluated per unit minichannel length because of different lengths the tested minichannels have.

All of three minichannels have a tendency of increase in pressure drop with increasing mass flux for each quality value specified. When the data of the first and second minichannels are investigated in the quality of 12% in Figure 35, it is observed that the inclination to increase in pressure drop with increasing mass flux is seen in higher pressure drop values in the same mass flux values for the second minichannel compared to the first minichannel.

Although higher pressure drops with increasing quality values are foreseen in the literature, the tendency of increase in pressure drop with increasing mass flux of the third minichannel becomes in the lower pressure drop values in the same mass fluxes than the other two minichannels'. When the data in this figure are considered, the third minichannel's causing less pressure drops even though in high qualities makes the idea which suggests that this minichannel may be the most appropriate one for refrigerator applications strong.

Table 26: Mass flux and pressure drop values at constant refrigerant qualities (Minichannel 1, 2, 3)

%7	Minichannel 1		%12	Minichannel 1		%12	Minichannel 2	
x	G	ΔP/L	x	G	ΔP/L	x	G	ΔP/L
%	kg/m²s	bar/m	%	kg/m²s	bar/m	%	kg/m²s	bar/m
6.52	79.96	0,0007	10.21	90.11	0,0159	11.25	96.06	0,0558
6.58	175.65	0,0366	11.35	156.33	0,0752	11.26	95.55	0,0479
6.71	274.63	0,1226	11.54	125.99	0,0433	12.53	95.85	0,0571
7.87	241.52	0,1207	11.81	130.42	0,0590	12.87	47.77	0,0189
8.08	231.30	0,1093	12.92	151.01	0,0818	12.93	47.64	0,0113
			13.95	115.54	0,0516	12.94	93.59	0,0561
						13.07	92.94	0,0577
						13.44	90.76	0,0543
						13.48	93.26	0,0612
						13.51	91.03	0,0583

%28	Minichannel 3		%35	Minichannel 3	
x	G	ΔP/L	x	G	ΔP/L
%	kg/m²s	bar/m	%	kg/m²s	bar/m
27.39	102.85	0,0595	32.40	111.62	0,0148
29.61	81.99	0,0136	34.23	69.31	0,0075
29.78	100.46	0,0103	34.69	108.50	0,0165
30.34	95.85	0,0145	34.78	93.72	0,0145
30.42	98.67	0,0137	37.59	63.92	0,0075
			38.16	79.82	0,0090

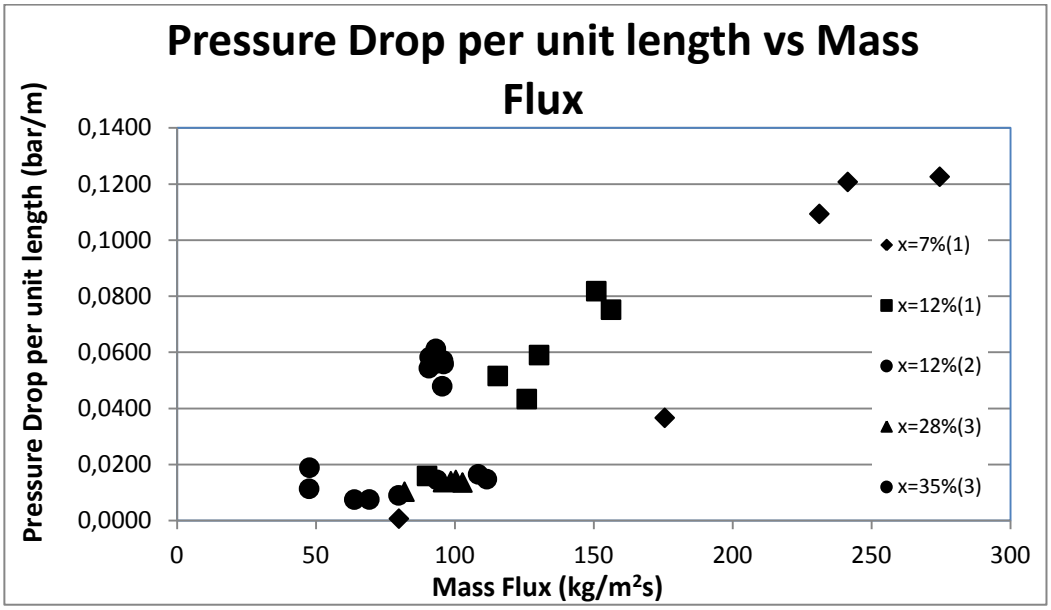

Figure 35: Change in pressure drop by mass flux for constant refrigerant qualities (Minichannel 1, 2, 3)

4.2.2 Constant Mass Flux

Under this title the experimental data, which was obtained with the two phase flow experiments, of the three minichannels are investigated by the qualities and pressure drops at the constant mass flux.

Minichannel 1

In this section the experimental data of the first minichannel are handled at the constant mass fluxes of 67 and 94 kg/m^{2}s. The properties which are compared at these constant mass fluxes are given in Table 27. In Figure 36 for the first minichannel pressure drop change depending on quality is shown.

At 67 and 94 kg/m^{2}s mass fluxes pressure drop increases with increasing quality as expected. Furthermore, trend to increase in pressure drop is higher at higher mass flux, 94 kg/m^{2}s.

Table 27: Pressure drops and qualities for constant mass fluxes (Minichannel 1)

67			94		
G	x	ΔP	G	x	ΔP
kg/m²s	%	bar	kg/m²s	%	bar
51.19	32.61	0.0083	90.11	10.21	0.0074
58.63	15.62	0.0027	90.67	14.07	0.0107
63.40	29.43	0.0116	91.55	17.48	0.0116
74.86	21.33	0.0106	92.12	9.60	0.0091
79.96	6.52	0.0003	94.78	19.16	0.0234
80.63	22.60	0.0142	96.59	16.49	0.0215
			98.31	21.93	0.0268

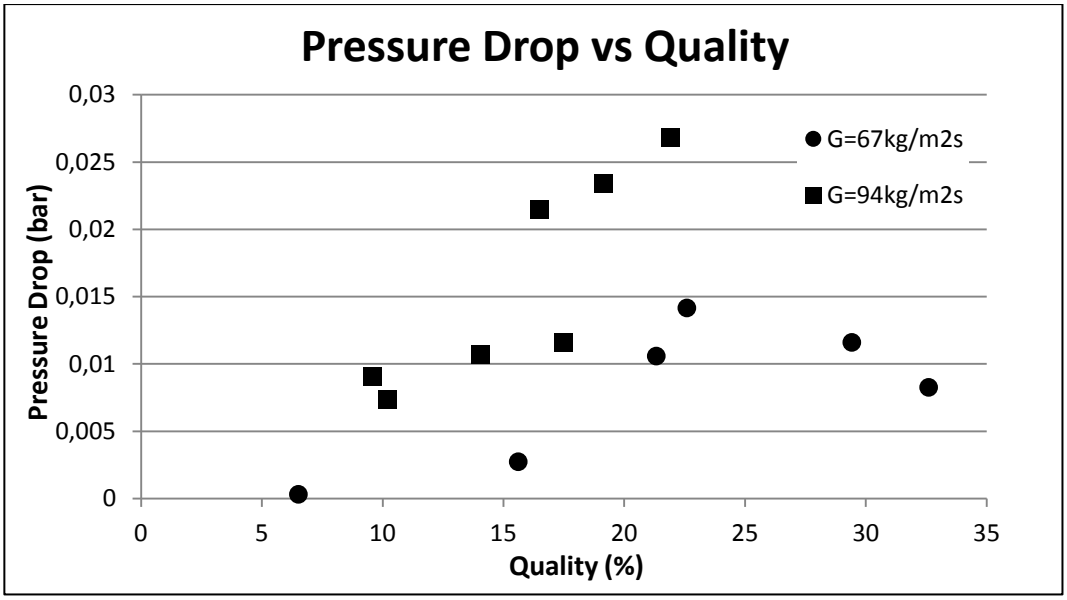

Figure 36: Change in pressure drop by quality value for constant mass fluxes (Minichannel 1)

Minichannel 2

In the second minichannel the constant mass flux values are determined as 48, 60, 67, 77, and 94 kg/m^{2}s. The values which are used in evaluations in terms of pressure drop in these mass fluxes are given in Table 28. Figure 37 includes the

diagram showing the trends between pressure drop and quality values in these specified 5 different mass flux values.

Table 28: Pressure drops and qualities for constant mass fluxes (Minichannel 2)

48			60			67		
G	x	ΔP	G	x	ΔP	G	x	ΔP
kg/m²s	%	bar	kg/m²s	%	bar	kg/m²s	%	bar
46.18	25.99	0.0097	58.25	1.89	0.0028	63.74	1.68	0.0029
46.94	27.18	0.0106	59.67	15.33	0.0133	64.34	14.08	0.0156
47.27	7.60	0.0041	59.94	2.00	0.0029	64.41	1.57	0.0027
47.27	7.85	0.0054	60.49	18.58	0.0166	65.70	1.85	0.0038
47.32	27.72	0.0108	60.98	3.11	0.0046	66.04	2.32	0.0044
47.64	12.93	0.0050	61.44	16.76	0.0151	67.32	2.50	0.0051
47.77	12.87	0.0083				68.61	1.39	0.0035
48.77	5.72	0.0033				68.77	2.81	0.0056
49.01	10.18	0.0058				69.73	1.16	0.0029
49.11	5.68	0.0029						
49.39	4.84	0.0047						
51.04	5.29	0.0025						
51.19	5.42	0.0033						

77			94		
G	x	ΔP	G	x	ΔP
kg/m²s	%	bar	kg/m²s	%	bar
74.07	3.25	0.0078	90.76	13.44	0.0239
75.19	3.44	0.0090	91.03	13.51	0.0256
77.10	3.22	0.0082	92.94	13.07	0.0254
78.21	4.49	0.0130	93.26	13.48	0.0269
78.26	3.49	0.0097	93.59	12.94	0.0247
78.45	4.50	0.0119	94.45	10.43	0.0202
78.48	2.99	0.0086	95.55	11.26	0.0211
79.36	4.13	0.0104	95.79	9.41	0.0194
79.55	3.84	0.0094	95.85	12.53	0.0251
79.58	5.18	0.0147	96.00	8.64	0.0184
79.65	4.46	0.0142	96.06	11.25	0.0246
			96.58	7.49	0.0158

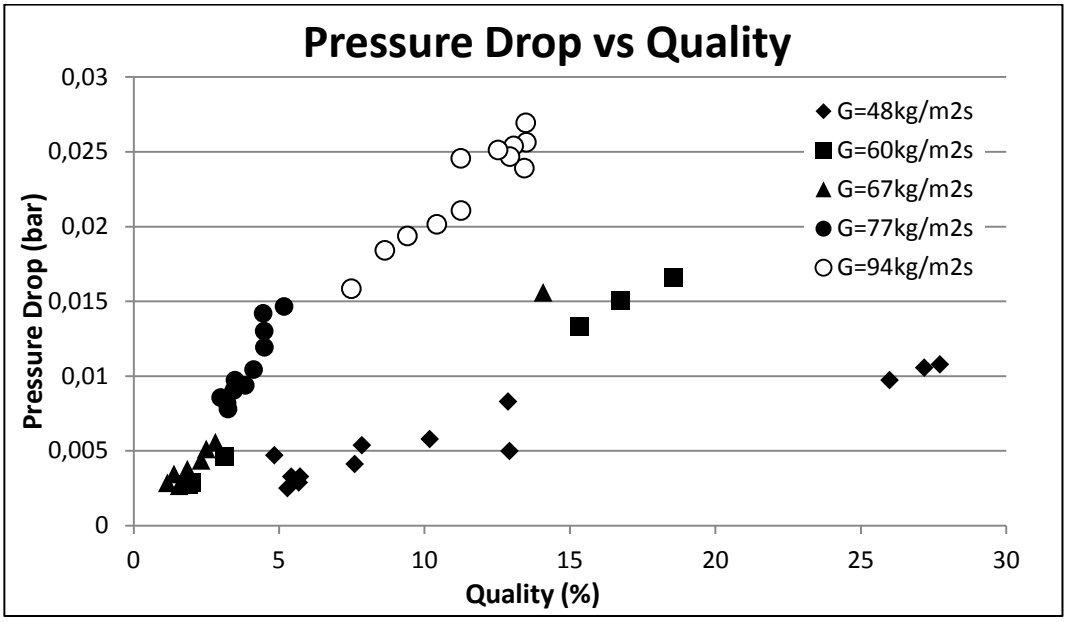

Figure 37: Change in pressure drop by quality value for constant mass fluxes (Minichannel 2)

As seen in Figure 37, in all five specified mass fluxes there is a linear relation between pressure drop and quality. Although there are not any data in some quality ranges at 48, 60, and 67 kg/m^{2}s, the data are enough to determine this direct proportional relation between quality and pressure drop. When examined the data at 48, 60 and 67 kg/m^{2}s mass fluxes together, in the higher mass fluxes at the same qualities higher pressure drops occur and for the same amount of increase in quality higher increases in pressure drop are observed. However though they are not evaluated at the same quality intervals, according to the data obtained from 77 to 94 kg/m^{2}s mass flux less increase in pressure drop depending on increase in quality is observed.

Minichannel 3

The experimental data of the third minichannel are evaluated at 65, 78 and 95 kg/m^{2}s mass fluxes. The information of the required data for investigation of pressure drop at these mass fluxes is given in Table 29. The diagram in Figure

38 shows the change of pressure drop depending on quality at these constant mass fluxes.

When the graph in Figure 38 is examined it is seen that at all mass fluxes there a similar tendency to increase in pressure drop with increase in quality. If the experimental data are examined for the same quality values, it is seen that an increase in mass flux brings with it an increase in pressure drop. This result is compatible with the information in the literature.

Table 29: Pressure drops and qualities for constant mass fluxes (Minichannel 3)

65			**78**			**95**		
Mass Flux	**x**	**ΔP**	**Mass Flux**	**x**	**ΔP**	**Mass Flux**	**x**	**ΔP**
kg/m²s	**%**	**bar**	**kg/m²s**	**%**	**bar**	**kg/m²s**	**%**	**bar**
60.02	77.18	0.0063	74.85	41.91	0.0052	91.14	45.43	0.0082
61.09	56.17	0.0047	76.00	56.14	0.0067	91.59	57.93	0.0092
63.92	37.59	0.0039	76.75	68.50	0.0088	93.72	34.78	0.0076
64.14	49.66	0.0042	79.82	38.16	0.0047	95.85	30.34	0.0072
69.31	34.23	0.0039	81.99	29.61	0.0054	97.82	46.00	0.0098
69.99	56.18	0.0062				98.67	30.42	0.0074

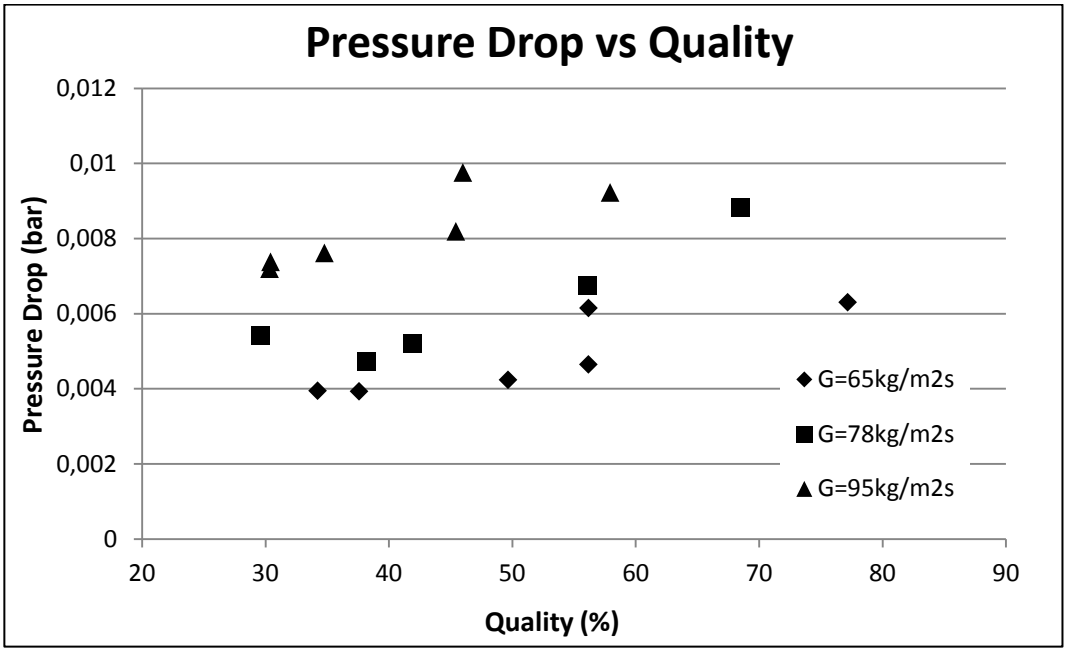

Figure 38: Change in pressure drop by quality value for constant mass fluxes (Minichannel 3)

Comparison of the Minichannels

In this section for the three minichannels the relation between qualities and pressure drops per unit minichannel length corresponding to the mass fluxes at which the minichannels can be compared is examined. The experimental data of the three minichannels to be examined in this section are given in Table 30 and Figure 39. Like comparison of the minichannels at constant qualities, comparison of them at constant mass fluxes is made evaluating pressure drop properties per unit minichannel length because of different lengths the tested minichannels have.

Table 30: Pressure drops and qualities for constant mass fluxes (Minichannel 1, 2, 3)

67	Minichannel 1		94	Minichannel 1		60	Minichannel 2	
G	x	ΔP/L	G	x	ΔP/L	G	x	ΔP/L
kg/m²s	%	bar/m	kg/m²s	%	bar/m	kg/m²s	%	bar/m
51.19	32.61	0,0178	90.11	10.21	0,0159	58.25	1.89	0,0063
58.63	15.62	0,0059	90.67	14.07	0,0231	59.67	15.33	0,0302
63.40	29.43	0,0250	91.55	17.48	0,0250	59.94	2.00	0,0065
74.86	21.33	0,0228	92.12	9.60	0,0195	60.49	18.58	0,0376
79.96	6.52	0,0007	94.78	19.16	0,0503	60.98	3.11	0,0104
80.63	22.60	0,0305	96.59	16.49	0,0462	61.44	16.76	0,0342
			98.31	21.93	0,0577			

67	Minichannel 2		77	Minichannel 2		94	Minichannel 2	
G	x	ΔP/L	G	x	ΔP/L	G	x	ΔP/L
kg/m²s	%	bar/m	kg/m²s	%	bar/m	kg/m²s	%	bar/m
63.74	1.68	0,0066	74.07	3.25	0,0177	90.76	13.44	0,0543
64.34	14.08	0,0355	75.19	3.44	0,0206	91.03	13.51	0,0583
64.41	1.57	0,0061	77.10	3.22	0,0186	92.94	13.07	0,0577
65.70	1.85	0,0086	78.21	4.49	0,0296	93.26	13.48	0,0612
66.04	2.32	0,0099	78.26	3.49	0,0221	93.59	12.94	0,0561
67.32	2.50	0,0117	78.45	4.50	0,0271	94.45	10.43	0,0458
68.61	1.39	0,0078	78.48	2.99	0,0195	95.55	11.26	0,0479
68.77	2.81	0,0127	79.36	4.13	0,0237	95.79	9.41	0,0440
69.73	1.16	0,0065	79.55	3.84	0,0213	95.85	12.53	0,0571
			79.58	5.18	0,0333	96.00	8.64	0,0418
			79.65	4.46	0,0323	96.06	11.25	0,0558
						96.58	7.49	0,0360

65	Minichannel 3		78	Minichannel 3		95	Minichannel 3	
G	x	ΔP/L	G	x	ΔP/L	G	x	ΔP/L
kg/m²s	%	bar/m	kg/m²s	%	bar/m	kg/m²s	%	bar/m
60.02	77.18	0,0120	74.85	41.91	0,0099	91.14	45.43	0,0156
61.09	56.17	0,0089	76.00	56.14	0,0128	91.59	57.93	0,0176
63.92	37.59	0,0075	76.75	68.50	0,0168	93.72	34.78	0,0145
64.14	49.66	0,0081	79.82	38.16	0,0090	95.85	30.34	0,0137
69.31	34.23	0,0075	81.99	29.61	0,0103	97.82	46.00	0,0186
69.99	56.18	0,0117				98.67	30.42	0,0141

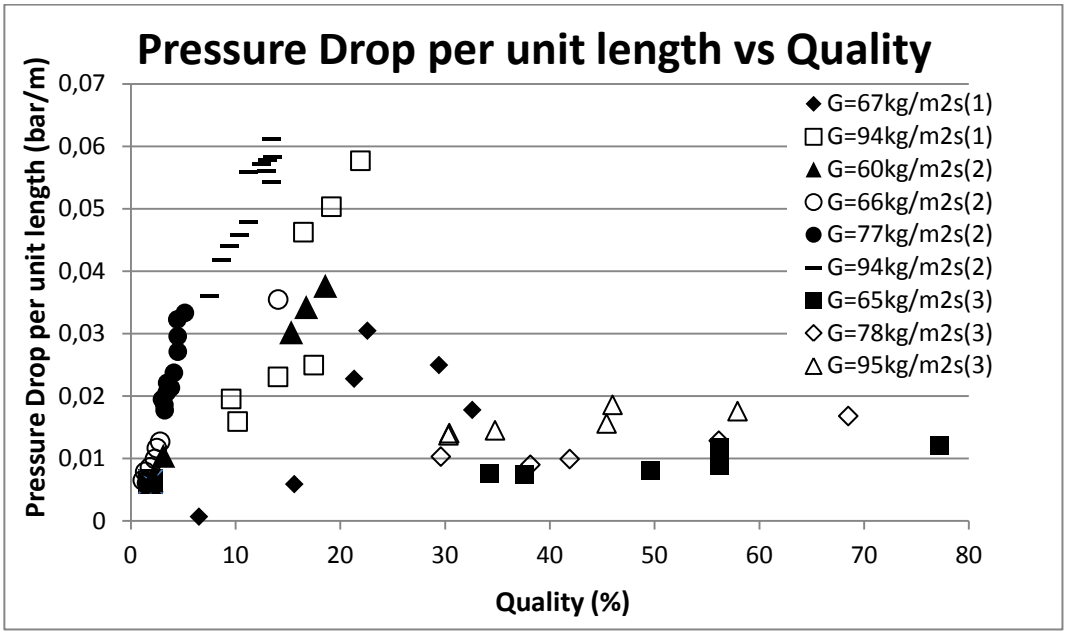

Figure 39: Change in pressure drop by quality value for constant mass fluxes (Minichannel 1, 2, 3)

In Figure 39 when the each minichannel are handled separately, it is understood that increasing mass fluxes result in steeper slopes in the graph, in other words increase in mass fluxes causes more increase in pressure drops with increasing quality values. If the first two minichannels are investigated at 67 kg/m^{2}s mass flux and the third minichannel is investigated at 65 kg/m^{2}s mass flux together, it is seen that the tendency of increase in pressure drop with increasing quality is in the lowest level in the third minichannel.

Also when the first and second minichannels are evaluated at 94 kg/m^{2}s mass flux and the third one is evaluated at 95 kg/m^{2}s mass flux together, the tendencies in the relation of pressure drop and quality of the minichannels are pot in an order from the highest to the lowest as 2nd, 1st, and 3rd minichannel. By looking the tendencies in mass fluxes of 77 kg/m^{2}s for the first minichannel and 78 kg/m^{2}s for the third minichannel the same order of minichannels is observed. In case that Figure 39 is evaluated deeply, in parallel with the results of comparison of the minichannels at constant qualities the third minichannel causes less pressure drops even in high mass fluxes than ones in other two

minichannels, moreover it is determined that this case is valid at high quality values too. When also pressure drop is considered, it is understood that the third minichannel is the most appropriate one for refrigerator applications among the minichannels examined.

4.3 UNCERTAINTY ANALYSIS

To determine the total uncertainty included in the calculated values, the contributions of each variable contained by this value must be considered. If the calculated parameter is "R" and n independent variables, which this parameter is dependent on, are x_1, x_2, x_3, … x_n, R can be written as R = R (x_1, x_2, x_3 , … x_n). Also if the uncertainties of each n independent variables are w_1, w_2, w_3, … w_n and the uncertainty of R is w_R, which can be written as [46]:

$$w_R = \left[\left(\frac{\partial R}{\partial x_1} w_1\right)^2 + \left(\frac{\partial R}{\partial x_2} w_2\right)^2 + \cdots + \left(\frac{\partial R}{\partial x_n} w_n\right)^2\right]^{1/2} \quad (20)$$

By using Eq. (20), the uncertainties of the heat transfer coefficients calculated as the result of two phase flow experiments can be calculated. In the similar way with the application of Eq. (20), it can be written that: $\bar{h}_{TP} = \bar{h}_{TP}(U_i, t, k_{Al})$, $U_i = U_i(\dot{Q}_W, A_i, \Delta T_{LM})$, $\dot{Q}_W = \dot{Q}_W(\dot{Q}_V, \dot{V}_W, \rho_W, h_{we} - h_{wi})$, $A_i = A_i(P_h, L)$, $\Delta T_{LM} = \Delta T_{LM}(T_w, T_{re}, T_{ri})$, $\dot{Q}_V = \dot{Q}_V(Re_W)$, $P_h = P_h(H_{ch}, w_{ch})$, $Re_W = Re_W(\rho_W, u_m, D_h, \mu_W)$, $u_m = u_m(\dot{V}_W, A_c)$, $D_h = D_h(A_c, P_w)$, $P_w = P_w(h_{Al}, w_{Al})$, $A_c = A_c(d, h_{ch}, w_{ch})$, $(h_{we} - h_{wi}) = (h_{we} - h_{wi})(C, (T_{we} - T_{wi}))$, $h_{ri} = h_{ri}(\dot{Q}_{RI}, T_{hi}, P_R)$. The uncertainty values of the measurements and calculated values are given in Table 31.

The uncertainties of the values read from the measurement devices were obtained from the catalogs prepared by the producer companies. The uncertainties of the fitted lines and curves shown in the graphs obtained for determination of fluid properties in both cycles and the rate of heat transferred to the refrigerant from the pre-heater were determined in the range of confidence level of 95% by using linear and polynomial regression methods with the help of MS Excel 2007 software.

Table 31: The values used and calculated in the uncertainty analysis of one experimental data set for each tested minichannels

		Minichannel 1		Minichannel 2		Minichannel 3	
Parameter	**Unit**	**Value**	**Uncertainty**	**Value**	**Uncertainty**	**Value**	**Uncertainty**
H_{ch} (1 port)	mm	1,50	±0,02	3,80	±0,02	1,30	±0,02
w_{ch} (1 port)	mm	1,94	±0,02	3,68	±0,02	2,35	±0,02
h_{Al}	mm	2,10	±0,02	5,00	±0,02	2,10	±0,02
w_{Al}	mm	16,00	±0,02	22,00	±0,02	20,00	±0,02
L	mm	465,00	±0,02	440,00	±0,02	525,00	±0,02
t	mm	0,30	±0,02	0,60	±0,02	0,40	±0,02
d	mm	49,60	±0,02	65,70	±0,02	49,60	±0,02
P_h	mm	48,20	±0,03	68,79	±0,03	51,80	±0,03
P_w	mm	192,02	±0,08	256,11	±0,08	200,02	±0,09
A_i	mm^2	22413,00	±13,19	30268,11	±12,52	27195,00	±14,89
A_{cw}	mm^2	1898,61	±6,24	3285,53	±6,24	1890,21	±6,24
D_{hW}	mm	39,55	±0,13	51,31	±0,10	37,80	±0,13
T_{wi}	˚C	12,55	±0,05	8,92	±0,05	21,77	±0,05
T_{we}	˚C	11,77	±0,05	8,00	±0,05	20,12	±0,05
$T_{w,mean}$	˚C	12,16	±0,03	8,46	±0,03	20,94	±0,03
T_w	˚C	6,40	±0,02	1,62	±0,02	10,87	±0,02
T_{hi}	˚C	-1,02	±0,05	-5,54	±0,05	7,65	±0,05
ΔT_{LM}	˚C	-3,50	±0,06	1,66	±0,09	-1,26	±0,11
P_R	bar	3,30	±0,07	2,90	±0,07	4,04	±0,07
DP	bar	0,0147	±0,0009	0,0147	±0,0009	0,0098	±0,0009
Q_V	W	8,26	±3,71	5,26	±3,22	15,59	±5,20
Q_{RI}	W	20,21	±7,21	34,90	±8,67	84,33	±13,30
Q_W	W	84,75	±7,97	109,72	±8,88	216,61	±10,64
U_i	W/m^2K	1079,19	±103,11	2183,75	±209,88	6304,28	±626,90
k_{Al}	W/mK	228,96	±0,00	228,84	±0,00	229,11	±0,00
h_{TP}	W/m^2K	1080,72	±145,26	2190,02	±469,33	6374,44	±3604,44

CHAPTER 5

SUMMARY, CONCLUSIONS AND FUTURE WORK

This thesis explains the two-phase flow experiments made in three different minichannels having hydraulic diameters of 1.69 mm (smooth), 3.85 mm (smooth) and 1.69 mm (grooved) with the refrigerant R134a and the comparison of these minichannels in terms of heat transfer and pressure drop performances. The benefits of usage of micro/minichannels in different areas and the need for developments on their performances were explained. Negligible saturation pressure effect on heat transfer coefficients in flow boiling was observed in the studies in the literature. Continuous increase or increase up to a peak then a decrease in heat transfer coefficients with increasing quality was another point faced in the literature. As distinct from the experimental studies in the literature, this experimental procedure involves constant wall temperature boundary approach on the minichannels. Also by considering usage of the minichannels in the evaporator section of the refrigerators, mass fluxes of the refrigerant used during the experiments were tried to be kept at lower levels than those used in the experimental studies in the literature.

The experimental set-up constructed for two-phase flow minichannel experiments and the copper minitube experiments carried out by Tekin [26] for the verification of the experimental set-up were mentioned. The changes made on the experimental set-up and the calibrations of the devices used after the verification of the experimental set-up such as replacement of minitube with minichannels and additional devices were explained.

The approach applied and the experimental conditions occurring during the two-phase flow experiments made in the three minichannels were explained in detail. The procedure followed in the minichannel experiments were shown in a flow

chart. By using the experimental data chosen to be used for evaluation of the minichannels, the heat transfer coefficients were calculated for the each minichannel. The heat transfer coefficients calculated and the pressure drops measured were used to compare the tested minichannels by keeping quality and mass flux constant at the specified levels.

As the result of investigations of the experimental data collected from the two-phase flow experiments with R134a in the three minichannels, the conclusions made are as follows:

1. The evaluations made for heat transfer coefficients showed that higher heat transfer coefficients were obtained in the third minichannel than those obtained in the other two minichannels.

2. At the quality of 12% for any constant mass flux value the higher heat transfer coefficients were acquired in the second minichannel with respect to those obtained in the first minichannel.

3. When the first and second minichannels were compared in terms of heat transfer coefficient, especially in the range of 7-22% qualities at 94 kg/m^{2}s mass flux, it is observed that the second minichannel had higher heat transfer coefficients.

4. Evaluation of the pressure drop measurements of the three minichannels showed that pressure drop increased with increasing mass flux and increasing quality. Moreover, the same amount of increases in mass flux and quality caused the highest pressure drop increase in the second minichannel among the three minichannels and the third minichannel had the lowest pressure drop increase.

5. The two-phase flow minichannel experiments showed that by contrast with the expected case increase in the surface roughness did not result in an increase in pressure drop (the third minichannel). It is understood that

the surface roughness decreased the effect of increasing pressure drop of bubble nucleation in two-phase flow in the working experiment conditions.

6. The smaller mass fluxes corresponding to the same mass flow rates were obtained in the second minichannel having larger hydraulic diameter than the other minichannels. For example, while in the first minichannel 2.8 g/s mass flow rate corresponds to 137 kg/m^{2}s mass flux, in the second minichannel 3.2 g/s mass flow rate corresponds to 48 kg/m^{2}s mass flux and in the third minichannel 2.3 g/s mass flow rate corresponds to 65 kg/m^{2}s mass flux. The highest pressure drops measured at these mass fluxes are; 0.0380 bar for the first minichannel, 0.0166 bar for the second minichannel and 0.0087 bar for the third minichannel. By contrast with the comparison of the minichannels for changes in pressure drops with changing mass fluxes, the comparison to be made for mass flow rates instead of mass fluxes shows that at the same mass flow rates the second minichannel would have the higher pressure drops than the first minichannel. For this reason, the second minichannel gets an edge over the first minichannel due to its advantage in heat transfer coefficient and its lower pressure drops at the same mass flow rates.

7. When the third minichannel is considered for pressure drop, it is observed that it is the most ideal minichannel among the three tested minichannels similarly with the case of investigation for heat transfer coefficients. The lowest pressure drop occurring in the third minichannel having a rough inner surface is not an expected result, because it is known that roughness is a factor increasing pressure drop along fluid flow. The low pressure drop value obtained in the third minichannel can be interpreted as follows: roughness of its inner surface prevents the pressure drop increase caused by two-phase flows by disturbing the bubble formation in flow boiling.

In light of the findings obtained as the result of this study, future work which can be carried out is suggested below:

1. The heat transfer coefficient correlations proposed for the similar experimental conditions with the conditions in the current study can be adopted to the experimental data in this study by modifying the experimental coefficients in these correlations.

2. The new correlations can be proposed by repeating two-phase flow experiments for the conditions in which the experimental data are considered to be insufficient or faulty.

3. The three minichannels tested for two-phase flow can be tested for the single phase flow as well.

4. The single or two-phase flow experiments can be carried out for the micro/minichannels whose diameters are determined by CFD analysis for optimum heat transfer in the same experimental set-up.

5. The channels placed vertically or in different positions by using different type of fluids can be tested for two-phase flows in the same experimental set-up. Alternatively the constant wall temperature approach on the channels can be replaced with the constant heat flux approach which can be applied easily.

6. By modifying some parts of the current experimental set-up, new experiments can be conducted by using nanofluids.

7. The two-phase flow correlations proposed in the lliterature may be solved numerically for the current experimental conditions and the results may be compared with the experimental results.

8. The flow regimes can be determined through flow visualization by using high speed cameras.

REFERENCES

[1] Energy Information Administration, Electricity Consumption by End Use in U.S. Households, 2001, http://www.eia.gov/emeu/reps/enduse/er01_us_tab1.html, last visited on 27.01.2012.

[2] Enerji Enstitüsü, Keban Barajı Elektrik Üretim, http://enerjienstitusu.com/tag/keban-baraji-elektrik-uretim/, last visited on 27.01.2012.

[3] Kandlikar, S.G., *Heat transfer mechanism during flow boiling in microchannels*, Journal of Heat Transfer, 2004, 126, pp. 5749-5763.

[4] Tuckerman, D.B., Pease, R.F.W., *High-performance heat sinking for VLSI*, IEEE Electron Dev. Lett. 2, 1981, pp. 126–129.

[5] Kew, P.A., Cornwell, K., *Correlations for the prediction of boiling heat transfer in small-diameter channels*, Applied Thermal Engineering, 1997, 17, pp. 705-715.

[6] Yan, Y.Y., Lin, T.F., *Evaporation heat transfer and pressure drop of refrigerant R-134a in a small pipe*, International Journal of Heat and Mass Transfer, 1998, 41, pp. 4183–4194.

[7] Yang, C.Y., Shieh, C.C., *Flow pattern of air-water and two-phase R134a in small circular tubes*, International Journal of Multiphase Flow, 2001, 27, pp. 1163-1177.

[8] Yarin, L.P., Ekelchik, L.A., Hetsroni, G., *Two-phase laminar flow in a heated microchannels*, International Journal of Multiphase Flow, 2002, 28, pp. 1589-1616.

[9] Agostini, B., Bontemps, A., *Vertical flow boiling of refrigerant R134a in small channels*, International Journal of Heat and Fluid Flow, 2005, 26, pp. 296-306.

[10] Harirchian, T., Garimella, S.V., *Effects of channel dimension, heat flux, and mass flux on flow boiling regimes in microchannels*, International Journal of Multiphase Flow, 2009, 35, pp. 349-362.

[11] Cavallini, A., Col, D.D., Matkovic, M., Rosetto, L., *Pressure drop during two-phase flow of R134a and R32 in a single minichannel*, Journal of Heat Transfer, 2009, doi:10.1115/1.3056556

[12] Consolini, L., Thome, J.R., *Micro-channel flow boiling heat transfer of R-134a, R-236fa, and R-245fa*, Microfluid Nanofluid, 2009, 6, pp. 731-746.

[13] In, S., Jeong, S., *Flow boiling heat transfer characteristics of R123 and R134a in a micro-channel*, International Journal of Multiphase Flow, 2009, 35, pp. 987-1000.

[14] Ong, C.L., Thome, J.R., *Flow boiling heat transfer of R134a, R236fa and R245fa in a horizontal 1.030 mm circular channel*, Experimental Thermal and Fluid Science, 2009, 33, pp. 651-663.

[15] Li, W., Wu, Z., *A general criterion for evaporative heat transfer in micro/mini-channels*, International Journal of Heat and Mass Transfer, 2010, 53, pp. 1967-1976.

[16] Kaew-On, J., Sakamatapan, K., Wongwises, S., *Flow boiling heat transfer of R134a in the multiport minichannel heat exchangers*, Experimental Thermal and Fluid Science, 2011, 35, pp. 364-374.

[17] Kaew-On, J., Sakamatapan, K., Wongwises, S., *Flow boiling pressure drop of R134a in the counter flow multiport minichannel heat exchangers*, Experimental Thermal and Fluid Science, 2012, 36, pp. 107-117.

[18] Dall'Olio, S., Marengo, M., *Boiling of R134a inside a glass minichannel. A new statistical approach of flow pattern characterization based on flow visualization*, International Journal of Heat and Mass Transfer, 2012, 55, pp. 1048–1065.

[19] Ali, R., Palm, B., *Dryout characteristics during flow boiling of R134a in vertical circular minichannels*, International Journal of Heat and Mass Transfer, 2011, 54, pp. 2434-2445.

[20] Mahmoud, M.M., Karayiannis, T.G., Kenning, D.B.R., *Surface effects in flow boiling of R134a in microtubes*, International Journal of Heat and Mass Transfer, 2011, 54, pp. 3334-3346.

[21] Costa-Patry, E., Olivier, J., Nichita, B.A., Michel, B., Thome, J.R., *Two-phase flow of refrigerants in 85 lm-wide multi-microchannels: Part I – Pressure drop*, International Journal of Heat and Fluid Flow, 2011, 32, pp. 451-463.

[22] Padovan, A., Col, D.D., Rossetto, L., *Experimental study on flow boiling of R134a and R410A in a horizontal microfin tube at high saturation temperatures*, Applied Thermal Engineering, 2011, 31, pp. 3814-3826.

[23] Maqbool, M.H., Palm, B., Khodabandeh, R., *Boiling heat transfer of ammonia in vertical smooth minichannels: Experimental results and predictions*, International Journal of Thermal Sciences, 2012, 54, pp. 13-21.

[24] Copetti, J.B., Macagnan, M.H., Zinani, F., Kunsler, N.L.F., *Flow boiling heat transfer and pressure drop of R-134a in a mini tube: an experimental investigation*, Experimental Thermal and Fluid Science, 2011, 35, pp. 636-644.

[25] Agartan, Y.A., Yazıcıoglu, A.G. (2011, September). *Experimental Comparison of the Heat Transfer Performance of Microchannel Geometries,* Paper presented at VIII Minsk International Seminar “Heat Pipes, Heat Pumps, Refrigerators, Power Sources”.

[26] Tekin, B. (2011). *Experimental Investigation of R134a Flow in a 1.65 mm Copper Minitube* (Master’s thesis, Middle East Technical University, Ankara, Turkey). Retrieved from http://etd.lib.metu.edu.tr/upload/12612952/index.pdf, last visited on 27.01.2012.

[27] Kakaç, S. and Liu, H., *Heat Exchangers: Selection, Rating, and Thermal Design*, CRC, Florida, 2002.

[28] Bertsch, S.S., Groll, E.A., Garimella, S.V., *A composite heat transfer correlation for saturated flow boiling in small channels*, International Journal of Heat and Mass Transfer, 2009, 52, pp. 2110-2118.

[29] Shiferaw, D., Karayiannis, T.G., Kenning, D.B.R., *Flow boiling in a 1.1 mm tube with R134a: Experimental results and comparison with model*, Int. J. Thermal Sciences, 2009, 48, pp. 331-341.

[30] Tibiriçá, C. B., Ribatski, G., *Flow boiling heat transfer of R134a and R245fa in a 2.3 mm tube*, Int. J. Heat and Mass Transfer, 2010, doi:10.1016/j.ijheatmasstransfer.2010.01.038

[31] Sonntag, R., E., Borgnakke, C., Van Wylen, G., J., Fundamentals of Thermodynamics, Wiley, 6th edition, Phoenix, 2003.

[32] Kerpiççi, H., Personal communication.

[33] Liu, D., Garimella, S.V., *Flow Boiling Heat Transfer in Microchannels, ASME Journal of Heat Transfer*, 2008, 129, pp. 1321-1332.

[34] Cole Parmer, Thermo Scientific NESLAB RTE-series Refrigerated Circulating Baths, http://www.coleparmer.com/catalog/product_view.asp?sku=1350030&pfx=KH, last visited on 29.01.2012.

[35] Cole Parmer, Benchtop Digital Drive, http://www.coleparmer.com/catalog/Product_view.asp?sku=7401455&pfx=KH&referred_id=2269, last visited on 29.01.2012.

[36] Procon, Standard Vane Pump, http://www.proconpumps.com/products/Series-2-Pump.html, last visited on 31.01.2012.

[37] Rhenoik, RHM Coriolis Flow Sensors & RHE Coriolis Flow Transmitters, http://www.ge-mcs.com/, last visited on 29.01.2012.

[38] Cole Parmer, Compact Pressure Transducer, http://www.coleparmer.com/catalog/product_view.asp?sku=6834740, last visited on 29.01.2012.

[39] Cole Parmer, Oakton Integral handle RTD probes, http://www.coleparmer.com/catalog/Product_view.asp?sku=0811780&pfx=KH&referred_id=2269, last visited on 29.01.2012.

[40] Cole Parmer, 30-gauge wire, http://www.coleparmer.co.uk/catalog/product_view.asp?sku=0854204&pfx=KH, last visited on 29.01.2012.

[41] Cole Parmer, 303 SS Flowmeters for Water, http://www.coleparmer.com/catalog/product_view.asp?sku=3220502, last visited on 29.01.2012.

[42] Validyne, Products® P55 Compact Differential Pressure Transducer, http://www.validyne.com/ProductDisplay.aspx?Pid=2, last visited on 29.01.2012.

[43] Egerate, MCH TECHNIC 305D-2 DC Power Supply, http://www.egerate-store.com/Default.aspx?_Args=ProductInfo,43&LNG=EN last visited on 29.01.2012.

[44] Agilent, 34970A Data Acquisition / Data Logger Switch Unit, http://www.home.agilent.com/agilent/product.jspx?cc=TR&lc=eng&ckey=1000001313:epsg:pro&nid=-33640.536881544.00&id=1000001313:epsg:pro, last visited on 29.01.2012.

[45] Incropera, F.P., Dewitt, D.P., Bergman, T.L. and Lavine, A.S., *Fundamentals of Heat and MassTransfer*, Wiley, 6th edition, Phoenix, 2007.

[46] Kline, S.J., and McClintock, F.A., Describing uncertainties in single-sample experiments, Mechanical Engineering, 1953, 75, p.p. 3-8.

APPENDIX A

SPECIFICATIONS OF DEVICES IN THE EXPERIMENTAL SET-UP

Many of the information given about the devices used in minichannel experiments in Appendix A are also involved in the thesis of Tekin [26] because the microchannel experiments were conducted in the same experimental set-up which was used in the copper minitube experiments mentioned by Tekin in his thesis.

A.1 REFRIGERATED CIRCULATING BATH

Here the information about the cooling baths used in the both water and refrigeration cycles is given [34].

Brand Name: Cole Parmer
Catalog Number: KH-13500-30

Bath Capacity 7 Liters
Temperature Range -40 to 200°C
Temperature stability ±0.01°C
Temperature control PID
Temperature setting Digital
Temperature display LED
Temperature sensor 100 Ω Pt RTD
Cooling capacity 800 W @ 20°C, 650 W @ 0°C, 500 W @ -10°C
Wattage: 2550 W total, 2000 W heater
Pressure pump: Max flow 15 L/min, Max head 5 psi
Compressor 1/2 hp

Refrigerant	R-404A
Bath opening	6 5/8" x 7 1/4”
Working depth	6"
Overall dimensions	26 5/8"W x 11 3/8"H x 18 7/8"D
Power Input	230 VAC, 50 Hz
Amperes	12 A

A.2 DIGITAL GEAR PUMP SYSTEM

The information about the pump used during the microchannel experiments in the refrigeration cycle is given below [35].

Brand Name: Cole Parmer
Catalog Number: KH-74014-55

Wetted parts	Body: 316 SS
	Gears: PPS
	Seals: PTFE

Flow rate:	0.316 mL/rev
	18.96 mL/min at 60 rpm
	1137.6 mL/min at 3600 rpm

Differential pressure	75 psi (max)
Max system pressure	300 psi
Max temperature	40°C (system)
Temperature range	-46 to 54°C
Port size	1/8" NPT(F)
Viscosity	0.2 to 1500 cp
Dimensions	7 3/4"L x 11 1/2"W x 7 1/4"H
Power VAC	220 VAC

A.3 STANDARD VANE PUMP SYSTEM

The information about the second pump used at the beginning of the microchannel experiments in the refrigeration cycle is given below [36].

Brand Name: PROCON
Serial Number: 104E240F11BA225

Body Material: Type 303 stainless steel
Capacity: 15 to 125 GPH
Nominal Speed: 1725 RPM
Typical Horsepower Required: .25 to .50 HP
Maximum Discharge Pressure: 250 PSI
Rotation (vievew from nameplate): Clockwise
Dry Weight: Approximately 2.5 lbs.
Dimensions: 3.56" x 3.49" x 3.86"
Self Priming (water): 6 ft. Maximum Lift
Port Size: 3/8 NPT Inlet and Outlet

A.4 MICRO-FLOWMETER

The information about the micro-flowmeter used in the refrigeration cycle for measuring the refrigerant flow rate is given below [37].

Brand Name: Rheonik
Flowmeter Model: RHM 04 Universal Coriolis Mass Flowmeter with particular Fast Response

Pressure	up to 250 bar
Range	from 0.1 kg/min to 10 kg/min
Minimal flow	0.05 kg/min
Response time	30 ms and better
Flow Accuracy	0.10%

Repeatability	0.05%

Transmitter Model: RHE 08 Rheonik advanced transmitters

Version	Wall mounting
Analog Outputs	Two (0/4 - 20/22 mA)
Pulse/frequency	1 output - 2 inputs
Supply voltages	Available in all common
Multifunctions	density, brix, concentration
Power consumption	< 15 W
Temperature range	-40°C to 60°C

A.5 COMPACT PRESSURE TRANSDUCER

The information about the compact pressure transducers used in both cycles for measurements of system pressures is given below [38].

Brand Name: Cole Parmer
Catalog Number: KH-68347-40

Output	4-20 mA
Process connection	1/4" NPT (M)
Range	200 psia
Accuracy	0.5% full scale
Power	8 to 30 VDC

A.6 RTD PROBE

The information about the RTDs used in specified locations of the experimental setup for temperature measurements is given below [39].

Brand Name: Cole Parmer
Catalog Number: KH-08117-80

Temp range	-50 to 500°C
Probe length	2"
Diameter	0.093"
Time constant	10 seconds
Sheath material	316 SS

A.7 THERMOCOUPLE WIRE

The information about the thermocouples used for wall temperature measurement on the outer surface of the minichannel is given below [40].

Brand Name: Cole Parmer
Catalog Number: KH-08542-04

Length	1000 ft
Temp range	-200 TO 204°C
Error limit	±1.5% reading from -200 to -65°C; ±1°C from -65 to 130°C ±0.75% reading from 130 to 350°C
Type	T
Advantages	Chemical, moisture and abrasion resistance
Gauge	30
ID	0.0100" (0.25 mm) dia
OD	0.030" x 0.048"
Model	T30-2-506

A.8 ROTAMETER

The information about two rotameters used in the water cycle is given below [41].

Brand Name: Cole Parmer
Catalog Number: EW-32205-02 (KH-32205-02)

Media	water
Max operating temperature	240°F (115°C)
Max pressure	6000 psi
Flow rate	water 0.2 to 1.8 LPM;
Accuracy	±2% full-scale
Connections	1/4" NPT(F)
Repeatability	±1.0%
Housing Material	304 Stainless Steel
Dimensions	1 3/4” W x 4 13/16” H x 1 15/16” D

A.9 DIFFERENTIAL PRESSURE TRANSDUCER

The information about the differential pressure transducer used in the test section for pressure drop measurement is given below [42].

Brand Name: Validyne
Catalog Number: 1-N-1-28-S-4-A

Dimensions	1.5"L x 1.5"W x 4.5"H
Output	±5 Vdc @0.5 mA
Operating temperature	-65 to 250°F (-54 to 121°C)
Process connection	1/8" NPT(F)
Range	±0.08 to ±3200 psid
Accuracy	±0.25% full scale
Power	9 to 55 Vdc

A.10 DC POWER SUPPLY

The information about the DC power supply used in the data acquisition system is given below [43].

Brand Name: MCH Technic
Catalog Number: MCH 305D-2 DC Power Supply

Voltage:	0-30V Adjustable	
Current:	0-5A Adjustable	
Dual-Output DC Power Source	Two Independent:	30V-5A
	With Serial Button:	60V-5A
	With Parallel Button:	30V-10A

Voltage	0 to Descripted Continuously Variable	
	Stability	Voltage: ≤0.01%+2mV
	Load:	≤0.0%+2mV
	Recover Time	≤100μS
	Ripple & Noise	≤1MVRMS（efficent）
	Temperature Factor	≤300PPM/ºC

Current	0 to Descripted Continuously Variable	
	Current, Load Stability	≤0.2%+3mA
	Ripple & Noise	≤3mArms

Working Condition		
	Line Power Supply	220V±10% 50/60Hz
	Operating Temperature:	-10ºC to 40ºC Moisture≤90%
	Storage Temperature:	-20ºC to 80ºC Moisture≤80%

A.11 DATA ACQUISITION SYSTEM

The information about the data acquisition system used to collect the measurements on the computer is given below [44].

Brand Name: Agilent
Catalog Number: 34970A Data Acquisition / Switch Unit

Slot	3
Interface	GPIB and RS232

Multimeter	Digital and internal with 6 1/2-digit (22-bit)
Scanning	up to 250 channels per second
Modules	8 switch and control plug-in
Memory	50k readings
Alarm	Hi/Lo on each channel
Measurement	Thermocouples, RTDs and thermistors, ac/dc volts and current; resistance; frequency and period
Software	Free Bench Link data logger software enables tests without programming

Brand Name: Agilent

Catalog Number: 34901A 20-Channel Multiplexer + 2 Current Channels Module (Built-in thermocouple reference junction)

Model description	34901A 20 ch Multiplexer+ 2 current channels
Type	2-wire armature (4-wire selectable)
Speed(ch/sec)	60
Max volts	300 V
Max amps	1 A

APPENDIX B

TECHNICAL DRAWINGS OF THE PARTS IN THE TEST SECTION

B.1 TECHNICAL DRAWING OF THE FLANGES

The units of the dimensions specified in Figure B.1 and B.2 are millimeters (mm)

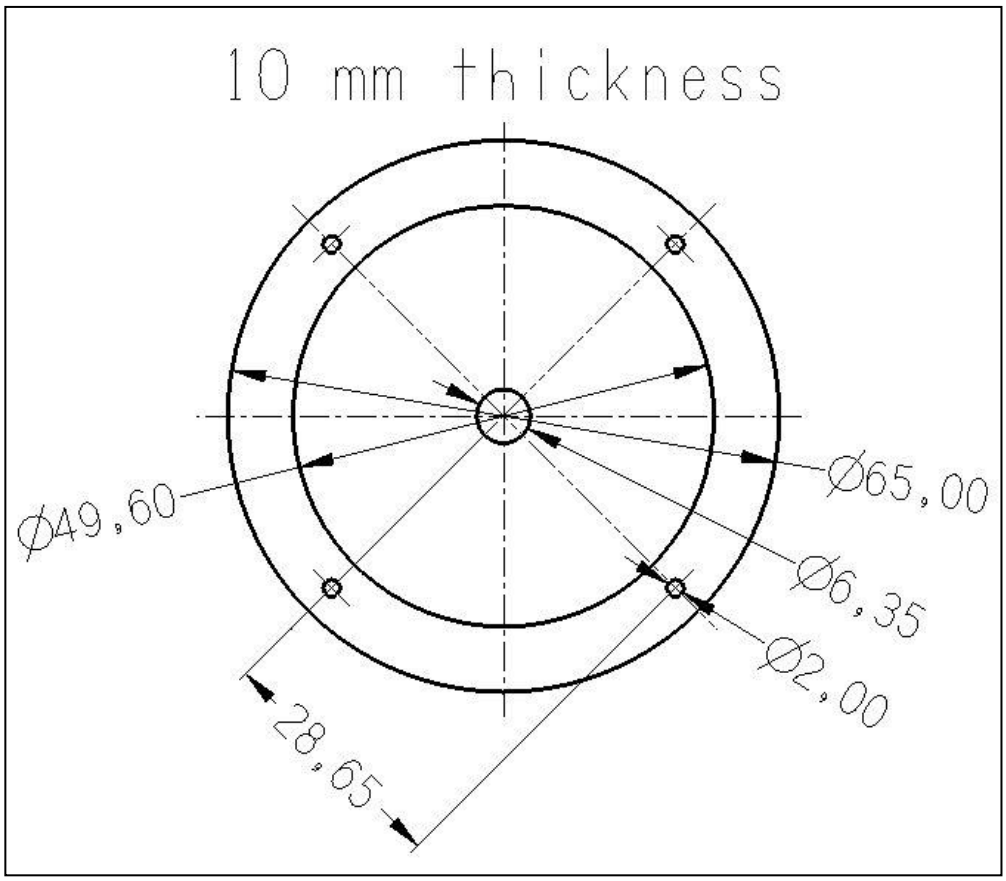

Figure B.1: Technical drawing of the flange used for the 1st and 3rd minichannels

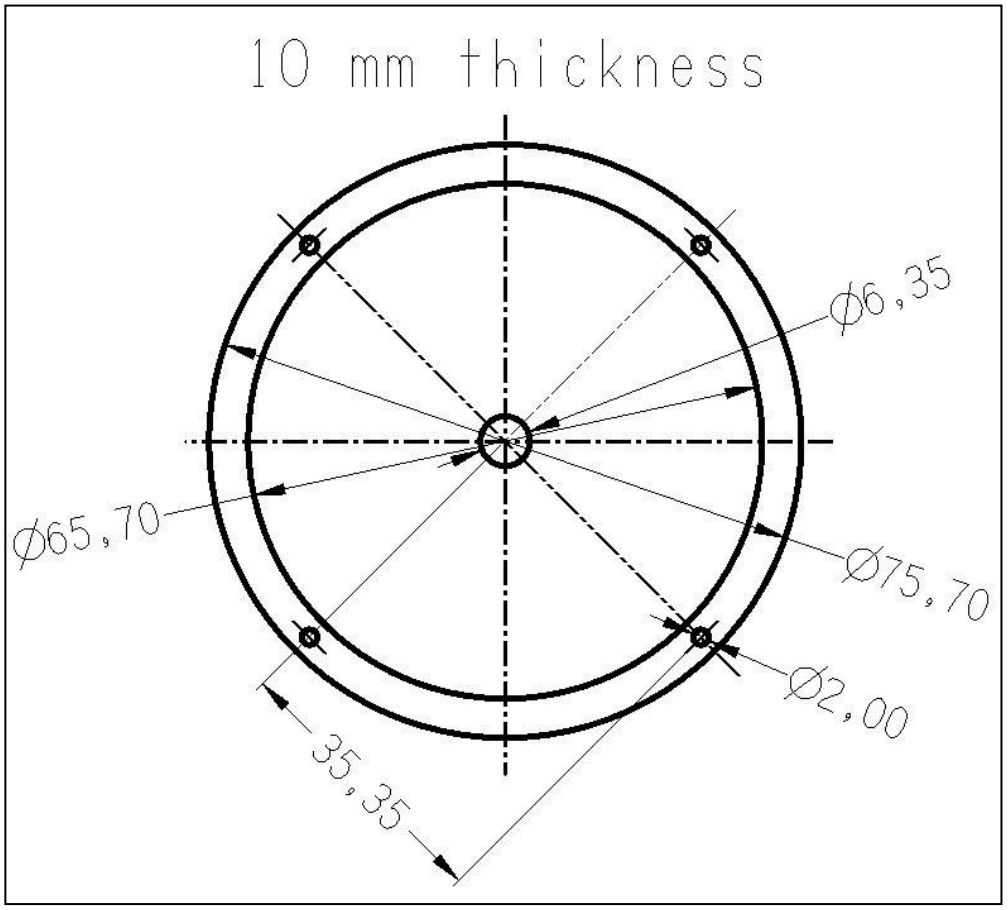

Figure B.2: Technical drawing of the flange used for the 2nd minichannel

B.2 TECHNICAL DRAWINGS OF THE SHELLS

The units of the dimensions specified in Figure B.3, B.4 and B.5 are millimeters (mm).

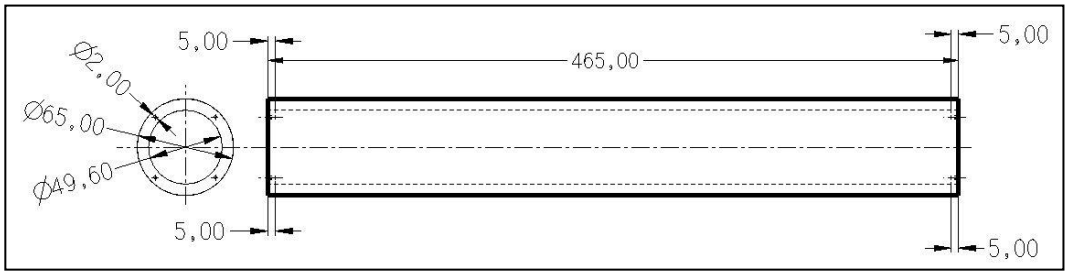

Figure B.3: Technical drawing of the first shell

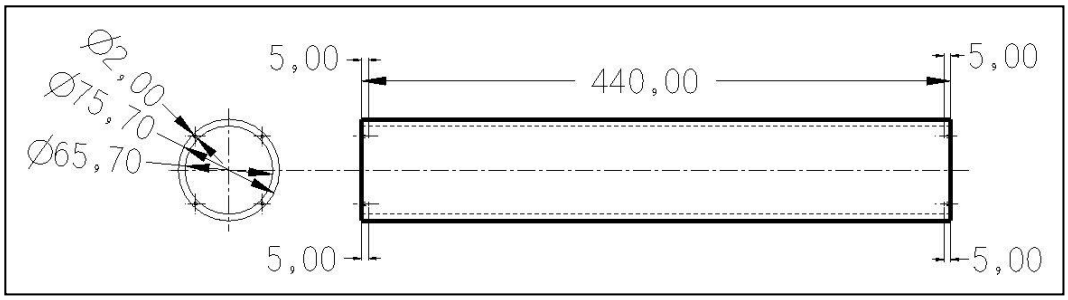

Figure B.4: Technical drawing of the second shell

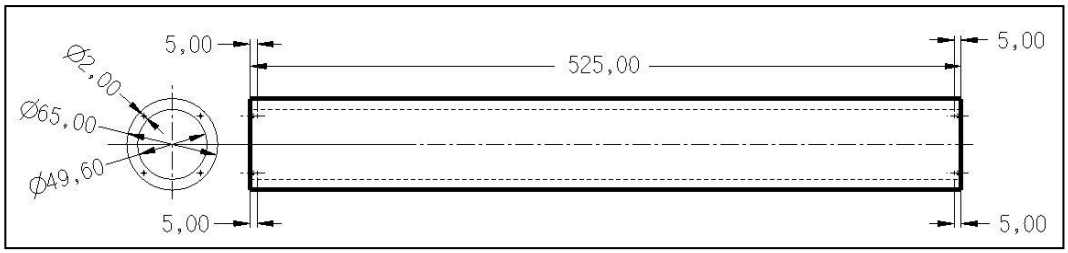

Figure B.5: Technical drawing of the third shell

APPENDIX C

THE CALIBRATION TABLES AND GRAPHS FOR MEASUREMENT DEVICES

The same calibration curves involved in the thesis of Tekin [26] is given here because the RTDs and the pressure transducers used in the minichannel experiments without recalibration after the copper minitube experiments made by Tekin.

C.1 A SAMPLE CALIBRATION CURVE FOR A CALIBRATED RTD

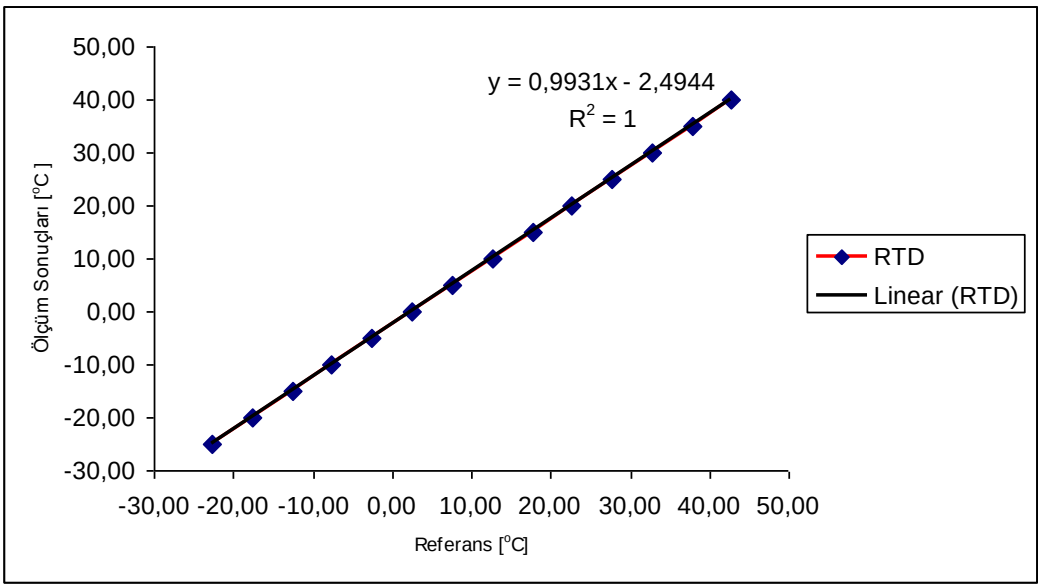

Figure C.1: A sample calibration curve for an RTD

C.2 THE CALIBRATION RESULTS FOR THE CPTS

Table C.1: The calibration results for the compact pressure transducers

PSI	221	222	PSI	221	222	PSI	221 (A)	222 (A)
0-200 psi çıkış			0-200 psi iniş			0-200 psi ortalama		
0	0,003983	0,003985	0	0,003982	0,003989	0	0,003983	0,003987
1	0,004064	0,004063	1	0,004061	0,004065	1	0,004063	0,004064
2	0,004137	0,004136	2	0,00414	0,004143	2	0,004138	0,00414
3	0,004212	0,004214	3	0,004216	0,004217	3	0,004214	0,004215
4	0,004291	0,004295	4	0,004298	0,004299	4	0,004295	0,004297
5	0,004366	0,00437	5	0,004376	0,004377	5	0,004371	0,004373
6	0,004445	0,004448	6	0,004453	0,004454	6	0,004449	0,004451
7	0,004524	0,004526	7	0,00453	0,00453	7	0,004527	0,004528
8	0,004601	0,004602	8	0,004606	0,004607	8	0,004603	0,004604
9	0,00468	0,00468	9	0,004683	0,004684	9	0,004681	0,004682
10	0,004759	0,004758	10	0,004764	0,004761	10	0,004761	0,00476
11	0,004838	0,004837	11	0,004841	0,004842	11	0,004839	0,00484
12	0,004917	0,004915	12	0,004918	0,004917	12	0,004917	0,004916
13	0,004997	0,004994	13	0,004996	0,004995	13	0,004997	0,004994
14	0,005078	0,005073	14	0,005078	0,005076	14	0,005078	0,005074
15	0,005152	0,005147	15	0,005156	0,005152	15	0,005154	0,00515
20	0,005543	0,005536	20	0,005551	0,005545	20	0,005547	0,00554
40	0,007121	0,007114	40	0,007133	0,007124	40	0,007127	0,007119
60	0,008742	0,008733	60	0,008706	0,008695	60	0,008724	0,008714
80	0,010273	0,01026	80	0,010282	0,010268	80	0,010277	0,010264
100	0,011859	0,011846	100	0,011862	0,011847	100	0,011861	0,011846
120	0,013432	0,013416	120	0,013435	0,013417	120	0,013433	0,013417
140	0,01502	0,015001	140	0,015017	0,014993	140	0,015018	0,014997
160	0,016588	0,016564	160	0,016597	0,016574	160	0,016592	0,016569
180	0,018162	0,018146	180	0,018169	0,018148	180	0,018165	0,018147
200	0,019752	0,019717	200	0,019747	0,019723	200	0,019749	0,01972

C.3 THE CALIBRATION CURVE FOR THE CPT 1

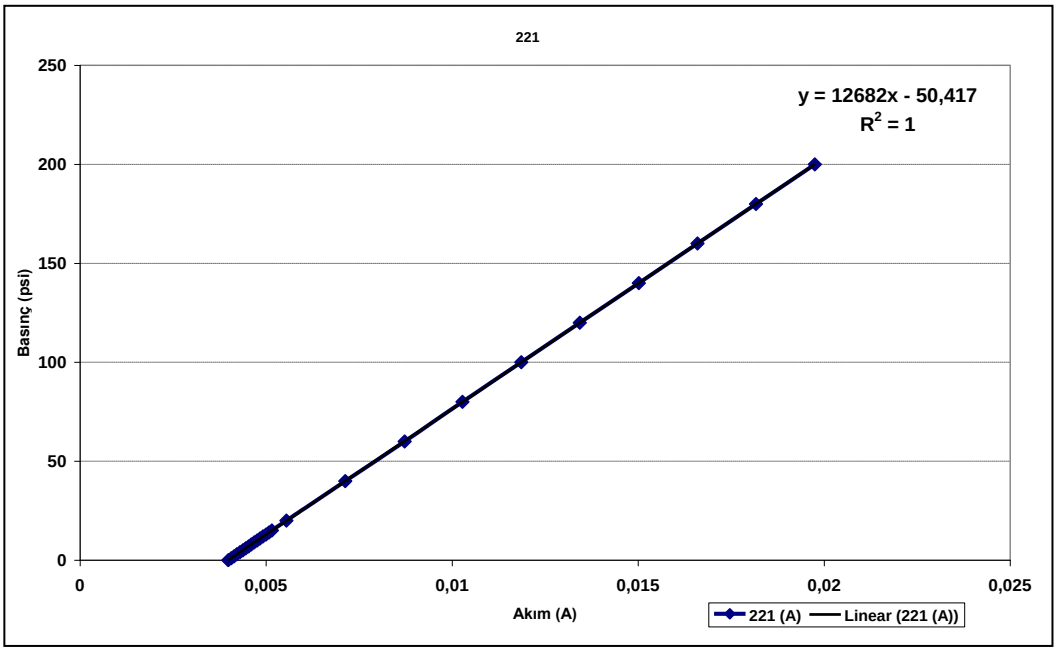

Figure C.2: The calibration curve for the compact pressure transducer 1

C.4: THE CALIBRATION CURVE FOR THE CPT 2

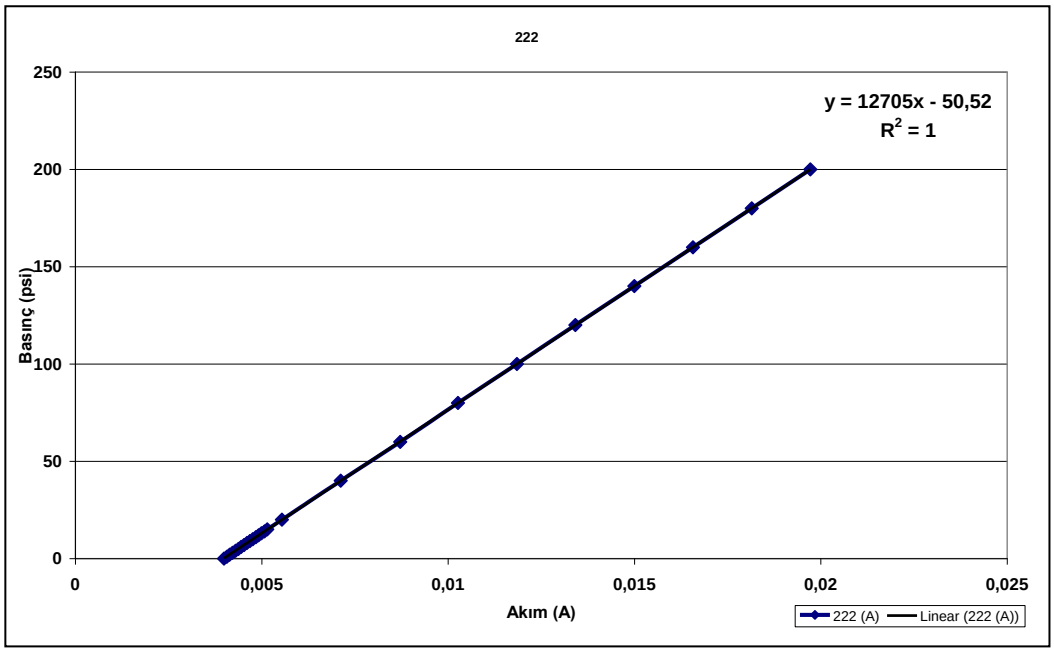

Figure C.3: The calibration curve for the compact pressure transducer 2

C.5 THE CALIBRATION RESULTS FOR THE DPT

Table C.2: The calibration results for the differential pressure transducer

bar	V
0,0	0,342348
0,5	0,88057
1,0	1,362816
1,5	1,85528
2,0	2,377242
2,5	2,746445
3,0	3,294953
3,5	3,660102
4,0	4,213051
4,5	4,685636
5,0	5,166647

C.6 THE CALIBRATION CURVE FOR THE DPT

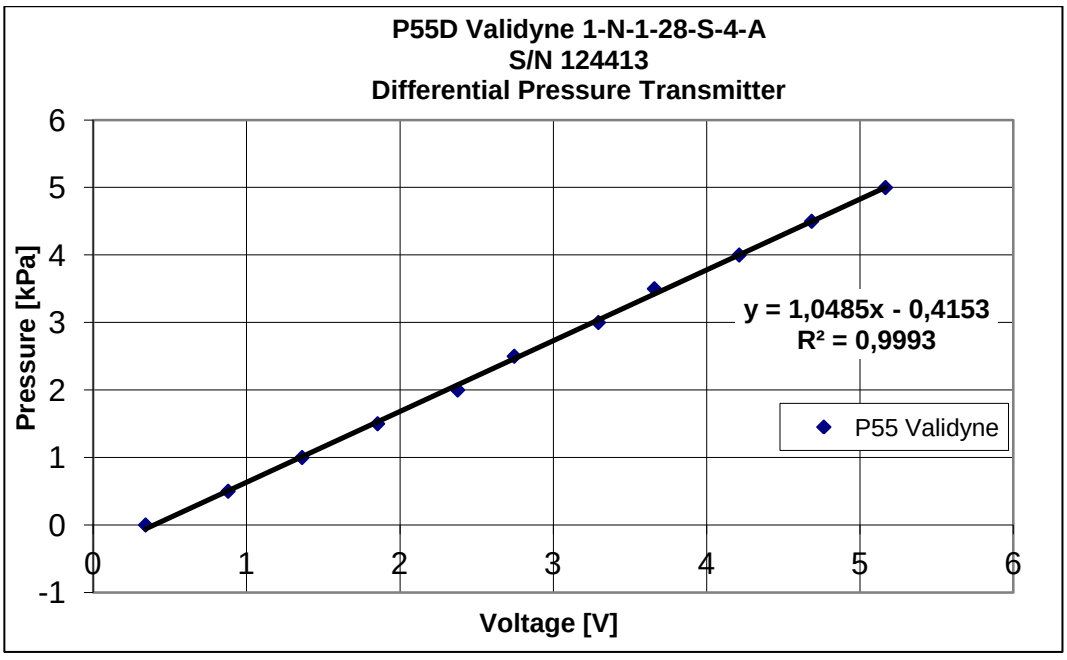

Figure C.4: The calibration curve for the differential pressure transducer

APPENDIX D

WATER-ETHYLENE GLYCOL 1:1 VOLUMETRIC MIXTURE PROPERTIES

The curves and the properties obtained and used to find the properties of water-ethylene glycol mixture in the water cycle which are presented in this section are also involved in the thesis of Tekin [26] because the same mixture was used in the copper minitube experiments made by him and the microchannel experiments mentioned in the current study and I was also involved in calculation of heat transfer coefficients for copper minitube in scope of the project covering minitube and minichannel experiments.

D.1: SPECIFIC GRAVITY OF THE MIXTURE

Table D.1: Specific gravity dependence on temperature for the water – ethylene glycol mixture

Temperature (°C)	Specific Gravity -
-17.8	1.1
4.4	1.088
26.7	1.077
48.9	1.064

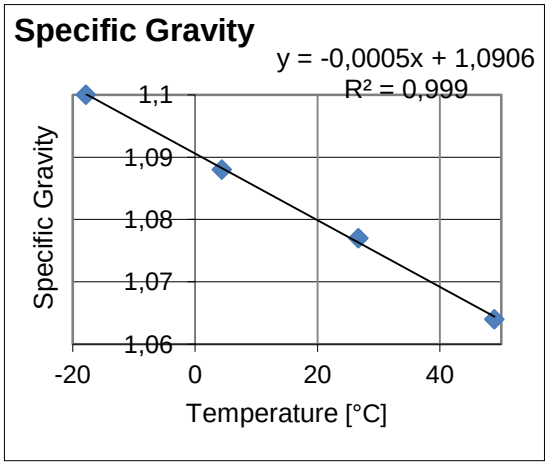

Figure D.1: Specific gravity versus temperature for the water – ethylene glycol mixture

D.2 SPECIFIC HEAT OF THE MIXTURE

Table D.2: Specific heat dependence on temperature for the water – ethylene glycol mixture

Temperature (°C)	Specific Heat (J/kgK)
-17.8	3265.704
4.4	3328.506
26.7	3412.242
48.9	3483.4176

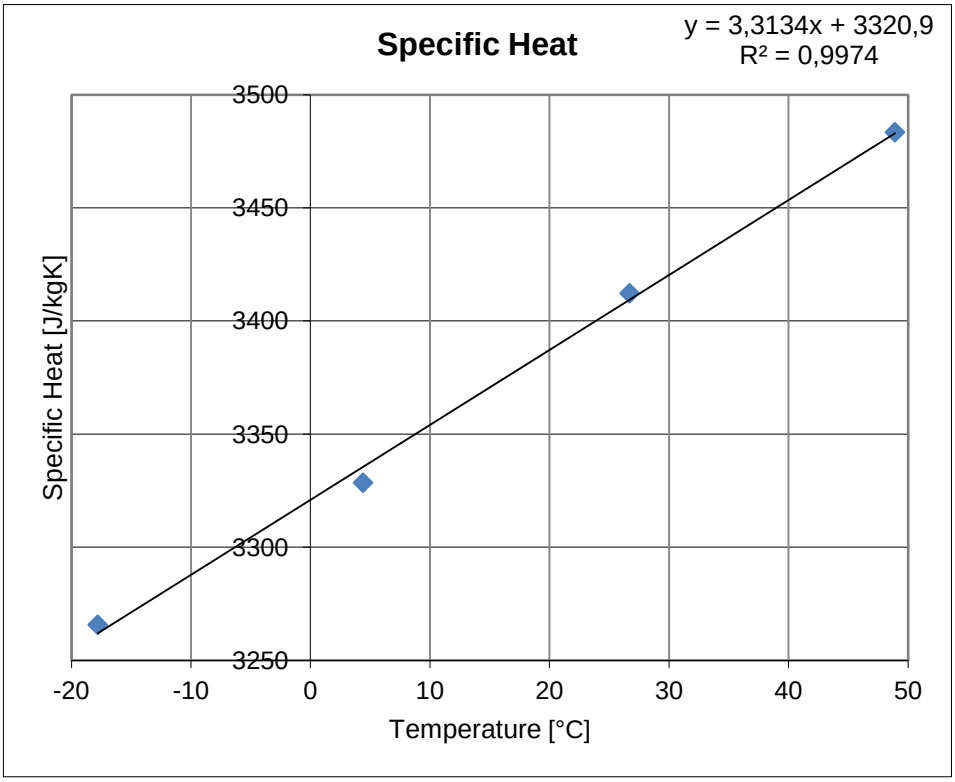

Figure D.2: Specific heat versus temperature for the water – ethylene glycol mixture

D.3 DYNAMIC VISCOSITY OF THE MIXTURE

Table D.3: Dynamic viscosity dependence on temperature for the water – ethylene glycol mixture

Temperature (°C)	Dynamic Viscosity (kg/ms)
-17.8	22
4.4	6.5
26.7	2.8
48.9	1.5

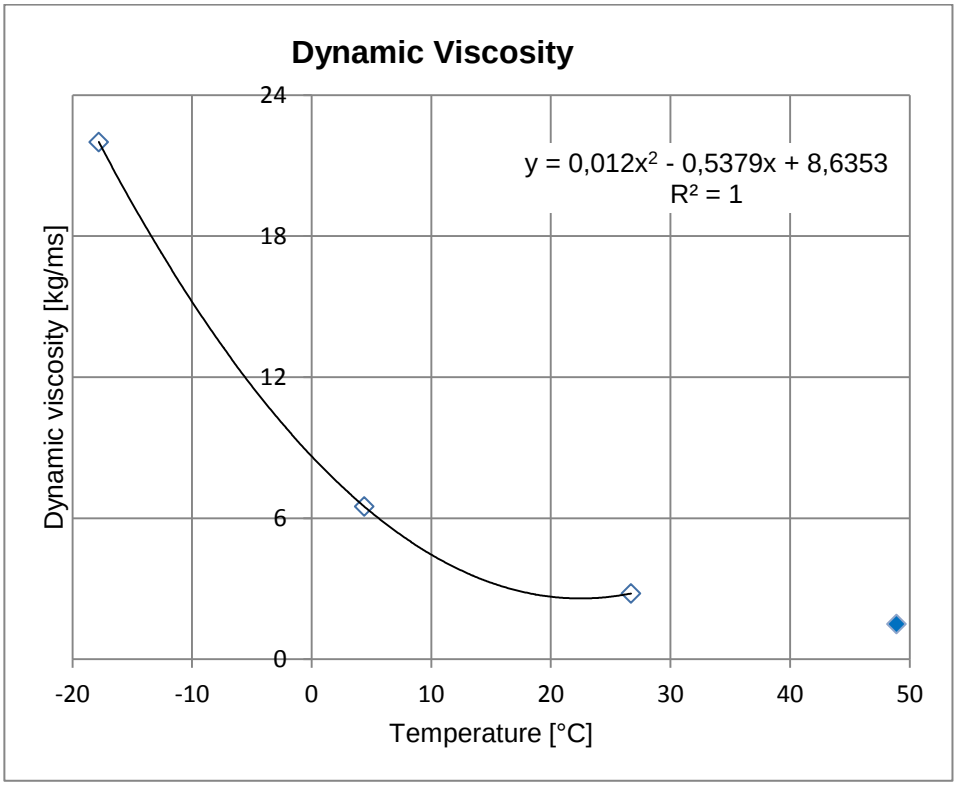

Figure D.3: Dynamic viscosity versus temperature for the water – ethylene glycol mixture

D.4 CONDUCTIVITY OF THE MIXTURE

Table D.4: Conductivity dependence on temperature for the water – ethylene glycol mixture

Temperature (°C)	Conductivity (W/mK)
-35	0.41
40	0.4
70	0.395

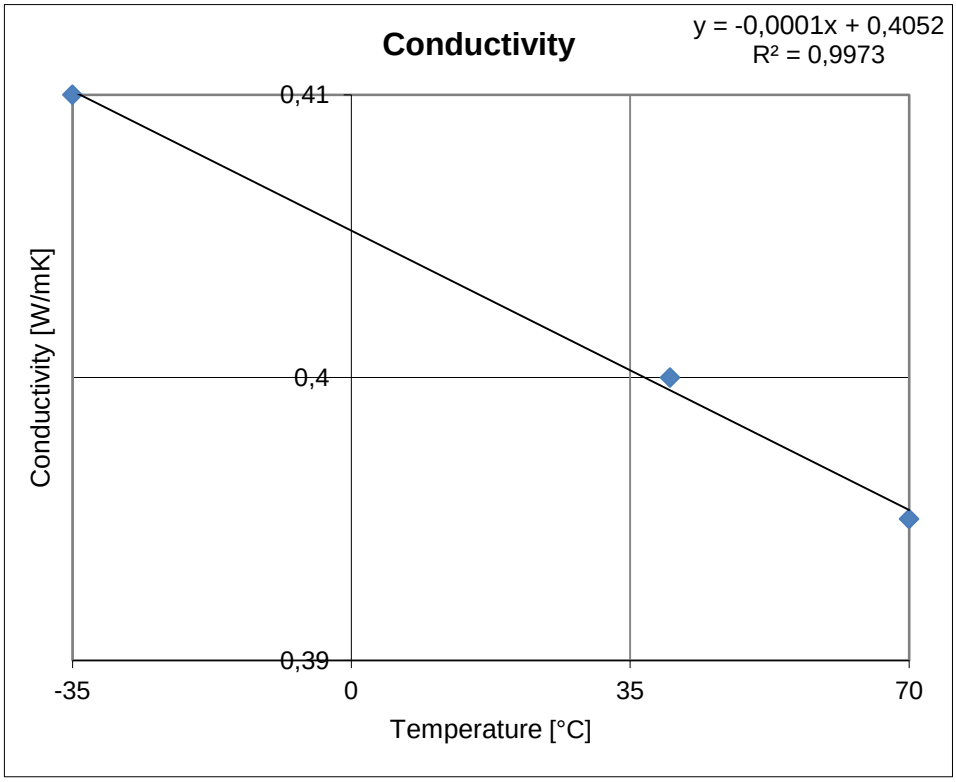

Figure D.4: Conductivity versus temperature for the water – ethylene glycol mixture

APPENDIX E

THE REFRIGERANT (R-134A) PROPERTIES

The curves and the properties obtained and used to find the properties of the refrigerant (R134a) in the refrigerant cycle which are presented in this section are also involved in the thesis of Tekin [26] because the same refrigerant was used in the copper minitube experiments made by him and the microchannel experiments mentioned in the current study and I was also involved in calculation of heat transfer coefficients for copper minitube in scope of the project covering minitube and minichannel experiments.

E.1 VISCOSITY OF THE REFRIGERANT IN LIQUID PHASE

Table E.1: Viscosity dependence on saturation pressure for R-134a in liquid phase [27]

Saturation pressure (bar)	Viscosity (liquid) (Pa.s)
0.728	0.000425
1.159	0.00037
1.765	0.000325
2.607	0.000288
3.721	0.000256
5.175	0.00023
7.02	0.000208
9.33	0.000189
12.16	0.000172
15.59	0.000158
19.71	0.000145

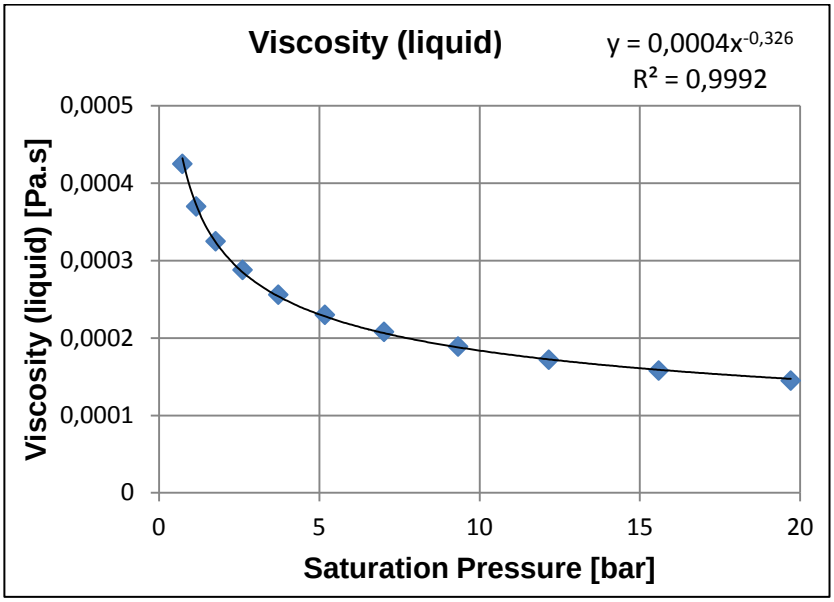

Figure E.1: Viscosity versus saturation pressure for R-134a in liquid phase

E.2 VISCOSITY OF THE REFRIGERANT IN VAPOR PHASE

Table E.2: Viscosity dependence on saturation pressure for R-134a in vapor phase [27]

Saturation pressure (bar)	Viscosity (vapor) (Pa.s)
0.728	0.0000095
1.159	0.0000099
1.765	0.0000104
2.607	0.0000108
3.721	0.0000112
5.175	0.0000117
7.02	0.0000121
9.33	0.0000125
12.16	0.0000129
15.59	0.0000133
19.71	0.0000137

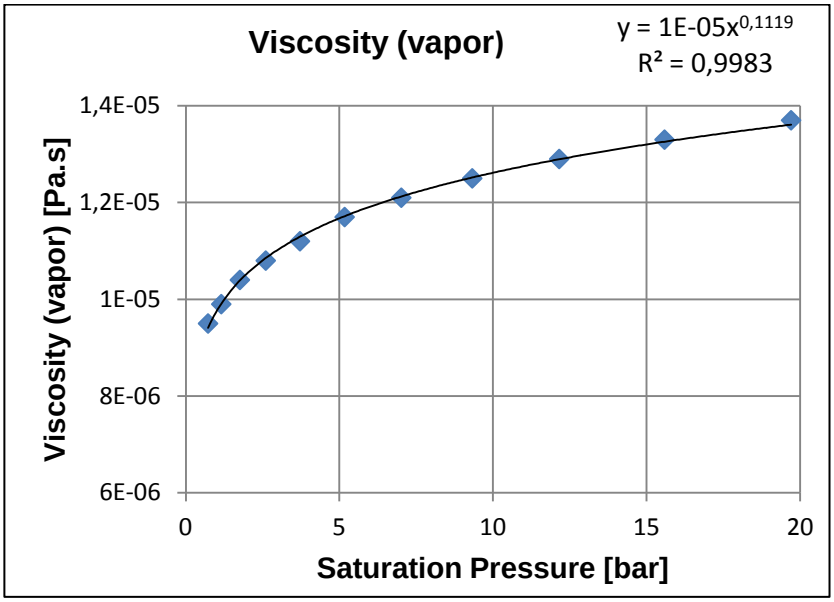

Figure E.2: Viscosity versus saturation pressure for R-134a in vapor phase

E.3 CONDUCTIVITY OF THE REFRIGERANT IN LIQUID PHASE

Table E.3: Conductivity dependence on saturation pressure for R-134a in liquid phase [27]

Saturation pressure (bar)	Conductivity (liquid) (W/mK)
0.728	0.099
1.159	0.095
1.765	0.091
2.607	0.087
3.721	0.083
5.175	0.079
7.02	0.075
9.33	0.071
12.16	0.068
15.59	0.064
19.71	0.06

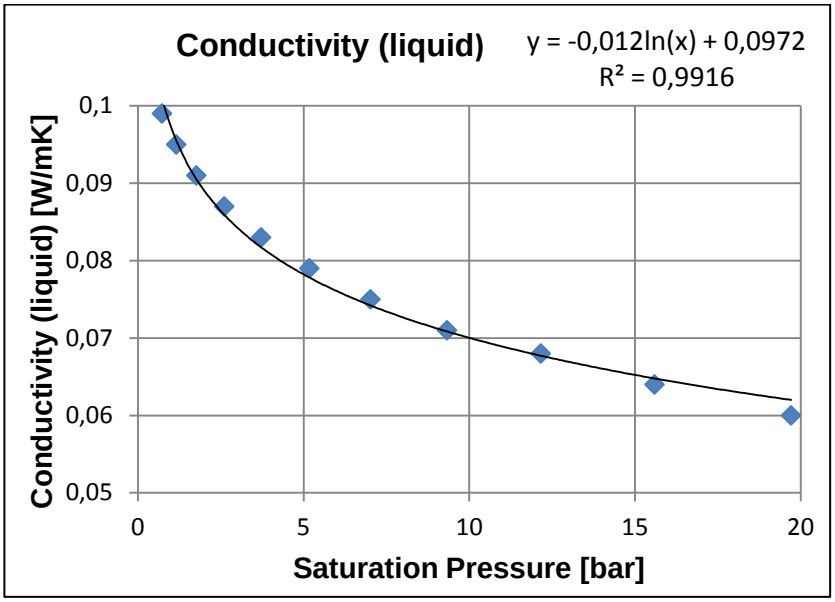

Figure E.3: Conductivity versus saturation pressure for R-134a in liquid phase

E.4 CONDUCTIVITY OF THE REFRIGERANT IN VAPOR PHASE

Table E.4: Conductivity dependence on saturation pressure for R-134a in vapor phase [27]

Saturation pressure (bar)	Conductivity (vapor) (W/mK)
0.728	0.008
1.159	0.008
1.765	0.008
2.607	0.009
3.721	0.009
5.175	0.01
7.02	0.01
9.33	0.01
12.16	0.011
15.59	0.011
19.71	0.012

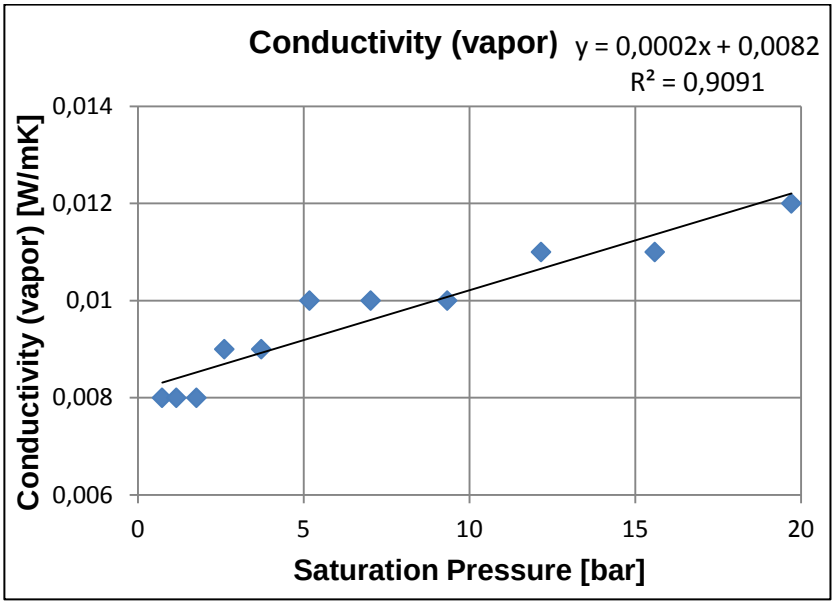

Figure E.4: Conductivity versus saturation pressure for R-134a in vapor phase

E.5 SPECIFIC HEAT OF THE REFRIGERANT IN LIQUID PHASE

Table E.5: Specific heat dependence on saturation pressure for R-134a in liquid phase [27]

Saturation pressure (bar)	Specific heat (liquid) (J/kgK)
0.728	1162
1.159	1212
1.765	1259
2.607	1306
3.721	1351
5.175	1397
7.02	1446
9.33	1497
12.16	1559
15.59	1638
19.71	1750

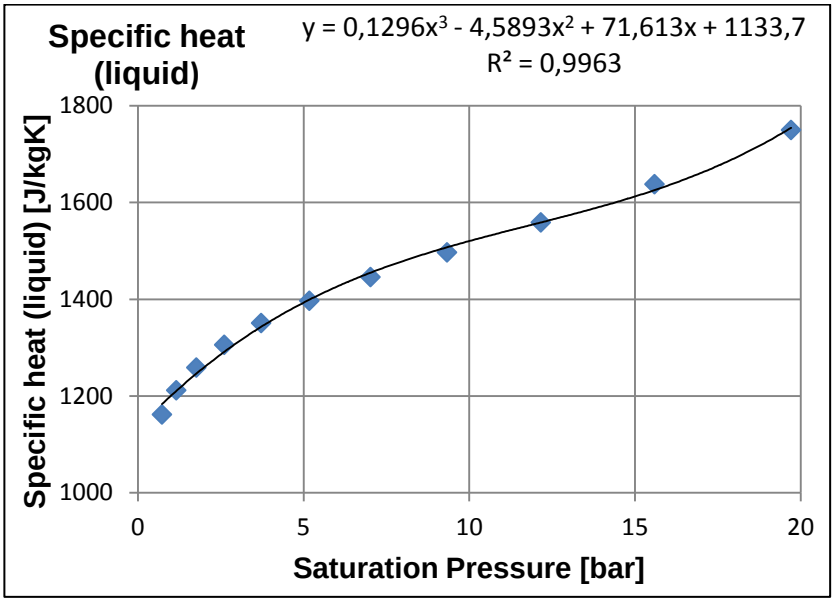

Figure E.5: Specific heat versus saturation pressure for R-134a in liquid phase

E.6 THERMAL CONDUCTIVITY OF ALUMINUM WHICH THE MINICHANNELS ARE MADE UP OF, THE REFRIGEREANT FLOWS THROUGH

Table E.6: Thermal conductivity of aluminum dependence on temperature [45]

Temperature (K)	Conductivity (Al) (W/mK)
100	302
200	237
400	240
600	231
800	218

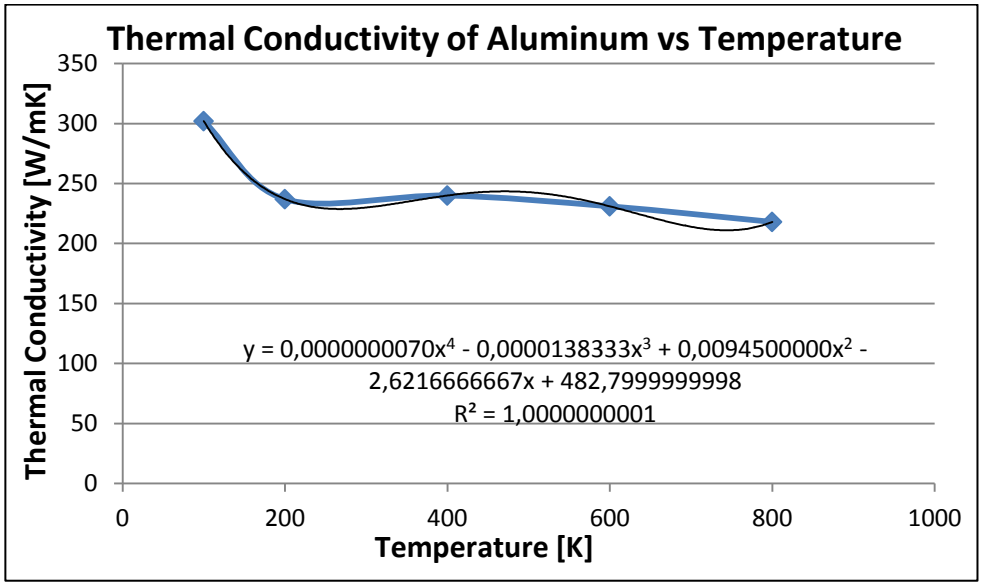

Figure E.6: Thermal conductivity of aluminum versus temperature

APPENDIX F

THE RESULTS FOR SAMPLE TWO-PHASE EXPERIMENTS

F.1 THE GEOMETRY OF BOTH SIDES IN THE TEST SECTION OF THREE MINICHANELLS

Table F.1: The geometry of refrigerant sides

Name	Unit	Minichannel 1	Minichannel 2	Minichannel 3
Width	mm	16	22	20
Height	mm	2.1	5	2.1
Wall thickness	mm	0.3	0.6	0.4
Channel height	mm	1.5	3.8	1.3
Channel width	mm	1.94	3.68	2.35
Channel number	mm	7	5	7
Channel length	mm	465	440	525
Cross sectional area	mm^2	20.4	66.27	21.84
Wetted parameter	mm	48.2	68.79	51.8
Hydraulic diameter	mm	1.69	3.85	1.69
Inner heat transfer area	mm^2	22413	30268	27195

Table F.2: The geometry of water sides

Name	Unit	Minichannel 1	Minichannel 2	Minichannel 3
Outer diameter	mm	49.6	65.7	49.6
Inner perimeter	mm	36.2	49.71	42.00
Outer perimeter	mm	155.82	206.40	155.82
Cross sectional area	mm^2	1898.61	3285.53	1890.21
Hydraulic diameter	mm	39.55	51.31	37.80

F.2 TEST CONDITIONS FOR THE MINICHANNEL EXPERIMENTS

Table F.3: Test conditions for the experiments

Name	Unit	Minichannel 1	Minichannel 2	Minichannel 3
Refrigerant mass flow rate	g/s	1.044	3.060	2.136
Refrigerant inlet pressure	bar	4.43	5.48	4.04
Refrigerant flowmeter	°C	4.98	13.18	7.64
Refrigerant inlet temperature	°C	12.59	19.27	9.67
Refrigerant exit temperature	°C	12.19	18.88	9.53
Refrigerant Pressure drop	bar	0.0083	0.0097	0.0098
Water inlet temperature	°C	16.17	22.83	21.77
Water exit temperature	°C	15.78	22.38	20.12
Water volumetric flow rate	l/min	1.65	1.90	2
Water mass flow rate	kg/s	0.030	0.034	0.036
Water mass flow rate	g/s	29.77	34.18	36.00
Test inlet wall temperature	°C	13.28	19.26	10.47
Test exit wall temperature	°C	13.11	20.20	11.27
Pre-heater voltage input	V	4	7	5
Pre-heater net power input	W	49.60	136.86	84.33
Viscous Heating	W	11.00	11.31	15.59
Net heat transfer rate	W	49.54	64.37	216.61

F.3 REFRIGERANT EXPERIMENT STATES

Table F.4: Refrigerant experiment states

Flowmeter State (Pre-heater inlet)	**Unit**	**Minichannel 1**	**Minichannel 2**	**Minichannel 3**
Refrigerant pressure	bar	4.43	5.48	4.04
Refrigerant temperature	°C	4.98	13.18	7.65
Refrigerant quality (%)	-	-	-	-
Refrigerant enthalpy	kJ/kg	206.74	217.97	210.36
Test Inlet (Pre-heater exit)				
Refrigerant pressure	bar	4.43	5.48	4.04
Refrigerant temperature	°C	12.00	13.18	9.24
Refrigerant quality (%)	-	20.04	20.24	19.49
Refrigerant enthalpy	kJ/kg	254.24	262.69	249.83
Test Exit				
Refrigerant pressure	bar	4.42	5.47	4.03
Refrigerant temperature	°C	11.94	18.58	9.16
Refrigerant quality (%)	-	45.17	31.74	72.51
Refrigerant enthalpy	kJ/kg	301.68	283.72	351.22

F.4 WATER SIDE PROPERTIES

Table F.5: Water side properties

Name	**Unit**	**Minichannel 1**	**Minichannel 2**	**Minichannel 3**
Velocity	m/s	0.0144	0.0096	0.0176
Density	kg/m³	1082.61	1079.30	1080.13
Viscosity	Pa.s	0.0031	0.0026	0.0026
Reynolds	-	200	205	273
Specific heat	J/kgK	3373.83	3395.80	3390.29
Average temperature	°C	15.98	22.61	20.94
Mass flow rate	kg/s	0.0298	0.0342	0.0360

F.5 REFRIGERANT EXPERIMENTAL CALCULATIONS

Table F.6: Refrigerant experimental calculations

Name	Unit	Minichannel 1	Minichannel 2	Minichannel 3
Net heat transfer rate	W	49.54	64.37	216.61
Heat flux	W/m²	2210.17	2126.52	7965.09
Mass flux	kg/m²s	51.19	46.18	97.82
Water average temperature	°C	15.98	22.61	20.94
Wall average temperature	°C	13.19	19.73	10.87
Water - wall temp. difference	°C	2.78	2.88	10.07
Refrigerant inlet temperature	°C	11.99	18.63	9.24
Refrigerant exit temperature	°C	11.94	18.58	9.16
Temp. Diff. Inlet	°C	-0.59	-0.32	-1.14
Temp. Diff. Exit	°C	-0.99	-1.00	-1.39
Log. Mean Temp. Diff.	°C	-0.78	-0.60	-1.26
U	W/m²K	2829.98	3551.19	6304.28
h	W/m²K	2840.50	3567.75	6374.44
Refrigerant average temp.	°C	11.97	18.61	9.20
Refrigerant saturation pres.	bar	4.43	5.47	4.04
Average quality (%)	-	32.61	25.99	46.00